G1-G2 scheme: Dramatic acceleration of nonequilibrium Green functions simulations within the Hartree-Fock generalized Kadanoff-Baym ansatz

Jan-Philip Joost, Niclas Schlünzen, and Michael Bonitz*
Institut für Theoretische Physik und Astrophysik, Christian-Albrechts-Universität zu Kiel, D-24098 Kiel, Germany

(Received 2 March 2020; revised manuscript received 27 April 2020; accepted 29 April 2020; published 1 June 2020)

The time evolution in quantum many-body systems after external excitations is attracting high interest in many fields, including dense plasmas, correlated solids, laser-excited materials, or fermionic and bosonic atoms in optical lattices. The theoretical modeling of these processes is challenging, and the only rigorous quantum-dynamics approach that can treat correlated fermions in two and three dimensions is nonequilibrium Green functions (NEGF). However, NEGF simulations are computationally expensive due to their T^3 scaling with the simulation duration T. Recently, T^2 scaling was achieved with the generalized Kadanoff-Baym ansatz (GKBA), for the second-order Born (SOA) self energy, which has substantially extended the scope of NEGF simulations. In a recent Letter [Schlünzen *et al.*, Phys. Rev. Lett. **124**, 076601 (2020)]. we demonstrated that GKBA-NEGF simulations can be efficiently mapped onto coupled time-local equations for the single-particle and two-particle Green functions on the time diagonal, hence the method has been called the G1-G2 scheme. This allows one to perform the same simulations with order T^1 scaling, both for SOA and *GW* self energies giving rise to a dramatic speedup. Here we present more details on the G1-G2 scheme, including derivations of the basic equations including results for a general basis, for Hubbard systems, and for jellium. Also, we demonstrate how to incorporate initial correlations into the G1-G2 scheme. Further, the derivations are extended to a broader class of self energies, including the T matrix in the particle-particle and particle-hole channels and the dynamically-screened-ladder approximation. Finally, we demonstrate that, for all self energies, the CPU-time scaling of the G1-G2 scheme with the basis dimension N_b can be improved compared to our first report: The overhead compared to the original GKBA is not more than an additional factor N_b, even for Hubbard systems.

DOI: 10.1103/PhysRevB.101.245101

I. INTRODUCTION

Nonequibrium Green functions (NEGF) [1–3] have proven highly successful in simulations of the dynamics of correlated many-body systems. This is due to a number of attractive properties that include conservation laws and the existence of systematic approximation schemes that are based on Feynman diagrams. Moreover, NEGF allow for a rigorous derivation of quantum kinetic equations and for their systematic improvement; for recent overviews, see the text books [4–6].

While early computational applications focused on spatially homogeneous systems such as nuclear matter [7,8], optically excited semiconductors [4,9], and dense plasmas [10,11], during the last 15 years the scope of applications has substantially broadened. This includes the excitation and ionization dynamics of small atoms and molecules [12–14], the correlated-electron dynamics in the Hubbard model [15–17], the dynamics of fermionic atoms [18,19], and the stopping of ions in correlated materials [20–22]. This success was caused, among other things, by progress in the numerical solution of the basic equations of NEGF—the Keldysh-Kadanoff-Baym equations (KBE) [12,23–25]. Furthermore, improved time propagation and integration schemes led to an increase in efficiency and accuracy of the simulations [26,27]. Moreover, the implementation of more advanced self energies, such as the T-matrix self energy, further increased the accuracy and predictive capability; for a recent review, see Ref. [28]. In particular, very good agreement with cold-atom experiments [18] and with *ab initio* density-matrix-renormalization-group (DMRG) simulations were reported [27]. A particular advantage of NEGF simulation is that they are well capable to treat strong electronic correlations, in contrast to density-functional theory (DFT), and that they are neither restricted to 1D systems, such as DMRG, nor to short times, such as continuous-time quantum Monte Carlo [29].

The main disadvantage of NEGF is their high numerical effort. The majority of many-body methods, including time-dependent DFT (TDDFT), Boltzmann-type quantum kinetic equations, hydrodynamics or semiclassical molecular dynamic—and even the exact solution of the time-dependent Schrödinger equation—require a simulation time that grows linearly with the physical time. In contrast, for NEGF, the propagation in the two-time plane, together with the memory integration in the scattering contributions, gives rise to a N_t^3

*bonitz@theo-physik.uni-kiel.de

scaling, where N_t is the propagation time (number of time steps). A substantial acceleration is possible when the generalized Kadanoff-Baym ansatz (GKBA) is applied [30] which restricts the propagation to a time stepping along the time diagonal. If combined with Hartree-Fock propagators (HF-GKBA) [31–33] the CPU-time scaling can be reduced to N_t^2, which has given rise to a drastic increase of the number of HF-GKBA simulations in recent years, see, e.g., Refs. [17,27,34–38]. However, this improved scaling is achieved only for the simplest self energy—the second-Born approximation (SOA). If the HF-GKBA is applied to improved self energies, such as the T-matrix self energy [19,27], which is required for strongly correlated systems [18], or the GW self energy [28] which is required to capture dynamical-screening effects, the CPU-time scaling is again increased to N_t^3.

In a recent Letter we reported a breakthrough for NEGF simulations within the HF-GKBA scheme: We demonstrated that *time-linear scaling*, i.e., a CPU time that is of order N_t^1, can be achieved if the equations of motion are properly reformulated, without any approximations. The alternative approach solves the time-local equations for the time-diagonal single- and two-particle Green functions and was called the G1-G2 scheme [39]. While the equivalence of the HF-GKBA to time-local equations was pointed out before [5,40], a comparison of the numerical behavior of both approaches was performed only in Ref. [39]. There we reported N_t^1 scaling for SOA and GW self energies and any type of single-particle basis. The scaling was demonstrated for small Hubbard clusters which turned out to be the most unfavorable case because the CPU time of the G1-G2 scheme was found to grow by a factor N_b^2 faster than for the standard HF-GKBA approach, where N_b is the dimension of the single-particle basis.

In this paper we present extensive additional results for the G1-G2 scheme. First, we present all necessary details for the derivation of the equation of motion for the time-diagonal two-particle Green function. The results are derived for a general basis, for the Hubbard model, and for jellium. Second, we discuss how initial correlations can be incorporated. Third, we extend the analysis to other self energies: the T-matrix approximation in the particle-particle (TPP) and particle-hole (TPH) channels and the dynamically-screened-ladder (DSL) approximation. Fourth, numerical results are presented for all self-energy approximations which clearly confirm the N_t^1 scaling, not only asymptotically, but already for rather small simulation durations, $N_t \lesssim 30$. Finally, we re-evaluate the N_b dependence of the CPU time and report an additional optimization that reduces the overhead of the new scheme from N_b^2 to only N_b^1, for the Hubbard model, for all self energies.

This paper is organized as follows: In Sec. II we summarize the main required formulas of NEGF theory and the properties of the two-particle Green function. In Sec. III we present the basic formulas for the G1-G2 scheme, for the case of the SOA self energy—separately for a general basis, the Hubbard basis, and for jellium. The same analysis is then extended to GW and T-matrix self energies in Secs. IV and V and to the screened-ladder approximation in Sec. VI. Finally, the analysis of the scaling behavior with N_t and N_b for all self energies and numerical results are presented in Sec. VII.

II. THEORETICAL FRAMEWORK

A. Keldysh-Kadanoff-Baym equations and two-particle Green function

We consider a nonequilibrium quantum many-particle system with the generic Hamiltonian

$$\hat{H}(t) = \sum_{ij} h_{ij}^{(0)}(t)\hat{c}_i^\dagger \hat{c}_j + \frac{1}{2}\sum_{ijkl} w_{ijkl}(t)\hat{c}_i^\dagger \hat{c}_j^\dagger \hat{c}_l \hat{c}_k\,, \tag{1}$$

containing a single-particle contribution $h^{(0)}$ and a pair interaction w. Note the twofold time dependencies of the Hamiltonian. The time dependence of the single-particle contribution $h^{(0)}$ covers the interaction with external electromagnetic fields, lasers, or particle impact (stopping) [20], or the variation (quench) of a confinement potential [18,41]. While the interaction potential w is time independent in most cases, a time dependence has to be taken into account when modeling interactions quenches (e.g., in cold-atom experiments) or for the numerical preparation of a correlated initial state via "adiabatic switching," cf. Sec. III E. Thus, for the sake of generality of our derivations, we will retain the full time dependence throughout this paper.

The matrix elements of the Hamiltonian are computed with a complete orthonormal system of single-particle orbitals $|i\rangle$. The creation ($\hat{c}_i^\dagger$) and annihilation ($\hat{c}_i$) operators of particles in state $|i\rangle$ define the one-body nonequilibrium Green function (correlation function) for contour-time arguments z on the Keldysh contour $\mathcal{C}$ [28] (examples of the contour are shown in Fig. 1),

$$G_{ij}(z,z') = \frac{1}{i\hbar}\langle \mathcal{T}_\mathcal{C}\{\hat{c}_i(z)\hat{c}_j^\dagger(z')\}\rangle\,.$$

Here, $\mathcal{T}_\mathcal{C}$ is the time-ordering operator on the contour, and the averaging is performed with the correlated unperturbed density operator of the system. The equations of motion (EOMs) for the NEGF are the Keldysh-Kadanoff-Baym equations [43]

$$\sum_k \left[i\hbar\frac{d}{dz}\delta_{ik} - h_{ik}^{(0)}(z)\right]G_{kj}(z,z') = \delta_{ij}\delta_\mathcal{C}(z,z') \pm i\hbar\sum_{klp}\int_\mathcal{C} d\bar{z}\, w_{iklp}(z,\bar{z})G^{(2)}_{lpjk}(z,\bar{z},z',\bar{z}^+)\,, \tag{2}$$

$$\sum_k G_{ik}(z,z')\left[-i\hbar\frac{\overleftarrow{\mathrm{d}}}{dz'}\delta_{kj} - h_{kj}^{(0)}(z')\right] = \delta_{ij}\delta_\mathcal{C}(z,z') \pm i\hbar\sum_{klp}\int_\mathcal{C} d\bar{z}\, G^{(2)}_{iklp}(z,\bar{z}^-,z',\bar{z})w_{lpjk}(\bar{z},z')\,. \tag{3}$$

Here, the times $z^\pm := z \pm \epsilon$ differ from z by an infinitesimally small positive constant ϵ to avoid ambiguities in the time ordering of field-operator products. Furthermore, a two-time version of the interaction potential is introduced using the delta function on the Keldysh contour, $w_{ijkl}(z,z') = \delta_\mathcal{C}(z,z')w_{ijkl}(z)$, see, e.g., Refs. [6,19,28]. The KBE couple to the two-particle Green function (terms on the

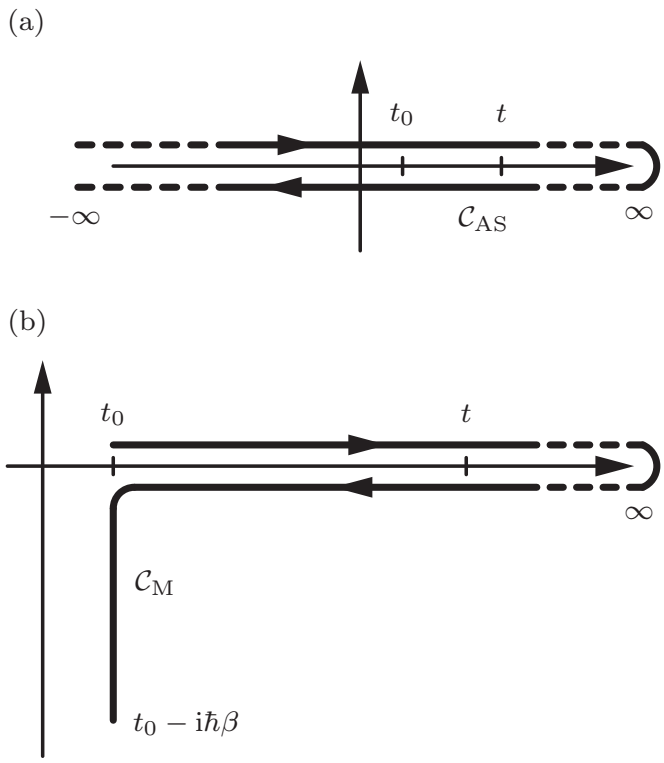

FIG. 1. Two examples of the Keldysh "round-trip" time contour that are used in NEGF theory to treat initial correlations, see, e.g., Ref. [2]. (a) Contour $\mathcal{C}_{\rm AS}$ containing an initial real-time interval (from $-\infty$ to t_0) to adiabatically "switch on" the pair interaction, starting from an uncorrelated state. (b) Contour $\mathcal{C}_{\rm M}$ with an imaginary branch allowing us to include thermodynamic-equilibrium correlations via Green functions which have one time argument on the real branch and one on the imaginary branch [33,42].

r.h.s.) which is defined by

$$G^{(2)}_{ijkl}(z_1,z_2,z_3,z_4) = \frac{1}{(i\hbar)^2}\langle \mathcal{T}_{\mathcal{C}}\{\hat{c}_i(z_1)\hat{c}_j(z_2)\hat{c}^\dagger_l(z_4)\hat{c}^\dagger_k(z_3)\}\rangle$$

and contains a mean-field (Hartree-Fock) and a correlation contribution

$$G^{(2)}_{ijkl}(z_1,z_2,z_3,z_4) = G^{(2),\rm H}_{ijkl}(z_1,z_2,z_3,z_4) \pm G^{(2),\rm F}_{ijkl}(z_1,z_2,z_3,z_4) + G^{(2),\rm corr}_{ijkl}(z_1,z_2,z_3,z_4)\,. \tag{4}$$

The Eqs. (2) and (3) for the one-particle NEGF are formulated on the Keldysh contour, cf. Fig. 1. They are equivalent to equations for Keldysh Green function matrices of real-time arguments where the matrix components differ by the location of the time arguments on the contour; for details see the text books [6,33]. Our G1-G2 scheme involves the special case of two-particle functions that depend either on one or two times and their real-time components that we define as follows:

$$\begin{aligned}
\mathcal{G}^{\rm H}_{ijkl}(z,z') &:= G^{(2),\rm H}_{ijkl}(z,z,z',z') = G_{ik}(z,z')G_{jl}(z,z')\,,\\
\mathcal{G}^{\rm F}_{ijkl}(z,z') &:= G^{(2),\rm F}_{ijkl}(z,z',z,z') = G_{il}(z,z')G_{jk}(z',z)\,,\\
\mathcal{G}^{\rm corr}_{ijkl}(z,z') &:= G^{(2),\rm corr}_{ijkl}(z,z,z',z^+)\,,\\
\mathcal{G}^{{\rm H},\gtrless}_{ijkl}(t,t') &:= G^{\gtrless}_{ik}(t,t')G^{\gtrless}_{jl}(t,t')\,,\\
\mathcal{G}^{{\rm F},\gtrless}_{ijkl}(t,t') &:= G^{\gtrless}_{il}(t,t')G^{\lessgtr}_{jk}(t',t)\,,\\
\mathcal{G}^{{\rm H},\gtrless}_{ijkl}(t) &:= \mathcal{G}^{{\rm H},\gtrless}_{ijkl}(t,t)\,,\\
\mathcal{G}^{{\rm F},\gtrless}_{ijkl}(t) &:= \mathcal{G}^{{\rm F},\gtrless}_{ijkl}(t,t)\,,\\
\mathcal{G}_{ijkl}(t) &:= \mathcal{G}^{{\rm corr},<}_{ijkl}(t,t)\,.
\end{aligned} \tag{5}$$

The time-diagonal two-particle Green function $\mathcal{G}(t)$, defined by Eq. (5), is the central quantity of the G1-G2 scheme. In general, and for all self-energy approximations considered in this work, it obeys the following (pair-) exchange symmetries,

$$\mathcal{G}_{ijkl}(t) = \mathcal{G}_{jilk}(t)\,, \tag{6}$$

$$\mathcal{G}_{ijkl}(t) = [\mathcal{G}_{klij}(t)]^*\,. \tag{7}$$

B. Time-diagonal KBE

In the following we are interested in the dynamics of the real-time components $G^{\gtrless}(t,t')$ and, in particular, the properties of $G^{\gtrless}_{ij}(t) := G^{\gtrless}_{ij}(t,t)$ on the real-time diagonal. The EOM for $G^<(t)$ has the form [19,44]

$$i\hbar\frac{d}{dt}G^<_{ij}(t) - [h^{\rm HF}, G^<]_{ij}(t) = [I + I^\dagger]_{ij}(t)\,, \tag{8}$$

$$I(t) = \mathcal{I}(t) + \mathcal{I}^{\rm IC}(t)\,, \tag{9}$$

where I is the collision integral of the kinetic equation that, in general, consists of the dynamical collision integral $\mathcal{I}$ and the initial-correlation contribution $\mathcal{I}^{\rm IC}$ which includes pair correlations existing in the system at the initial time $t = t_0$. In NEGF theory initial correlations can be described [6,21], e.g., by including contributions from the imaginary track of the Keldysh contour (lower part of Fig. 1) or via building up initial correlations dynamically via a prior dynamics that starts from an uncorrelated state ("adiabatic switching," upper part of Fig. 1). We will discuss this issue more in detail below, in Sec. III E where we also show how initial correlations are taken into account in the G1-G2 scheme. For now we focus on the first collision integral, i.e., $I(t) = \mathcal{I}(t)$, assuming that the system is prepared in an uncorrelated (ideal) initial state at time t_0. In that case the buildup of dynamical correlations is described by

$$\begin{aligned}
I_{ij}(t) &= \pm i\hbar\sum_{klp} w_{iklp}(t)\mathcal{G}_{lpjk}(t)\\
&= \sum_k \int_{t_0}^t d\bar{t}\,[\Sigma^>_{ik}(t,\bar{t})G^<_{kj}(\bar{t},t) - \Sigma^<_{ik}(t,\bar{t})G^>_{kj}(\bar{t},t)]\,.
\end{aligned} \tag{10}$$

Here, the first line follows directly from the r.h.s. of Eqs. (2) and (3), where the time integral has been taken with the help of the delta function in the two-time potential. In the second line the two-particle Green function has been eliminated by introducing the correlation self-energy functions $\Sigma^{\gtrless}$ [the notion "correlation self energy" means that the Hartree-Fock self-energy contributions have been subtracted from $\Sigma^{\gtrless}$; they are included in the Hamiltonian $h^{\rm HF}$ on the l.h.s., cf. Eq. (12)]—which is the standard approach in the NEGF framework. The self energy is the only unknown function in the theory. If it was known exactly, the description of the dynamics would be

exact. This is, of course, not the case in most situations and, thus, approximations are required. In the following sections we will consider several key approximations that are currently broadly used in various fields of many-body physics. Note that for the approximations studied in this paper, the self energies $\Sigma^{\gtrless}(t,t')$ are nonsingular functions. This means, the collision integral $I_{ij}(t)$ in Eq. (10) vanishes for $t \to t_0$.

Before we start the analysis with the second-order Born approximation for the self energy, in Sec. III, we summarize a few important properties of Eq. (8). First, on the time diagonal the less component of the NEGF can be written as

$$G^{<}_{ij}(t) = G^{>}_{ij}(t) - \frac{1}{i\hbar}\delta_{ij} = \pm\frac{1}{i\hbar}n_{ij}(t)\,, \tag{11}$$

where n_{ij} is the single-particle density matrix. Further, as was noted above, in Eq. (8) the mean-field part of the two-particle Green function, cf. Eq. (4) (or, equivalently, the self energy), is included in an effective single-particle Hartree-Fock Hamiltonian which is defined as [28]

$$h^{\mathrm{HF}}_{ij}(t) = h^{(0)}_{ij}(t) \pm i\hbar\sum_{kl} w^{\pm}_{ikjl}(t)G^{<}_{lk}(t,t)\,, \tag{12}$$

where we introduced the (anti-)symmetrized interaction potential which we define via its four-dimensional matrix with respect to the single-particle basis

$$w^{\pm}_{ijkl}(t) := w_{ijkl}(t) \pm w_{ijlk}(t)\,.$$

The interaction tensor obeys the same symmetries as $\mathcal{G}(t)$ [cf. Eqs. (6) and (7)]:

$$w_{ijkl}(t) = w_{jilk}(t)\,, \tag{13}$$

$$w_{ijkl}(t) = [w_{klij}(t)]^*\,, \tag{14}$$

which also leads to

$$w^{\pm}_{ijkl}(t) = \pm w^{\pm}_{ijlk}(t)\,.$$

III. SECOND-ORDER BORN SELF ENERGY

In the following we introduce the G1-G2 scheme for the simplest case of choosing the self energy in the second-Born approximation [19],

$$\Sigma^{\gtrless}_{ij}(t,t') = \pm(i\hbar)^2\sum_{klpqrs} w_{iklp}(t)w^{\pm}_{qrjs}(t') \times G^{\gtrless}_{lq}(t,t')G^{\gtrless}_{pr}(t,t')G^{\lessgtr}_{sk}(t',t)\,.$$

With that, the collision integral of the time-diagonal equation (10) transforms into:

$$\begin{aligned} I_{ij}(t) &= \pm(i\hbar)^2\sum_{klpqrsu} w_{iklp}(t)\int_{t_0}^{t} d\bar{t}\, w^{\pm}_{qrsu}(\bar{t}) \\ &\times [G^{>}_{lq}(t,\bar{t})G^{>}_{pr}(t,\bar{t})G^{<}_{uk}(\bar{t},t)G^{<}_{sj}(\bar{t},t) \\ &- G^{<}_{lq}(t,\bar{t})G^{<}_{pr}(t,\bar{t})G^{>}_{uk}(\bar{t},t)G^{>}_{sj}(\bar{t},t)] \\ &= \pm(i\hbar)^2\sum_{klpqrsu} w_{iklp}(t)\int_{t_0}^{t} d\bar{t}\, w^{\pm}_{qrsu}(\bar{t}) \\ &\times \left[\mathcal{G}^{\mathrm{H},>}_{lpqr}(t,\bar{t})\mathcal{G}^{\mathrm{H},<}_{sujk}(\bar{t},t) - \mathcal{G}^{\mathrm{H},<}_{lpqr}(t,\bar{t})\mathcal{G}^{\mathrm{H},>}_{sujk}(\bar{t},t)\right] \\ &= \pm(i\hbar)^2\sum_{klpqrsu} w_{iklp}(t)\int_{t_0}^{t} d\bar{t}\, w^{\pm}_{qrsu}(\bar{t}) \\ &\times \left[\mathcal{G}^{\mathrm{F},>}_{ljqs}(t,\bar{t})\mathcal{G}^{\mathrm{F},<}_{urkp}(\bar{t},t) - \mathcal{G}^{\mathrm{F},<}_{ljqs}(t,\bar{t})\mathcal{G}^{\mathrm{F},>}_{urkp}(\bar{t},t)\right], \end{aligned}$$

where we presented several equivalent formulations that will be used below. At this point, it is possible to identify $\mathcal{G}$ [cf. Eq. (10)] in SOA,

$$\mathcal{G}_{ijkl}(t) = i\hbar\sum_{pqrs}\int_{t_0}^{t} d\bar{t}\, w^{\pm}_{pqrs}(\bar{t}) \times \left[\mathcal{G}^{\mathrm{H},>}_{ijpq}(t,\bar{t})\mathcal{G}^{\mathrm{H},<}_{rskl}(\bar{t},t) - \mathcal{G}^{\mathrm{H},<}_{ijpq}(t,\bar{t})\mathcal{G}^{\mathrm{H},>}_{rskl}(\bar{t},t)\right]. \tag{15}$$

A. $\mathcal{G}$ within the GKBA

The G1-G2 scheme is a reformulation of the ordinary solution of the time-diagonal KBE in the HF-GKBA. When applying the GKBA the time-off-diagonal elements of the less and greater NEGF are reconstructed from the time-diagonal value via [19]

$$G^{\gtrless}_{ij}(t,t') = i\hbar\sum_{k}\left[G^{\mathrm{R}}_{ik}(t,t')G^{\gtrless}_{kj}(t') - G^{\gtrless}_{ik}(t)G^{\mathrm{A}}_{kj}(t,t')\right], \tag{16}$$

with the retarded and advanced Green functions that are defined by

$$\begin{aligned} G^{\mathrm{R}}_{ij}(t,t') &= \Theta(t-t')[G^{>}_{ij}(t,t') - G^{<}_{ij}(t,t')]\,, \\ G^{\mathrm{A}}_{ij}(t,t') &= -\Theta(t'-t)[G^{>}_{ij}(t,t') - G^{<}_{ij}(t,t')]\,, \end{aligned}$$

where $G^{\mathrm{R}}(t,t')$ $[G^{\mathrm{A}}(t,t')]$ is nonzero only for $t \geqslant t'$ $(t \leqslant t')$. We now show that, in the reconstruction expression (16), the individual functions $G^{\mathrm{R/A}}$ can be eliminated in favor of their difference

$$\mathcal{U}_{ij}(t,t') = G^{\mathrm{R}}_{ij}(t,t') - G^{\mathrm{A}}_{ij}(t,t')\,. \tag{17}$$

In the case of the HF-GKBA the propagator $\mathcal{U}(t,t')$ has the properties of a time-evolution operator, as is shown in Appendix A. It possesses the group property [Eq. (A4)] and obeys a Schrödinger equation, cf. Eqs. (A6) and (A7), with the initial value

$$\mathcal{U}_{ij}(t,t) = G^{\mathrm{R}}_{ij}(t,t) - G^{\mathrm{A}}_{ij}(t,t) = G^{>}_{ij}(t) - G^{<}_{ij}(t) = \frac{1}{i\hbar}\delta_{ij}\,. \tag{18}$$

We now demonstrate the appearance of $\mathcal{U}$ by rewriting Eq. (16) separately, for $t = t'$ and $t > t'$,

$$\begin{aligned} G^{\gtrless}_{ij}(t'=t) &= i\hbar\sum_{k}\Big[\underbrace{G^{\mathrm{R}}_{ik}(t,t)G^{\gtrless}_{kj}(t)}_{=G^{\gtrless}_{ik}(t)G^{\mathrm{R}}_{kj}(t,t)} - G^{\gtrless}_{ik}(t)G^{\mathrm{A}}_{kj}(t,t)\Big] \\ &= i\hbar\sum_{k} G^{\gtrless}_{ik}(t)\Big[G^{\mathrm{R}}_{kj}(t,t) - G^{\mathrm{A}}_{kj}(t,t)\Big]\,, \\ G^{\gtrless}_{ij}(t'<t) &= -i\hbar\sum_{k} G^{\gtrless}_{ik}(t')G^{\mathrm{A}}_{kj}(t',t) \\ &= i\hbar\sum_{k} G^{\gtrless}_{ik}(t')\Big[\underbrace{G^{\mathrm{R}}_{kj}(t',t)}_{=0} - G^{\mathrm{A}}_{kj}(t',t)\Big]\,. \end{aligned}$$

Similar relations can be found for $t \leqslant t'$. These results can be combined to an alternative form of the GKBA

$$G^{\gtrless}_{ij}(t' \leqslant t) = i\hbar \sum_k G^{\gtrless}_{ik}(t')\mathcal{U}_{kj}(t', t)\,, \tag{19}$$

$$G^{\gtrless}_{ij}(t \geqslant t') = i\hbar \sum_k \mathcal{U}_{ik}(t, t')G^{\gtrless}_{kj}(t')\,. \tag{20}$$

Using the results of Eqs. (19) and (20), for the Green functions [taking into account that in the collision integral only $G^{>}(t \geqslant \bar{t})$ and $G^{<}(\bar{t} \leqslant t)$ appear], we reformulate Eq. (15) for the two-particle Green function on the time diagonal (cf. Appendix A 1)

$$\mathcal{G}_{ijkl}(t) = i\hbar \sum_{pqrsuvxy} \int_{t_0}^{t} d\bar{t}\, w^{\pm}_{pqrs}(\bar{t}) \times \mathcal{U}^{(2)}_{ijuv}(t, \bar{t})\Phi^{uvrs}_{pqxy}(\bar{t})\mathcal{U}^{(2)}_{xykl}(\bar{t}, t)\,,$$

where we introduced short notations for the two-particle propagator $\mathcal{U}^{(2)}$ and define the occupation factors $\Phi^{\gtrless}$,

$$\mathcal{U}^{(2)}_{ijkl}(t, t') = \mathcal{U}_{ik}(t, t')\mathcal{U}_{jl}(t, t') = \mathcal{U}^{(2)}_{jilk}(t, t'), \tag{21}$$

$$\Phi^{ijkl}_{pqrs}(t) = \Phi^{ijkl,>}_{pqrs}(t) - \Phi^{ijkl,<}_{pqrs}(t)\,,$$

$$\Phi^{ijkl,\gtrless}_{pqrs}(t) = (i\hbar)^4 \mathcal{G}^{\mathrm{H},\gtrless}_{ijpq}(t)\mathcal{G}^{\mathrm{H},\lessgtr}_{klrs}(t) = (i\hbar)^4 \mathcal{G}^{\mathrm{F},\gtrless}_{ikrp}(t)\mathcal{G}^{\mathrm{F},\gtrless}_{jlsq}(t) = (i\hbar)^4 \mathcal{G}^{\mathrm{F},\gtrless}_{ilsp}(t)\mathcal{G}^{\mathrm{F},\lessgtr}_{kjqr}(t)\,.$$

A more compact and intuitive notation can be achieved by introducing the two-particle source term

$$\Psi^{\pm}_{ijkl}(t) = \frac{1}{(i\hbar)^2} \sum_{pqrs} w^{\pm}_{pqrs}(t)\Phi^{ijrs}_{pqkl}(t)\,,$$

which results in

$$\mathcal{G}_{ijkl}(t) = (i\hbar)^3 \sum_{pqrs} \int_{t_0}^{t} d\bar{t}\, \mathcal{U}^{(2)}_{ijpq}(t, \bar{t})\Psi^{\pm}_{pqrs}(\bar{t})\mathcal{U}^{(2)}_{rskl}(\bar{t}, t) \tag{22}$$

and allows for a straightforward interpretation: Pair correlations $\mathcal{G}_{ijkl}$ existing in the system at time t are due to pair correlations existing at all times $\bar{t}$ with $t_0 \leqslant \bar{t} \leqslant t$ that are time evolved with the propagators $\mathcal{U}^{(2)}$. The function $\Psi^{\pm}$ has the meaning of pair correlations produced in the system via two-particle scattering per unit time. The appearance of two propagators indicates that $\mathcal{G}_{ijkl}(t)$ does not obey a Schrödinger-type equation but a commutator equation, that we will derive below, in Sec. III B. There we will also show that the time integral in Eq. (22) can be eliminated.

B. Time-linear differential solution for $\mathcal{G}$: SOA-G1-G2 equations for a general basis

There are two ways to transform Eq. (22) into a scheme that scales linearly with propagation time. The first is based on the integral representation for $\mathcal{G}$ while the second uses, instead, coupled time-local differential equations for $G^{<}(t)$ and $\mathcal{G}(t)$. Here and throughout this paper we will concentrate on the second approach as it turns out to be more efficient. The first approach is discussed, for completeness, in Appendix B.

In the following we first derive the differential equation scheme (G1-G2 scheme) for a general single-particle basis that corresponds to the generic Hamiltonian defined in Eq. (1), where spin degrees of freedom are included in the basis index. Below we will separately consider the special cases of a Hubbard basis and the jellium model for electrons where the two spin projections will be indicated explicitly. In order to find the differential equation for $\mathcal{G}$, the EOMs for the retarded/advanced Green functions in HF-GKBA along both time directions are repeated [19]:

$$i\hbar \frac{d}{dt} G^{\mathrm{R/A}}_{ij}(t, t') = \sum_k h^{\mathrm{HF}}_{ik}(t)G^{\mathrm{R/A}}_{kj}(t, t') + \delta_{ij}\delta(t, t')$$

$$i\hbar \frac{d}{dt} G^{\mathrm{R/A}}_{ij}(t', t) = -\sum_k G^{\mathrm{R/A}}_{ik}(t', t)h^{\mathrm{HF}}_{kj}(t) - \delta_{ij}\delta(t, t')\,. \tag{23}$$

For the two-particle propagators similar Schrödinger-type EOMs hold as shown in Appendix A 3,

$$\frac{d}{dt}\mathcal{U}^{(2)}_{ijkl}(t, t') = \frac{1}{i\hbar} \sum_{pq} h^{(2),\mathrm{HF}}_{ijpq}(t)\mathcal{U}^{(2)}_{pqkl}(t, t')\,, \tag{24}$$

$$\frac{d}{dt}\mathcal{U}^{(2)}_{ijkl}(t', t) = -\frac{1}{i\hbar} \sum_{pq} \mathcal{U}^{(2)}_{ijpq}(t', t)h^{(2),\mathrm{HF}}_{pqkl}(t)\,, \tag{25}$$

where we define the two-particle Hartree-Fock Hamiltonian as the sum of two single-particle parts:

$$h^{(2),\mathrm{HF}}_{ijkl}(t) = \delta_{jl}h^{\mathrm{HF}}_{ik}(t) + \delta_{ik}h^{\mathrm{HF}}_{jl}(t)\,. \tag{26}$$

With that we now compute the time derivative of the time-diagonal two-particle Green function within the HF-GKBA (22), $\mathcal{G}$, which contains two parts,

$$\frac{d}{dt}\mathcal{G}_{ijkl}(t) = \left[\frac{d}{dt}\mathcal{G}_{ijkl}(t)\right]_{\int} + \left[\frac{d}{dt}\mathcal{G}_{ijkl}(t)\right]_{\mathcal{U}^{(2)}}\,.$$

The first contribution ($\int$) originates from the integration boundaries,

$$\left[\frac{d}{dt}\mathcal{G}_{ijkl}(t)\right]_{\int} = (i\hbar)^3 \sum_{pqrs} \mathcal{U}^{(2)}_{ijpq}(t, t)\Psi^{\pm}_{pqrs}(t)\mathcal{U}^{(2)}_{rskl}(t, t) = \frac{1}{i\hbar}\Psi^{\pm}_{ijkl}(t)\,, \tag{27}$$

where the latter equation holds due to the identity [cf. Eqs. (18) and (21)]

$$\mathcal{U}^{(2)}_{ijkl}(t, t) = \frac{1}{(i\hbar)^2}\delta_{ik}\delta_{jl}\,.$$

The second contribution to the derivative results from the time dependence of the integrand, i.e., of $\mathcal{U}^{(2)}$,

$$\left[\frac{d}{dt}\mathcal{G}_{ijkl}(t)\right]_{\mathcal{U}^{(2)}} = (i\hbar)^3 \sum_{pqrs} \int_{t_0}^{t} d\bar{t}\, \Psi^{\pm}_{pqrs}(\bar{t}) \times \left\{\left[\frac{d}{dt}\mathcal{U}^{(2)}_{ijpq}(t, \bar{t})\right]\mathcal{U}^{(2)}_{rskl}(\bar{t}, t) + \mathcal{U}^{(2)}_{ijpq}(t, \bar{t})\left[\frac{d}{dt}\mathcal{U}^{(2)}_{rskl}(\bar{t}, t)\right]\right\},$$

and, using the results from Eqs. (24) and (25), we obtain

$$\left[\frac{d}{dt}\mathcal{G}_{ijkl}(t)\right]_{\mathcal{U}^{(2)}} = (i\hbar)^3 \sum_{pqrs}\int_{t_0}^{t} d\bar{t} \times \left\{\left[\frac{1}{i\hbar}\sum_{uv} h^{(2),\mathrm{HF}}_{ijuv}(t)\mathcal{U}^{(2)}_{uvpq}(t,\bar{t})\right]\Psi^{\pm}_{pqrs}(\bar{t})\mathcal{U}^{(2)}_{rskl}(\bar{t},t) + \mathcal{U}^{(2)}_{ijpq}(t,\bar{t})\Psi^{\pm}_{pqrs}(\bar{t})\left[-\frac{1}{i\hbar}\sum_{uv}\mathcal{U}^{(2)}_{rsuv}(\bar{t},t)h^{(2),\mathrm{HF}}_{uvkl}(t)\right]\right\},$$

where we identify $\mathcal{G}$ again, to get

$$\left[\frac{d}{dt}\mathcal{G}_{ijkl}(t)\right]_{\mathcal{U}^{(2)}} = \frac{1}{i\hbar}\sum_{pq} h^{(2),\mathrm{HF}}_{ijpq}(t)\,\mathcal{G}_{pqkl}(t) - \frac{1}{i\hbar}\sum_{lf}\mathcal{G}_{ijpq}(t)\,h^{(2),\mathrm{HF}}_{pqkl}(t)\,. \tag{28}$$

With that, the full derivative of the time-diagonal two-particle Green function is obtained by adding up the results of Eqs. (27) and (28) [45]

$$i\hbar\frac{d}{dt}\mathcal{G}_{ijkl}(t) - \left[h^{(2),\mathrm{HF}},\mathcal{G}\right]_{ijkl}(t) = \Psi^{\pm}_{ijkl}(t)\,. \tag{29}$$

We now summarize the equations of the G1-G2 scheme for the second-order Born self energy, for a general basis. The scheme consists of the equation for the time-diagonal element of the single-particle Green function, cf. Eq. (8),

$$i\hbar\frac{d}{dt}G^{<}_{ij}(t) = [h^{\mathrm{HF}},G^{<}]_{ij}(t) + [I+I^{\dagger}]_{ij}(t)\,, \tag{30}$$

$$I_{ij}(t) = \pm i\hbar\sum_{klp} w_{iklp}(t)\mathcal{G}_{lpjk}(t)\,, \tag{31}$$

coupled to Eq. (29)—the EOM of the time-diagonal element of the two-particle Green function. Equations (29), (30), and (31) constitute a closed system of time-local differential equations, for which the computational effort for a numerical implementation scales linearly with time. This was achieved by eliminating the non-Markovian (memory) structure of the collision integral. All transformations so far introduce no further approximations resulting in an exact reformulation of the standard HF-GKBA, as was demonstrated in Ref. [39]. The linear scaling with N_t, as opposed to the quadratic scaling of the standard HF-GKBA in SOA, is the basis for a potentially dramatic speedup of NEGF simulations. The price to pay is the need to compute the entire matrix of the time-diagonal two-particle Green function, the effort for which only depends on the basis dimension N_b. This will be analyzed in detail in Sec. VII.

In a similar manner as for the SOA self energy, a time-local equation for $\mathcal{G}$ corresponding to more advanced self energies can be derived for which the speedup of the G1-G2 scheme is even larger. This will be demonstrated in the subsequent sections. But before that, we consider the G1-G2 scheme in SOA for two important special cases of basis sets—the Hubbard basis and the spatially uniform jellium model (plane-wave basis).

C. SOA-G1-G2 equations for the Hubbard model

The Hubbard model [46] is among the fundamental models in condensed-matter physics, in particular, for the analysis of strong electronic correlations. More recently it has been widely used to study the behavior of fermionic and bosonic atoms in optical lattices [47] and, in particular, time-dependent correlation phenomena, see, e.g, Refs. [16,17,41,48]. For the Fermi-Hubbard model, the general pair-interaction matrix element becomes ($\bar{\delta}_{\alpha\beta} := 1-\delta_{\alpha\beta}$)

$$w^{\alpha\beta\gamma\delta}_{ijkl}(t) = U(t)\delta_{ij}\delta_{ik}\delta_{il}\delta_{\alpha\gamma}\delta_{\beta\delta}\bar{\delta}_{\alpha\beta}\,, \tag{32}$$

with the on-site interaction U and the spin projection labeled by greek indices. Recall that we allow for a time dependence of the interaction to capture the adiabatic-switching protocol of initial correlations (see Sec. III E) as well as nonequilibrium processes such as an interaction quench, cf. the discussion of Eq. (1) above. The kinetic-energy matrix is replaced by a hopping Hamiltonian,

$$h^{(0)}_{ij} = -\delta_{\langle i,j\rangle}J\,,$$

which includes hopping processes between nearest-neighbor sites $\langle i,j\rangle$ with amplitude J. Thus, the total Hamiltonian is given by

$$\hat{H}(t) = -J\sum_{\langle i,j\rangle}\sum_{\alpha}\hat{c}^{\dagger}_{i\alpha}\hat{c}_{j\alpha} + U(t)\sum_{i}\hat{n}^{\uparrow}_{i}\hat{n}^{\downarrow}_{i}\,. \tag{33}$$

Extensions to more complicated models, going beyond the nearest-neighbor single-band case are straightforward but will not be considered here.

The time-diagonal EOM for the single-particle Green function, Eq. (8), takes the following form (from here we give all Hubbard equations for the spin-up component; the spin-down equations follow from the replacement $\uparrow \leftrightarrow \downarrow$.)

$$i\hbar\frac{d}{dt}G^{<,\uparrow}_{ij}(t) = [h^{\mathrm{HF},\uparrow},G^{<,\uparrow}]_{ij}(t) + [I+I^{\dagger}]^{\uparrow}_{ij}(t)\,, \tag{34}$$

$$I^{\uparrow}_{ij}(t) = -i\hbar U(t)\mathcal{G}^{\uparrow\downarrow\uparrow\downarrow}_{iiji}(t)\,, \tag{35}$$

where for electrons there exist two collision integrals, $I^{\uparrow}$ and $I^{\downarrow}$, that enter the single-particle EOMs. The Hartree-Fock Hamiltonian in Eq. (34) in the Hubbard basis becomes [cf. Eq. (12)]:

$$h^{\mathrm{HF},\uparrow}_{ij}(t) = h^{(0)}_{ij} - i\hbar\delta_{ij}U(t)G^{<,\downarrow}_{ii}(t)\,.$$

The equation for the time-diagonal two-particle Green function, Eq. (29), now reads

$$i\hbar\frac{d}{dt}\mathcal{G}^{\uparrow\downarrow\uparrow\downarrow}_{ijkl}(t) - \left[h^{(2),\mathrm{HF}}_{\uparrow\downarrow},\mathcal{G}^{\uparrow\downarrow\uparrow\downarrow}\right]_{ijkl}(t) = \frac{1}{(i\hbar)^2}U(t)\,\Phi^{\uparrow\downarrow\uparrow\downarrow}_{ijkl}(t) =: \Psi^{\uparrow\downarrow\uparrow\downarrow}_{ijkl}(t)\,, \tag{36}$$

where

$$h^{(2),\mathrm{HF}}_{ijkl,\uparrow\downarrow}(t) = \delta_{jl}h^{\mathrm{HF},\uparrow}_{ik}(t) + \delta_{ik}h^{\mathrm{HF},\downarrow}_{jl}(t)\,, \tag{37}$$

and

$$\Phi^{\uparrow\downarrow\uparrow\downarrow}_{ijkl}(t) := (i\hbar)^4 \sum_p \big[G^{>,\uparrow}_{ip}(t)G^{>,\downarrow}_{jp}(t)G^{<,\uparrow}_{pk}(t)G^{<,\downarrow}_{pl}(t) - G^{<,\uparrow}_{ip}(t)G^{<,\downarrow}_{jp}(t)G^{>,\uparrow}_{pk}(t)G^{>,\downarrow}_{pl}(t)\big]. \quad (38)$$

The Eqs. (34) and (36) together with their spin-down counterparts form a coupled system of four equations. For SOA, no further spin combinations of $\mathcal{G}$ contribute. Numerical examples will be presented in Sec. VII.

D. SOA-G1-G2 equations for jellium

As the second example we consider the jellium Hamiltonian [49],

$$\hat{H}(t) = \sum_{p\alpha} \frac{\boldsymbol{p}^2}{2m} \hat{c}^\dagger_{p\alpha}\hat{c}_{p\alpha} + \sum_{pp'q\alpha\beta} v_{|q|}(t)\hat{c}^\dagger_{p+q\alpha}\hat{c}^\dagger_{p'-q\beta}\hat{c}_{p'\beta}\hat{c}_{p\alpha}\,, \quad (39)$$

with the vector-sized momenta $\boldsymbol{p}, \boldsymbol{p}', \boldsymbol{q}$ and the Coulomb matrix element $v_{|q|} = \frac{4\pi e^2}{|q|^2}$ [we again allow for a time-dependent pair interaction to also describe adiabatic-switching processes, cf. the discussion of Eq. (1) above]. This model is of relevance for the electron gas in metals [50,51], for electron-hole plasmas in semiconductors [4], and for dense quantum plasmas, e.g., Refs. [5,10], as well as for model development [49,51]. The matrix element of the pair interaction in a plane-wave basis is

$$w^{\alpha\beta\gamma\delta}_{\boldsymbol{k_1}\boldsymbol{k_2}\boldsymbol{k_3}\boldsymbol{k_4}}(t) = \delta_{\alpha\gamma}\delta_{\beta\delta}\delta(\boldsymbol{k_1}+\boldsymbol{k_2}-\boldsymbol{k_3}-\boldsymbol{k_4})v_{|\boldsymbol{k_1}-\boldsymbol{k_3}|}(t)\,, \quad (40)$$

where v_q denotes the spatial Fourier transform of the pair potential, and the delta function arises from momentum conservation (spatial homogeneity).

The EOM for the single-particle Green function, Eq. (8), is now

$$i\hbar\frac{d}{dt}G^{<,\alpha}_{\boldsymbol{p}}(t) = [I + I^\dagger]^\alpha_{\boldsymbol{p}}(t)\,, \quad (41)$$

with

$$I^\alpha_{\boldsymbol{p}}(t) = \pm i\hbar \sum_{\bar{\boldsymbol{p}}.\boldsymbol{q}} \sum_\beta v_{|\boldsymbol{q}|}(t)\mathcal{G}^{\alpha\beta}_{\boldsymbol{p}\bar{\boldsymbol{p}}\boldsymbol{q}}(t)\,,$$

where we defined

$$\mathcal{G}^{\alpha\beta}_{\boldsymbol{p},\bar{\boldsymbol{p}}.\boldsymbol{q}}(t) := \mathcal{G}^{\alpha\beta\alpha\beta}_{\boldsymbol{p}-\boldsymbol{q},\bar{\boldsymbol{p}}+\boldsymbol{q},\boldsymbol{p},\bar{\boldsymbol{p}}}(t)\,, \quad (42)$$

and the equation for the time-diagonal two-particle Green function becomes

$$\begin{aligned} &i\hbar\frac{d}{dt}\mathcal{G}^{\alpha\beta}_{\boldsymbol{p}\bar{\boldsymbol{p}}\boldsymbol{q}}(t) - \mathcal{G}^{\alpha\beta}_{\boldsymbol{p}\bar{\boldsymbol{p}}\boldsymbol{q}}(t)\big(h^{\mathrm{HF},\alpha}_{\boldsymbol{p}-\boldsymbol{q}} + h^{\mathrm{HF},\beta}_{\bar{\boldsymbol{p}}+\boldsymbol{q}} - h^{\mathrm{HF},\alpha}_{\boldsymbol{p}} - h^{\mathrm{HF},\beta}_{\bar{\boldsymbol{p}}}\big)(t) \\ &= \frac{1}{(i\hbar)^2}\big[v_{|\boldsymbol{q}|}(t) \pm \delta_{\alpha\beta}v_{|\boldsymbol{p}-\boldsymbol{q}-\bar{\boldsymbol{p}}|}(t)\big]\Phi^{\alpha\beta}_{\boldsymbol{p}\bar{\boldsymbol{p}}\boldsymbol{q}}(t) \\ &=: \Psi^{\pm,\alpha\beta}_{\boldsymbol{p}\bar{\boldsymbol{p}}\boldsymbol{q}}(t)\,, \end{aligned} \quad (43)$$

where

$$h^{\mathrm{HF},\alpha}_{\boldsymbol{p}}(t) = \frac{\boldsymbol{p}^2}{2m} + i\hbar\sum_{\bar{\boldsymbol{p}}} v_{|\boldsymbol{p}-\bar{\boldsymbol{p}}|}(t)G^{<,\alpha}_{\bar{\boldsymbol{p}}}(t)\,,$$

and

$$\Phi^{\alpha\beta}_{\boldsymbol{p}\bar{\boldsymbol{p}}\boldsymbol{q}}(t) = (i\hbar)^4\big[G^{>,\alpha}_{\boldsymbol{p}-\boldsymbol{q}}(t)G^{>,\beta}_{\bar{\boldsymbol{p}}+\boldsymbol{q}}(t)G^{<,\alpha}_{\boldsymbol{p}}(t)G^{<,\beta}_{\bar{\boldsymbol{p}}}(t) - G^{<,\alpha}_{\boldsymbol{p}-\boldsymbol{q}}(t)G^{<,\beta}_{\bar{\boldsymbol{p}}+\boldsymbol{q}}(t)G^{>,\alpha}_{\boldsymbol{p}}(t)G^{>,\beta}_{\bar{\boldsymbol{p}}}(t)\big].$$

This result agrees with the one derived in Refs. [5,32].

E. Initial pair correlations in the G1-G2 scheme

We conclude this section by returning to the question of initial correlations in NEGF theory that we briefly discussed in the context of Eq. (8) and analyze how they show up in the present G1-G2 scheme. For NEGF theory and the GKBA, the question of initial correlations has been extensively discussed before, see, e.g., Refs. [6,7,11,52], for more recent investigations, see Refs. [21,36,53]. As we mentioned below Eq. (10), the collision integral $I(t) = \mathcal{I}(t)$ vanishes for $t \to t_0$ which is correct only for a system that is uncorrelated at the initial time t_0. In the presence of finite initial correlations, one also has to consider the second contribution of the collision integral, Eq. (9), with $\lim_{t\to t_0} I(t) = \mathcal{I}^{\mathrm{IC}}(t_0)$. In NEGF theory there are three common equivalent approaches to take into account initial correlations and to derive the additional collision integral $\mathcal{I}^{\mathrm{IC}}(t)$:

(i): Derivation of an additional self energy Σ^{IC} that depends on initial correlations. This self energy can be shown to be singular, i.e., it contains a delta function $\delta(t, t_0)$ which gives rise to a finite value of the time integral from t_0 to t in $I(t)$, in the limit $t \to t_0$. This approach has been developed in Refs. [5,10,52,54], where also explicit expressions for the second-order Born and T-matrix approximations for the self energy have been derived.

(ii): Incorporation of thermodynamic-equilibrium initial correlations given by an imaginary-time Green function (Matsubara function). This leads to an extension of the Keldysh time contour $\mathcal{C}$ that is shown in the lower part of Fig. 1. When making the transition from the Green function on this contour to real-time quantities, i.e., from Eqs. (2) and (3) to the equations of motion for $G^{\gtrless}(t, t')$, an additional collision integral appears that involves the mixed Green functions $G(t, \tau)$ and $G(\tau, t)$ where the argument t runs along the real-time part of the contour and τ along the imaginary-time branch of $\mathcal{C}_{\mathrm{M}}$. This approach was introduced by Danielewicz [7] and is explained in detail in Refs. [6,33].

(iii): Incorporation of arbitrary initial correlations at time $t = t_0$ that are computed via a preceding time evolution that starts from an uncorrelated initial state in the remote past ($t \to -\infty$). This is the "adiabatic-switching" procedure that was discussed already by Keldysh [1,2]. There the interaction is smoothly turned on, i.e., $w_{ijkl}(t) = f(t)w_{ijkl}$, where the scalar function $f(t)$ starts from zero and approaches one at t_0. Correspondingly, the contour is extended to real times well before t_0 (see the contour $\mathcal{C}_{\mathrm{AS}}$ in the upper part of Fig. 1) and the collision integral I again has a finite value at $t = t_0$. For recent applications of this approach, see Refs. [17,28,55].

It is characteristic for these NEGF approaches [except for (i)] that the correlated initial state is prepared without explicitly specifying the two-particle Green function $G^{(2)}$ or the pair-correlation function. This is in line with the standard

NEGF approach to formally eliminate the two-particle Green function in favor of the single-particle self energy.

In contrast, the G1-G2 scheme recovers the two-particle Green function on the time diagonal $\mathcal{G}(t)$ from the collision integral $I(t)$. Its equation is solved simultaneously with the equation for the single-particle NEGF. This allows for a different and more straightforward approach to initial correlations as we discuss in the remainder of this section.

As shown in Ref. [5], the previous expression (22) for $\mathcal{G}(t)$ is only a particular solution of the inhomogeneous differential equation (29), whereas the complete solution contains, in addition, the general solution of the homogeneous equations (corresponding to the neglect of $\Psi^{\pm}$) which is directly related to initial correlations and which we denote $\mathcal{G}^{\mathrm{IC}}(t)$. Thus the total solution becomes

$$\mathcal{G}(t) \to \mathcal{G}(t) + \mathcal{G}^{\mathrm{IC}}(t)\,, \tag{44}$$

$$\mathcal{G}^{\mathrm{IC}}_{ijkl}(t) = (i\hbar)^4 \sum_{pqrs} \mathcal{U}^{(2)}_{ijpq}(t,t_0)\,\mathcal{G}^0_{pqrs}\,\mathcal{U}^{(2)}_{rskl}(t_0,t)\,. \tag{45}$$

For the special case $t = t_0$, the first term in Eq. (44) vanishes but the second reduces exactly to the initial correlation, $\mathcal{G}^{\mathrm{IC}}(t_0) = \mathcal{G}^0$. Thus, we have identified the initial conditions for the differential equations (30), for $G^<(t)$, and (29), for $\mathcal{G}(t)$. Recalling the definitions (11) and (5), the former is related to the initial value of the single-particle density matrix and the latter to the initial value of the correlated part of the two-particle density matrix $n^0_{ijkl} := n_{ijkl}(t_0)$:

$$G^{0,<}_{ij} = \pm\frac{1}{i\hbar} n_{ij}(t_0) =: \pm\frac{1}{i\hbar} n^0_{ij}\,,$$
$$\mathcal{G}^0_{ijkl} = \frac{1}{(i\hbar)^2}\left\{n^0_{ijkl} - n^0_{ik}n^0_{jl} \mp n^0_{il}n^0_{jk}\right\},$$

i.e., to pair correlations existing in the system at the initial time $t = t_0$. The two expressions, (45) and (22), can be combined into the total solution for the time-diagonal two-particle Green function according to

$$\mathcal{G}_{ijkl}(t) = (i\hbar)^4 \sum_{pqrs} \int_{t_0}^{t} d\bar{t}\, \mathcal{U}^{(2)}_{ijpq}(t,\bar{t}) \times \left[\delta(t_0,\bar{t})\mathcal{G}^0_{pqrs} + \frac{1}{i\hbar}\Psi^{\pm}_{pqrs}(\bar{t})\right]\mathcal{U}^{(2)}_{rskl}(\bar{t},t)\,. \tag{46}$$

Mathematically, of course, arbitrary initial conditions can be used to time evolve the differential equations for $G^<(t)$ and $\mathcal{G}(t)$. At the same time, however, restrictions should be imposed by selecting only physically realistic correlations (see below). An important example is initial correlations that correspond to the correlated ground state or thermodynamic-equilibrium state. This can be achieved using concept (iii) above to adiabatically turn on the interaction, starting from an uncorrelated system in the remote past. This results in the following "initial" pair-correlation function (corresponding to the second-Born approximation)

$$\mathcal{G}^0_{ijkl} = (i\hbar)^3 \sum_{pqrs} \int_{-\infty}^{t_0} d\bar{t}\, \mathcal{U}^{(2)}_{ijpq}(t_0,\bar{t})\Psi^{\pm}_{pqrs}(\bar{t})\mathcal{U}^{(2)}_{rskl}(\bar{t},t_0)\,. \tag{47}$$

In practice, a sufficiently long but finite adiabatic-switching time has to be chosen to generate the correlated ground state [19]. Inserting the adiabatic-switching result (47) into the general expression for the time-dependent initial-correlation contribution, Eq. (45), we obtain

$$\mathcal{G}^{\mathrm{IC}}_{ijkl}(t) = (i\hbar)^3 \sum_{pqrs} \int_{-\infty}^{t_0} d\bar{t}\, \mathcal{U}^{(2)}_{ijpq}(t,\bar{t})\Psi^{\pm}_{pqrs}(\bar{t})\mathcal{U}^{(2)}_{rskl}(\bar{t},t)\,,$$

where we took into account the group property of the two-particle propagators, cf. Appendix A 2. Interestingly, this result is of exactly the same mathematical form as the collision-induced contribution, Eq. (22), except for the limits of the time integration, which are t_0 and t, in the latter case. This means, in the case of initial correlations that are produced via adiabatic switching, both contributions to the two-particle function can be combined into

$$\mathcal{G}_{ijkl}(t) = (i\hbar)^3 \sum_{pqrs} \int_{-\infty}^{t} d\bar{t}\, \mathcal{U}^{(2)}_{ijpq}(t,\bar{t})\Psi^{\pm}_{pqrs}(\bar{t})\mathcal{U}^{(2)}_{rskl}(\bar{t},t)\,, \tag{48}$$

which is a special case of the general result (46). This result also shows that the "initial" point t_0 is arbitrary: The dynamics that started at $-\infty$ can be interrupted at any time $t_1 \in (-\infty, t]$, and the result (48) for $\mathcal{G}(t_1)$ can be used as the new "initial" correlation $\mathcal{G}^0$, whereas the collision-induced contribution now contains an integral running from t_1 to t. Of course, the dynamics are time reversible: Starting at time t and changing the Hamiltonian $\hat{H}(t+\bar{t}) \to -\hat{H}(t-\bar{t})$ will return the system to the same initial state at t_1 [56].

While expression (47) was based on adiabatic switching, in principle, the initial value for $\mathcal{G}^0$ can be generated by other methods [e.g. (i) and (ii) above], as long as certain physical restrictions are satisfied, as was discussed, e.g., in Refs. [21,57]. The result can be summarized as follows: In a closed (isolated) system, only such pair correlations are physically relevant that are produced for the same system within the same many-body approximations as the subsequent dynamics. In contrast, initial correlations that are produced by different approximations will, in general, lead to discontinuities in the dynamics, for $t > t_0$. This has relevance in open systems, in cases where the initial state is produced externally, by a separate process such as an interaction quench, e.g., Refs. [10,58–60] or a spin switch [61,62]. When the general result, Eq. (46), is inserted into the kinetic equation (30), this will give rise to the total collision integral, $I(t)$, Eq. (9), where the term containing $\Psi^{\pm}$ will produce the dynamical collision integral $\mathcal{I}(t)$, whereas the term containing $\mathcal{G}^0$ will give rise to the second contribution $\mathcal{I}^{\mathrm{IC}}(t)$, in agreement with the discussion above.

With this we succeeded to derive the complete formal solution for the time-diagonal two-particle Green function that is equivalent to the coupled system of differential equations for $G^<(t)$ and $\mathcal{G}(t)$ [Eqs. (30) and (29)] with the initial conditions $G^{<0}$ and $\mathcal{G}^0$, respectively. While the results in Eqs. (46) and (48) hold for the second-Born approximation for the self energy, this functional form is generally valid. The main difference, for more complicated self energies, is the explicit form of the two-particle propagators. For the additional approximations considered in this work [*GW* (Sec. IV),

T matrix (Sec. V)] the respective expressions are presented in Appendix D.

IV. *GW* SELF ENERGY

The static second-Born approximation that was considered above neglects screening effects and the dynamics of screening. These effects are captured by the *GW* approximation for which the self energy is given by

$$\Sigma^{\gtrless}_{ij}(t,t') = i\hbar \sum_{kl} W^{\gtrless}_{ilkj}(t,t') G^{\gtrless}_{kl}(t,t') . \tag{49}$$

Here, W is the dynamically screened interaction, which can be expressed in terms of the bare interaction and the inverse dielectric function,

$$W^{\gtrless}_{ijkl}(t,t') = \sum_{pq} w_{ipkq}(t) \varepsilon^{-1,\gtrless}_{pjql}(t,t') , \tag{50}$$

which allows us to transform the self energy (49) into

$$\Sigma^{\gtrless}_{ij}(t,t') = i\hbar \sum_{klpq} w_{ipkq}(t) \varepsilon^{-1,\gtrless}_{plqj}(t,t') G^{\gtrless}_{kl}(t,t') .$$

The collision integral of the time-diagonal equation then becomes

$$\begin{aligned} I_{ij}(t) &= \sum_{k} \int_{t_0}^{t} d\bar{t} \left[\Sigma^{>}_{ik}(t,\bar{t}) G^{<}_{kj}(\bar{t},t) - \Sigma^{<}_{ik}(t,\bar{t}) G^{>}_{kj}(\bar{t},t) \right] \\ &= i\hbar \sum_{klpqr} w_{ipkq}(t) \int_{t_0}^{t} d\bar{t} \\ &\quad \times \left[\varepsilon^{-1,>}_{plqr}(t,\bar{t}) \mathcal{G}^{\mathrm{F},>}_{krjl}(t,\bar{t}) - \varepsilon^{-1,<}_{plqr}(t,\bar{t}) \mathcal{G}^{\mathrm{F},<}_{krjl}(t,\bar{t}) \right] . \end{aligned}$$

Recalling the definition (10), we identify the time-diagonal element of the two-particle Green function in *GW* approximation,

$$\begin{aligned} \mathcal{G}_{ijkl}(t) = \pm \sum_{pq} \int_{t_0}^{t} d\bar{t} \big[& \varepsilon^{-1,>}_{lpjq}(t,\bar{t}) \mathcal{G}^{\mathrm{F},>}_{iqkp}(t,\bar{t}) \\ & - \varepsilon^{-1,<}_{lpjq}(t,\bar{t}) \mathcal{G}^{\mathrm{F},<}_{iqkp}(t,\bar{t}) \big] . \end{aligned}$$

By construction, the screened-interaction tensor obeys the following symmetry [cf. Eq. (13)],

$$W^{\gtrless}_{ijkl}(t,t') = W^{\lessgtr}_{jilk}(t',t) . \tag{51}$$

From Hedin's equations [63] we derive the following relation for the dynamically screened interaction W from which we subtract the singular part, i.e., $W^{\gtrless}_{ijkl}(t,t') \to W^{\gtrless}_{ijkl}(t,t') - w_{ijkl}\delta(t-t')$ [28],

$$\begin{aligned} W^{\gtrless}_{ijkl}(t,t') = & \pm i\hbar \sum_{pqrs} w_{ipkq}(t) w_{rjsl}(t') \mathcal{G}^{\mathrm{F},\gtrless}_{qspr}(t,t') \\ & \pm i\hbar \sum_{pqrs} w_{ipkq}(t) \\ & \times \Bigg[\int_{t_0}^{t} d\bar{t} \left(\mathcal{G}^{\mathrm{F},>}_{qspr}(t,\bar{t}) - \mathcal{G}^{\mathrm{F},<}_{qspr}(t,\bar{t}) \right) W^{\gtrless}_{rjsl}(\bar{t},t') \\ & + \int_{t_0}^{t'} d\bar{t}\, \mathcal{G}^{\mathrm{F},\gtrless}_{qspr}(t,\bar{t}) (W^{<}_{rjsl}(\bar{t},t') - W^{>}_{rjsl}(\bar{t},t')) \Bigg] . \end{aligned} \tag{52}$$

By comparison with Eq. (50) and using the symmetry of Eq. (51) one can identify a recursive equation for ε^{-1},

$$\begin{aligned} \varepsilon^{-1,\gtrless}_{ijkl}(t,t') = & \pm i\hbar \sum_{pq} w_{pjql}(t') \mathcal{G}^{\mathrm{F},\gtrless}_{kqip}(t,t') \\ & \pm i\hbar \sum_{pqrs} w_{jrls}(t') \\ & \times \Bigg[\int_{t_0}^{t} d\bar{t} \left(\mathcal{G}^{\mathrm{F},>}_{kqip}(t,\bar{t}) - \mathcal{G}^{\mathrm{F},<}_{kqip}(t,\bar{t}) \right) \varepsilon^{-1,\lessgtr}_{rpsq}(t',\bar{t}) \\ & + \int_{t_0}^{t'} d\bar{t}\, \mathcal{G}^{\mathrm{F},\gtrless}_{kqip}(t,\bar{t}) \left(\varepsilon^{-1,>}_{rpsq}(t',\bar{t}) - \varepsilon^{-1,<}_{rpsq}(t',\bar{t}) \right) \Bigg] . \end{aligned}$$

The time-diagonal equation for the inverse dielectric function can be further simplified,

$$\begin{aligned} \varepsilon^{-1,\gtrless}_{ijkl}(t,t) = & \pm i\hbar \sum_{pq} w_{pjql}(t) \mathcal{G}^{\mathrm{F},\gtrless}_{kqip}(t) \pm i\hbar \sum_{pqrs} w_{jrls}(t) \\ & \times \int_{t_0}^{t} d\bar{t} \left(\mathcal{G}^{\mathrm{F},>}_{kqip}(t,\bar{t}) \varepsilon^{-1,>}_{rpsq}(t,\bar{t}) \right. \\ & \left. - \mathcal{G}^{\mathrm{F},<}_{kqip}(t,\bar{t}) \varepsilon^{-1,<}_{rpsq}(t,\bar{t}) \right) \\ = & \pm i\hbar \sum_{pq} w_{pjql}(t) \mathcal{G}^{\mathrm{F},\gtrless}_{kqip}(t) \\ & + i\hbar \sum_{pq} w_{pjql}(t) \mathcal{G}_{kqip}(t) . \end{aligned} \tag{53}$$

A. *GW* approximation within the HF-GKBA

We now apply the HF-GKBA [cf. (16) and (17)] and obtain the following expressions for $\mathcal{G}$,

$$\begin{aligned} \mathcal{G}_{ijkl}(t) = \pm (i\hbar)^2 \sum_{pqrs} \int_{t_0}^{t} d\bar{t}\, \mathcal{U}_{ir}(t,\bar{t}) \big[& \varepsilon^{-1,>}_{lpjq}(t,\bar{t}) \mathcal{G}^{\mathrm{F},>}_{rqsp}(\bar{t}) \\ & - \varepsilon^{-1,<}_{lpjq}(t,\bar{t}) \mathcal{G}^{\mathrm{F},<}_{rqsp}(\bar{t}) \big] \mathcal{U}_{sk}(\bar{t},t) , \end{aligned}$$

as well as for ε^{-1},

$$\begin{aligned} & \varepsilon^{-1,\gtrless}_{ijkl}(t \geqslant t') \\ & = \pm (i\hbar)^3 \sum_{pqrs} w_{pjql}(t') \mathcal{U}_{kr}(t,t') \mathcal{G}^{\mathrm{F},\gtrless}_{rqsp}(t') \mathcal{U}_{si}(t',t) \\ & \quad \pm (i\hbar)^3 \sum_{pqrsuv} w_{jrls}(t') \Bigg[\int_{t_0}^{t} d\bar{t}\, \mathcal{U}_{ku}(t,\bar{t}) \\ & \quad \times \left(\mathcal{G}^{\mathrm{F},>}_{uqvp}(\bar{t}) - \mathcal{G}^{\mathrm{F},<}_{uqvp}(\bar{t}) \right) \mathcal{U}_{vi}(\bar{t},t) \varepsilon^{-1,\lessgtr}_{rpsq}(t',\bar{t}) \\ & \quad + \int_{t_0}^{t'} d\bar{t}\, \mathcal{U}_{ku}(t,\bar{t}) \mathcal{G}^{\mathrm{F},\gtrless}_{uqvp}(\bar{t}) \mathcal{U}_{vi}(\bar{t},t) \\ & \quad \times \left(\varepsilon^{-1,>}_{rpsq}(t',\bar{t}) - \varepsilon^{-1,<}_{rpsq}(t',\bar{t}) \right) \Bigg] , \end{aligned} \tag{54}$$

where $\mathcal{U}$ obeys Eqs. (A6) and (A7). By using the symmetry relation of Eq. (51) we easily find an expression for the time derivative of the off-diagonal inverse dielectric

function,

$$\begin{aligned}\frac{d}{dt}\varepsilon^{-1,\gtrless}_{ijkl}(t\geqslant t') &= \frac{1}{i\hbar}\sum_p\left\{h^{\mathrm{HF}}_{kp}(t)\varepsilon^{-1,\gtrless}_{ijpl}(t\geqslant t') - \varepsilon^{-1,\gtrless}_{pjkl}(t\geqslant t')h^{\mathrm{HF}}_{pi}(t)\right\}\\ &\pm i\hbar\sum_{pqrs}w_{prqs}(t)\left[\mathcal{G}^{\mathrm{F},>}_{kqip}(t)-\mathcal{G}^{\mathrm{F},<}_{kqip}(t)\right]\varepsilon^{-1,\gtrless}_{rjsl}(t\geqslant t')\\ &= \frac{1}{i\hbar}\sum_{pq}\left[\mathfrak{h}^{\varepsilon,\mathrm{HF}}_{pkqi}(t)+\mathfrak{h}^{\varepsilon,\mathrm{corr}}_{pkqi}(t)\right]\varepsilon^{-1,\gtrless}_{pjql}(t\geqslant t'),\end{aligned}$$

where we introduced the modified two-particle Hartree-Fock Hamiltonian

$$\mathfrak{h}^{\varepsilon,\mathrm{HF}}_{ijkl}(t)=\delta_{il}h^{\mathrm{HF}}_{jk}(t)-\delta_{jk}h^{\mathrm{HF}}_{il}(t),$$

which matches the index structure of the effective quasi-Hamiltonian, defined as

$$\mathfrak{h}^{\varepsilon,\mathrm{corr}}_{ijkl}(t)=\pm(i\hbar)^2\sum_{pq}w_{qipk}(t)\left[\mathcal{G}^{\mathrm{F},>}_{jplq}(t)-\mathcal{G}^{\mathrm{F},<}_{jplq}(t)\right]. \tag{55}$$

Combining these Hamiltonians into a single one,

$$\mathfrak{h}^{\varepsilon}_{ijkl}(t)=\mathfrak{h}^{\varepsilon,\mathrm{HF}}_{ijkl}(t)+\mathfrak{h}^{\varepsilon,\mathrm{corr}}_{ijkl}(t), \tag{56}$$

we observe that the inverse dielectric function, within the *GW*-HF-GKBA, obeys a time-dependent two-particle Schrödinger equation,

$$i\hbar\frac{d}{dt}\varepsilon^{-1,\gtrless}_{ijkl}(t\geqslant t')=\sum_{pq}\mathfrak{h}^{\varepsilon}_{pkqi}(t)\varepsilon^{-1,\gtrless}_{pjql}(t\geqslant t'), \tag{57}$$

with the Hamiltonian (56), that is equivalent to the rather complicated integral equation (54). In the following, we demonstrate that, for the *GW*-HF-GKBA, again, a time-local G1-G2 scheme can be derived which retains time-linear scaling [39].

B. *GW*-G1-G2 equations for a general basis

To derive the G1-G2 scheme, we compute the time derivative of $\mathcal{G}$, yielding

$$\frac{d}{dt}\mathcal{G}_{ijkl}(t)=\left[\frac{d}{dt}\mathcal{G}_{ijkl}(t)\right]_{\int}+\left[\frac{d}{dt}\mathcal{G}_{ijkl}(t)\right]_{\varepsilon}+\left[\frac{d}{dt}\mathcal{G}_{ijkl}(t)\right]_{\mathcal{U}}, \tag{58}$$

where the first contribution, which originates from the derivative of the integration boundaries, is given by

$$\begin{aligned}\left[\frac{d}{dt}\mathcal{G}_{ijkl}(t)\right]_{\int} &= \pm\sum_{pq}\left[\varepsilon^{-1,>}_{lpjq}(t,t)\mathcal{G}^{\mathrm{F},>}_{iqkp}(t)-\varepsilon^{-1,<}_{lpjq}(t,t)\mathcal{G}^{\mathrm{F},<}_{iqkp}(t)\right]\\ &= i\hbar\sum_{pqrs}w_{rpsq}(t)\left[\mathcal{G}^{\mathrm{F},>}_{jslr}(t)\mathcal{G}^{\mathrm{F},>}_{iqkp}(t)-\mathcal{G}^{\mathrm{F},<}_{jslr}(t)\mathcal{G}^{\mathrm{F},<}_{iqkp}(t)\right]\\ &\pm i\hbar\sum_{pqrs}w_{rpsq}(t)\mathcal{G}_{jslr}(t)\left[\mathcal{G}^{\mathrm{F},>}_{iqkp}(t)-\mathcal{G}^{\mathrm{F},<}_{iqkp}(t)\right]\\ &= \frac{1}{i\hbar}\Psi_{ijkl}(t)-\frac{1}{i\hbar}\sum_{pq}\mathcal{G}_{qjpl}(t)\left[\mathfrak{h}^{\varepsilon,\mathrm{corr}}_{qkpi}(t)\right]^*.\end{aligned}$$

Here, the two-particle source term is defined as

$$\Psi_{ijkl}(t)=\frac{1}{(i\hbar)^2}\sum_{pqrs}w_{pqrs}(t)\Phi^{ijrs}_{pqkl}(t).$$

The second contribution to Eq. (58), resulting from the time derivative of ε^{-1}, is given by

$$\begin{aligned}\left[\frac{d}{dt}\mathcal{G}_{ijkl}(t)\right]_{\varepsilon} &= \pm(i\hbar)^2\sum_{pqrs}\int_{t_0}^{t}d\bar{t}\,\mathcal{U}_{ir}(t,\bar{t})\left[\left(\frac{d}{dt}\varepsilon^{-1,>}_{lpjq}(t,\bar{t})\right)\mathcal{G}^{\mathrm{F},>}_{rqsp}(\bar{t})\right.\\ &\left.-\left(\frac{d}{dt}\varepsilon^{-1,<}_{lpjq}(t,\bar{t})\right)\mathcal{G}^{\mathrm{F},<}_{rqsp}(\bar{t})\right]\mathcal{U}_{sk}(\bar{t},t)\\ &= \frac{1}{i\hbar}\sum_{pq}\left[\mathfrak{h}^{\varepsilon,\mathrm{HF}}_{pjql}(t)+\mathfrak{h}^{\varepsilon,\mathrm{corr}}_{pjql}(t)\right]\mathcal{G}_{iqkp}(t),\end{aligned}$$

whereas the third contribution to Eq. (58), which stems from the derivative of the propagators, is

$$\begin{aligned}\left[\frac{d}{dt}\mathcal{G}_{ijkl}(t)\right]_{\mathcal{U}} &= \pm(i\hbar)^2\sum_{pqrs}\int_{t_0}^{t}d\bar{t}\left(\frac{d}{dt}\mathcal{U}_{ir}(t,\bar{t})\right)\left[\varepsilon^{-1,>}_{lpjq}(t,\bar{t})\mathcal{G}^{\mathrm{F},>}_{rqsp}(\bar{t})\right.\\ &\left.-\varepsilon^{-1,<}_{lpjq}(t,\bar{t})\mathcal{G}^{\mathrm{F},<}_{rqsp}(\bar{t})\right]\mathcal{U}_{sk}(\bar{t},t)\\ &\pm(i\hbar)^2\sum_{pqrs}\int_{t_0}^{t}d\bar{t}\,\mathcal{U}_{ir}(t,\bar{t})\left[\varepsilon^{-1,>}_{lpjq}(t,\bar{t})\mathcal{G}^{\mathrm{F},>}_{rqsp}(\bar{t})\right.\\ &\left.-\varepsilon^{-1,<}_{lpjq}(t,\bar{t})\mathcal{G}^{\mathrm{F},<}_{rqsp}(\bar{t})\right]\left(\frac{d}{dt}\mathcal{U}_{sk}(\bar{t},t)\right)\\ &= \frac{1}{i\hbar}\sum_{p}\left[h^{\mathrm{HF}}_{ip}(t)\mathcal{G}_{pjkl}(t)-\mathcal{G}_{ijpl}(t)h^{\mathrm{HF}}_{pk}(t)\right]\\ &= -\frac{1}{i\hbar}\sum_{pq}\mathcal{G}_{qjpl}(t)\left[\mathfrak{h}^{\varepsilon,\mathrm{HF}}_{qkpi}(t)\right]^*.\end{aligned}$$

Finally, the three contributions to the derivative of $\mathcal{G}$ are combined to reveal

$$\begin{aligned}i\hbar\frac{d}{dt}\mathcal{G}_{ijkl}(t) &= \Psi_{ijkl}(t)+\sum_{pq}\left\{\mathfrak{h}^{\varepsilon}_{qjpl}(t)[\mathcal{G}_{qkpi}(t)]^*\right.\\ &\left.-\mathcal{G}_{qjpl}(t)\left[\mathfrak{h}^{\varepsilon}_{qkpi}(t)\right]^*\right\},\end{aligned} \tag{59}$$

where $\mathfrak{h}^{\varepsilon}(t)$ was defined in Eq. (56). With this we have obtained the equations of the G1-G2 scheme for the *GW* approximation. For $\mathfrak{h}^{\varepsilon,\mathrm{corr}}(t)\equiv 0$, we recover the equations from the SOA, cf. Eq. (29), since the remaining Hamiltonian contribution can be expressed as a commutator. Equation (59) is the most compact formulation that visualizes the intrinsic structure of $\mathcal{G}$ in the *GW* approximation.

For practical use, it is convenient to separate the correlation contributions from the mean-field terms via the introduction of an additional quantity:

$$\begin{aligned}i\hbar\frac{d}{dt}\mathcal{G}_{ijkl}(t)-\left[h^{(2),\mathrm{HF}},\mathcal{G}\right]_{ijkl}(t)\\ =\Psi_{ijkl}(t)+\Pi_{ijkl}(t)-[\Pi_{lkji}(t)]^*,\end{aligned} \tag{60}$$

where polarization effects are included in

$$\Pi_{ijkl}(t) = \sum_{pq} \mathfrak{h}^{\varepsilon,\mathrm{corr}}_{qjpl}(t)\mathcal{G}_{ipkq}(t)\,. \tag{61}$$

Equation (59) agrees with the polarization approximation of density-matrix theory, cf. Refs. [5,64]. In the Markov limit this leads to the quantum generalization of the Balescu-Lenard kinetic equation [65–67].

Here, we have employed the standard definition of *GW* in NEGF theory, which is widely used in literature (see, e.g., Refs. [15,28,68]), in which the screened interaction [Eq. (52)] does not include exchange terms. The generalization to also describe exchange processes is, however, straightforwardly carried out. For the G1-G2 scheme, this is achieved by simply replacing $\Psi_{ijkl}(t)$ by $\Psi^{\pm}_{ijkl}(t)$ in Eqs. (59) and (60).

Again we have succeeded to eliminate all time integrations which means that Eq. (59) can be solved with an effort that is first order in N_t. Note that the conventional HF-GKBA scheme with *GW* self energy scales as N_t^3 indicating a huge advantage of the G1-G2 formulation [39]. More computational details will be given below, in Sec. VII.

C. *GW*-G1-G2 equations for the Hubbard model

For the Hubbard system [cf. Eq. (33)] we again use the interaction matrix of Eq. (32). With that, the equations of motion (60) become,

$$\begin{aligned} &i\hbar\frac{d}{dt}\mathcal{G}^{\uparrow\downarrow\uparrow\downarrow}_{ijkl}(t) - \left[h^{(2),\mathrm{HF}}_{\uparrow\downarrow}, \mathcal{G}^{\uparrow\downarrow\uparrow\downarrow}\right]_{ijkl}(t) \\ &\quad = \Psi^{\uparrow\downarrow\uparrow\downarrow}_{ijkl}(t) + \Pi^{\uparrow\downarrow\uparrow\downarrow}_{ijkl}(t) - [\Pi^{\uparrow\downarrow\uparrow\downarrow}_{lkji}(t)]^* \quad \text{and} \end{aligned} \tag{62}$$

$$\begin{aligned} &i\hbar\frac{d}{dt}\mathcal{G}^{\uparrow\uparrow\uparrow\uparrow}_{ijkl}(t) - \left[h^{(2),\mathrm{HF}}_{\uparrow\uparrow}, \mathcal{G}^{\uparrow\uparrow\uparrow\uparrow}\right]_{ijkl}(t) \\ &\quad = \Pi^{\uparrow\uparrow\uparrow\uparrow}_{ijkl}(t) - [\Pi^{\uparrow\uparrow\uparrow\uparrow}_{lkji}(t)]^*\,, \end{aligned} \tag{63}$$

where we introduced the polarization terms,

$$\begin{aligned} \Pi^{\uparrow\downarrow\uparrow\downarrow}_{ijkl}(t) = -(i\hbar)^2 U(t) \sum_p &[G^{>,\downarrow}_{jp}(t)G^{<,\downarrow}_{pl}(t) \\ &- G^{<,\downarrow}_{jp}(t)G^{>,\downarrow}_{pl}(t)]\mathcal{G}^{\uparrow\uparrow\uparrow\uparrow}_{ipkp}(t), \end{aligned} \tag{64}$$

$$\begin{aligned} \Pi^{\uparrow\uparrow\uparrow\uparrow}_{ijkl}(t) = -(i\hbar)^2 U(t) \sum_p &[G^{>,\uparrow}_{jp}(t)G^{<,\uparrow}_{pl}(t) \\ &- G^{<,\uparrow}_{jp}(t)G^{>,\uparrow}_{pl}(t)]\mathcal{G}^{\uparrow\downarrow\uparrow\downarrow}_{ipkp}(t)\,. \end{aligned} \tag{65}$$

Notice that there are two separate spin combinations (four when considering $\uparrow \leftrightarrow \downarrow$) for the two-particle Green function that enter Eqs. (62) and (63). Due to the cross coupling in the two polarization terms, they cannot be solved independently [28,69]. Numerical results for the *GW*-G1-G2 scheme are presented in Sec. VII.

D. *GW*-G1-G2 equations for jellium

For the uniform electron gas [cf. Eq. (39)] we again use the interaction matrix of Eq. (40) and define

$$\Pi^{\alpha\beta}_{\boldsymbol{p},\bar{\boldsymbol{p}},\boldsymbol{q}}(t) := \Pi^{\alpha\beta\alpha\beta}_{\boldsymbol{p}-\boldsymbol{q},\bar{\boldsymbol{p}}+\boldsymbol{q},\boldsymbol{p},\bar{\boldsymbol{p}}}(t)\,.$$

With that, the equation (60) for the time-diagonal two-particle Green function [recall the definition (42)] becomes

$$\begin{aligned} &i\hbar\frac{d}{dt}\mathcal{G}^{\alpha\beta}_{\boldsymbol{p}\bar{\boldsymbol{p}}\boldsymbol{q}}(t) - \mathcal{G}^{\alpha\beta}_{\boldsymbol{p}\bar{\boldsymbol{p}}\boldsymbol{q}}(t)\big(h^{\mathrm{HF},\alpha}_{\boldsymbol{p}-\boldsymbol{q}} + h^{\mathrm{HF},\beta}_{\bar{\boldsymbol{p}}+\boldsymbol{q}} - h^{\mathrm{HF},\alpha}_{\boldsymbol{p}} - h^{\mathrm{HF},\beta}_{\bar{\boldsymbol{p}}}\big)(t) \\ &\quad = \underbrace{\frac{1}{(i\hbar)^2} v_{|\boldsymbol{q}|}(t)\Phi^{\alpha\beta}_{\boldsymbol{p}\bar{\boldsymbol{p}}\boldsymbol{q}}(t)}_{=:\Psi^{\alpha\beta}_{\boldsymbol{p}\bar{\boldsymbol{p}}\boldsymbol{q}}(t)} + \Pi^{\alpha\beta}_{\boldsymbol{p},\bar{\boldsymbol{p}},\boldsymbol{q}}(t) - \left[\Pi^{\beta\alpha}_{\bar{\boldsymbol{p}}+\boldsymbol{q},\boldsymbol{p}-\boldsymbol{q},\boldsymbol{q}}(t)\right]^*, \end{aligned}$$

with the momentum representation of the polarization term, given by

$$\begin{aligned} \Pi^{\alpha\beta}_{\boldsymbol{p},\bar{\boldsymbol{p}},\boldsymbol{q}}(t) = \pm (i\hbar)^2 &\left[G^{>,\beta}_{\bar{\boldsymbol{p}}+\boldsymbol{q}}(t)G^{<,\beta}_{\bar{\boldsymbol{p}}}(t) - G^{<,\beta}_{\bar{\boldsymbol{p}}+\boldsymbol{q}}(t)G^{>,\beta}_{\bar{\boldsymbol{p}}}(t)\right] \\ &\times v_{|\boldsymbol{q}|}(t)\sum_{\boldsymbol{k},\sigma}\mathcal{G}^{\alpha\sigma}_{\boldsymbol{pkq}}(t)\,. \end{aligned} \tag{66}$$

As we will discuss in Sec. VII, the *GW* equations for jellium can be solved particularly efficiently.

V. *T*-MATRIX SELF ENERGIES

We next turn to the case of strong coupling where the second-Born approximation is not applicable. It is well known that the entire Born series can be summed up, giving rise to the *T*-matrix (or binary-collision or ladder) approximation. Here we first consider the case of a static pair interaction. The extension to a dynamically screened *T* matrix will be considered in Sec. VI. We start by considering, in Sec. V A, the *T* matrix in the particle-particle channel after which we analyze, in Sec. V B, the *T* matrix in the particle-hole channel.

A. *T* matrix in the particle-particle channel

For the particle-particle *T* matrix, the self energy has the form [3,19],

$$\Sigma^{\gtrless}_{ij}(t,t') = i\hbar\sum_{kl} T^{\mathrm{pp},\gtrless}_{ikjl}(t,t')G^{\lessgtr}_{lk}(t',t)\,. \tag{67}$$

Here, the *T* matrix is expressed as

$$T^{\mathrm{pp},\gtrless}_{ijkl}(t,t') = \sum_{pq} w_{ijpq}(t)\Omega^{\mathrm{pp},\gtrless}_{pqkl}(t,t')\,, \tag{68}$$

which allows us to rewrite the self energy (67):

$$\Sigma^{\gtrless}_{ij}(t,t') = i\hbar\sum_{klpq} w_{ikpq}(t)\Omega^{\mathrm{pp},\gtrless}_{pqjl}(t,t')G^{\lessgtr}_{lk}(t',t)\,. \tag{69}$$

In Eqs. (68) and (69) the quantity Ω^{pp} is the nonequilibrium generalization of the Møller operator from scattering theory [70,71]. The collision integral (10) of the time-diagonal equation then becomes,

$$\begin{aligned} I_{ij}(t) &= i\hbar\sum_{klpqr} w_{ipqr}(t)\int_{t_0}^{t} d\bar{t}\left[\Omega^{\mathrm{pp},>}_{qrkl}(t,\bar{t})\mathcal{G}^{\mathrm{H},<}_{kljp}(\bar{t},t)\right. \\ &\quad \left. - \Omega^{\mathrm{pp},<}_{qrkl}(t,\bar{t})\mathcal{G}^{\mathrm{H},>}_{kljp}(\bar{t},t)\right] \\ &= \pm i\hbar\sum_{klp} w_{iklp}(t)\mathcal{G}_{kpjl}(t)\,, \end{aligned}$$

which results in the following expression for the time-diagonal element of the two-particle Green function,

$$\mathcal{G}_{ijkl}(t) = \pm \sum_{pq} \int_{t_0}^{t} d\bar{t} \left[\Omega^{\mathrm{pp},>}_{ijpq}(t,\bar{t}) \mathcal{G}^{\mathrm{H},<}_{pqkl}(\bar{t},t) - \Omega^{\mathrm{pp},<}_{ijpq}(t,\bar{t}) \mathcal{G}^{\mathrm{H},>}_{pqkl}(\bar{t},t) \right].$$

By construction, the T matrix obeys the following symmetry [cf. Eq. (14)],

$$T^{\mathrm{pp},\gtrless}_{ijkl}(t,t') = -\left[T^{\mathrm{pp},\gtrless}_{klij}(t',t) \right]^{*}. \tag{70}$$

The T matrix sums up the particle-particle collisions via the recursive equation (nonequilibrium Lippmann-Schwinger equation; compared to the standard definition of the T matrix, here the singular part has been subtracted [19,28]),

$$\begin{aligned} T^{\mathrm{pp},\gtrless}_{ijkl}(t,t') = \pm i\hbar \sum_{pqrs} w_{ijpq}(t) \mathcal{G}^{\mathrm{H},\gtrless}_{pqrs}(t,t') w^{\pm}_{rskl}(t') + i\hbar \sum_{pqrs} w_{ijpq}(t) \Bigg\{ \int_{t_0}^{t} d\bar{t} \left[\mathcal{G}^{\mathrm{H},>}_{pqrs}(t,\bar{t}) \right. \\ \left. - \mathcal{G}^{\mathrm{H},<}_{pqrs}(t,\bar{t}) \right] T^{\mathrm{pp},\gtrless}_{rskl}(\bar{t},t') + \int_{t_0}^{t'} d\bar{t}\, \mathcal{G}^{\mathrm{H},\gtrless}_{pqrs}(t,\bar{t}) \left[T^{\mathrm{pp},<}_{rskl}(\bar{t},t') - T^{\mathrm{pp},>}_{rskl}(\bar{t},t') \right] \Bigg\}. \end{aligned}$$

Following this and using the symmetries of Eqs. (14) and (70) the relation for the Møller operator is readily derived,

$$\begin{aligned} \Omega^{\mathrm{pp},\gtrless}_{ijkl}(t,t') &= \pm i\hbar \sum_{pq} \mathcal{G}^{\mathrm{H},\gtrless}_{ijpq}(t,t') w^{\pm}_{pqkl}(t') + i\hbar \sum_{pqrs} \Bigg\{ \int_{t_0}^{t} d\bar{t} \left[\mathcal{G}^{\mathrm{H},>}_{ijpq}(t,\bar{t}) - \mathcal{G}^{\mathrm{H},>}_{ijpq}(t,\bar{t}) \right] w_{pqrs}(\bar{t}) \Omega^{\mathrm{pp},\gtrless}_{rskl}(\bar{t},t') \\ &\quad + \int_{t_0}^{t'} d\bar{t}\, \mathcal{G}^{\mathrm{H},\gtrless}_{ijpq}(t,\bar{t}) w_{pqrs}(\bar{t}) \left[\Omega^{\mathrm{pp},<}_{rskl}(\bar{t},t') - \Omega^{\mathrm{pp},>}_{rskl}(\bar{t},t') \right] \Bigg\} \\ &= \pm i\hbar \sum_{pq} \mathcal{G}^{\mathrm{H},\gtrless}_{ijpq}(t,t') w^{\pm}_{pqkl}(t') + i\hbar \sum_{pqrs} \Bigg\{ \int_{t_0}^{t} d\bar{t}\, \Omega^{\mathrm{pp},\gtrless}_{rspq}(t',\bar{t}) \left[\mathcal{G}^{\mathrm{H},<}_{pqij}(\bar{t},t) - \mathcal{G}^{\mathrm{H},>}_{pqij}(\bar{t},t) \right] \\ &\quad + \int_{t_0}^{t'} d\bar{t} \left[\Omega^{\mathrm{pp},>}_{rspq}(t',\bar{t}) - \Omega^{\mathrm{pp},<}_{rspq}(t',\bar{t}) \right] \mathcal{G}^{\mathrm{H},\gtrless}_{pqij}(\bar{t},t) \Bigg\}^{*} w_{rskl}(t'). \end{aligned}$$

The time-diagonal equation for Ω^{pp} can be further simplified,

$$\begin{aligned} \Omega^{\mathrm{pp},\gtrless}_{ijkl}(t,t) &= \pm i\hbar \sum_{pq} \mathcal{G}^{\mathrm{H},\gtrless}_{ijpq}(t) w^{\pm}_{pqkl}(t) + i\hbar \sum_{pqrs} \left[\int_{t_0}^{t} d\bar{t} \left(\Omega^{\mathrm{pp},>}_{pqrs}(t,\bar{t}) \mathcal{G}^{\mathrm{H},<}_{rsij}(\bar{t},t) - \Omega^{\mathrm{pp},<}_{pqrs}(t,\bar{t}) \mathcal{G}^{\mathrm{H},>}_{rsij}(\bar{t},t) \right) \right]^{*} w_{pqkl}(t) \\ &= \pm i\hbar \sum_{pq} \mathcal{G}^{\mathrm{H},\gtrless}_{ijpq}(t) w^{\pm}_{pqkl}(t) \pm i\hbar \sum_{pq} \left[\mathcal{G}_{pqij}(t) \right]^{*} w_{pqkl}(t). \end{aligned}$$

1. T^{pp} approximation within the HF-GKBA

We now apply the HF-GKBA [cf. Eqs. (16) and (17)] and find the following expressions for $\mathcal{G}$,

$$\mathcal{G}_{ijkl}(t) = \pm (i\hbar)^2 \sum_{pqrs} \int_{t_0}^{t} d\bar{t} \left[\Omega^{\mathrm{pp},>}_{ijpq}(t,\bar{t}) \mathcal{G}^{\mathrm{H},<}_{pqrs}(\bar{t}) - \Omega^{\mathrm{pp},<}_{ijpq}(t,\bar{t}) \mathcal{G}^{\mathrm{H},>}_{pqrs}(\bar{t}) \right] \mathcal{U}^{(2)}_{rskl}(\bar{t},t),$$

as well as for Ω^{pp},

$$\begin{aligned} \Omega^{\mathrm{pp},\gtrless}_{ijkl}(t \geqslant t') = \pm (i\hbar)^3 \sum_{pqrs} \mathcal{U}^{(2)}_{ijrs}(t,t') \mathcal{G}^{\mathrm{H},\gtrless}_{rspq}(t') w^{\pm}_{pqkl}(t') + (i\hbar)^3 \sum_{pqrsuv} \Bigg[\int_{t_0}^{t} d\bar{t}\, \mathcal{U}^{(2)}_{ijrs}(t,\bar{t}) \left(\mathcal{G}^{\mathrm{H},>}_{rspq}(\bar{t}) - \mathcal{G}^{\mathrm{H},<}_{rspq}(\bar{t}) \right) w_{pquv}(\bar{t}) \Omega^{\mathrm{pp},\gtrless}_{uvkl}(\bar{t},t') \\ + \int_{t_0}^{t'} d\bar{t}\, \mathcal{U}^{(2)}_{ijrs}(t,\bar{t}) \mathcal{G}^{\mathrm{H},\gtrless}_{rspq}(\bar{t}) w_{pquv}(\bar{t}) \left(\Omega^{\mathrm{pp},<}_{uvkl}(\bar{t},t') - \Omega^{\mathrm{pp},>}_{uvkl}(\bar{t},t') \right) \Bigg], \end{aligned} \tag{71}$$

where $\mathcal{U}^{(2)}$ obeys Eqs. (24) and (25). With Eq. (71) we easily find an expression for the time derivative of Ω^{pp},

$$\frac{d}{dt} \Omega^{\mathrm{pp},\gtrless}_{ijkl}(t \geqslant t') = \frac{1}{i\hbar} \sum_{pq} \left(\mathfrak{h}^{\Omega^{\mathrm{pp}},\mathrm{HF}}_{ijpq}(t) + \mathfrak{h}^{\Omega^{\mathrm{pp}},\mathrm{corr}}_{ijpq}(t) \right) \Omega^{\mathrm{pp},\gtrless}_{pqkl}(t \geqslant t'). \tag{72}$$

As for the case of the *GW* self energy, here we introduced two quasi-Hamiltonians,

$$\mathfrak{h}^{\Omega^{\rm pp},\rm HF}_{ijkl}(t) = h^{(2),\rm HF}_{ijkl}(t)\,,$$
$$\mathfrak{h}^{\Omega^{\rm pp},\rm corr}_{ijkl}(t) = (i\hbar)^2 \sum_{pq} \left[\mathcal{G}^{\rm H,>}_{ijpq}(t) - \mathcal{G}^{\rm H,<}_{ijpq}(t)\right] w_{pqkl}(t). \quad (73)$$

Combining these Hamiltonians again into a single one,

$$\mathfrak{h}^{\Omega^{\rm pp}}_{ijkl}(t) = \mathfrak{h}^{\Omega^{\rm pp},\rm HF}_{ijkl}(t) + \mathfrak{h}^{\Omega^{\rm pp},\rm corr}_{ijkl}(t)\,, \quad (74)$$

the equation (72) for the Møller operator is transformed into a time-dependent two-particle Schrödinger equation,

$$i\hbar \frac{d}{dt} \Omega^{\rm pp,\gtrless}_{ijkl}(t \gtrless t') = \sum_{pq} \mathfrak{h}^{\Omega^{\rm pp}}_{ijpq}(t) \Omega^{\rm pp,\gtrless}_{pqkl}(t \gtrless t')\,. \quad (75)$$

This equation is analogous to the Schrödinger equation for the inverse dielectric function, Eq. (57), the main difference being the modified Hamiltonian (74).

2. $T^{\rm pp}$-G1-G2 equations for a general basis

To derive the G1-G2 scheme for the particle-particle T matrix, we have to take the derivative of $\mathcal{G}$, yielding,

$$\frac{d}{dt}\mathcal{G}_{ijkl}(t) = \left[\frac{d}{dt}\mathcal{G}_{ijkl}(t)\right]_{\int} + \left[\frac{d}{dt}\mathcal{G}_{ijkl}(t)\right]_{\Omega^{\rm pp}} + \left[\frac{d}{dt}\mathcal{G}_{ijkl}(t)\right]_{\mathcal{U}^{(2)}},$$

The derivative of the integration boundaries results in,

$$\begin{aligned}\left[\frac{d}{dt}\mathcal{G}_{ijkl}(t)\right]_{\int} &= \pm \sum_{pq} \left[\Omega^{\rm pp,>}_{ijpq}(t,t)\mathcal{G}^{\rm H,<}_{pqkl}(t) - \Omega^{\rm pp,<}_{ijpq}(t,t)\mathcal{G}^{\rm H,>}_{pqkl}(t)\right] \\ &= i\hbar \sum_{pqrs} w^{\pm}_{rspq}(t)\left[\mathcal{G}^{\rm H,>}_{ijrs}(t)\mathcal{G}^{\rm H,<}_{pqkl}(t) - \mathcal{G}^{\rm H,<}_{ijrs}(t)\mathcal{G}^{\rm H,>}_{pqkl}(t)\right] \\ &\quad + i\hbar \sum_{pqrs} [\mathcal{G}_{rsij}(t)]^* w_{rspq}(t)\left[\mathcal{G}^{\rm H,<}_{pqkl}(t) - \mathcal{G}^{\rm H,>}_{pqkl}(t)\right] \\ &= \frac{1}{i\hbar}\Psi^{\pm}_{ijkl}(t) - \frac{1}{i\hbar}\sum_{pq}\left[\mathfrak{h}^{\Omega^{\rm pp},\rm corr}_{klpq}(t)\mathcal{G}_{pqij}(t)\right]^*,\end{aligned}$$

while the time derivative of the Møller operator yields

$$\begin{aligned}\left[\frac{d}{dt}\mathcal{G}_{ijkl}(t)\right]_{\Omega^{\rm pp}} &= \pm(i\hbar)^2 \sum_{pqrs}\int_{t_0}^{t} d\bar{t}\left[\left(\frac{d}{dt}\Omega^{\rm pp,>}_{ijpq}(t,\bar{t})\right)\mathcal{G}^{\rm H,<}_{pqrs}(\bar{t}) - \left(\frac{d}{dt}\Omega^{\rm pp,<}_{ijpq}(t,\bar{t})\right)\mathcal{G}^{\rm H,>}_{pqrs}(\bar{t})\right]\mathcal{U}^{(2)}_{rskl}(\bar{t},t) \\ &= \frac{1}{i\hbar}\sum_{pq}\left(\mathfrak{h}^{\Omega^{\rm pp},\rm HF}_{ijpq}(t) + \mathfrak{h}^{\Omega^{\rm pp},\rm corr}_{ijpq}(t)\right)\mathcal{G}_{pqkl}(t)\,.\end{aligned}$$

The last contribution originates from the derivative of the two-particle propagator,

$$\begin{aligned}\left[\frac{d}{dt}\mathcal{G}_{ijkl}(t)\right]_{\mathcal{U}^{(2)}} &= \pm(i\hbar)^2 \sum_{pqrs}\int_{t_0}^{t} d\bar{t}\left[\Omega^{\rm pp,>}_{ijpq}(t,\bar{t})\mathcal{G}^{\rm H,<}_{pqrs}(\bar{t}) - \Omega^{\rm pp,<}_{ijpq}(t,\bar{t})\mathcal{G}^{\rm H,>}_{pqrs}(\bar{t})\right]\left(\frac{d}{dt}\mathcal{U}^{(2)}_{rskl}(\bar{t},t)\right) \\ &= \frac{1}{i\hbar}\sum_{pq}\mathcal{G}_{ijpq}(t)\mathfrak{h}^{\Omega^{\rm pp},\rm HF}_{pqkl}(t).\end{aligned}$$

Combining the three contributions to the derivative of $\mathcal{G}$ reveals

$$i\hbar\frac{d}{dt}\mathcal{G}_{ijkl}(t) = \Psi^{\pm}_{ijkl}(t) + \sum_{pq}\left\{\mathfrak{h}^{\Omega^{\rm pp}}_{ijpq}(t)[\mathcal{G}_{klpq}(t)]^* - \mathcal{G}_{ijpq}(t)\left[\mathfrak{h}^{\Omega^{\rm pp}}_{klpq}(t)\right]^*\right\}, \quad (76)$$

where $\mathfrak{h}^{\Omega^{\rm pp}}(t)$ was introduced in Eq. (74). This is the central equation for the G1-G2 scheme in T-matrix approximation for the particle-particle channel [5,71]. Compared to the equation of motion for $\mathcal{G}$ in second-Born approximation, Eq. (29), this equation contains, in addition, the particle-particle ladder terms which are generated by the quasi-Hamiltonian of Eq. (73). Again, for practical use, it is convenient to separate the correlation contributions from the mean-field terms via the introduction of an additional quantity:

$$i\hbar\frac{d}{dt}\mathcal{G}_{ijkl}(t) - \left[h^{(2),\rm HF},\mathcal{G}\right]_{ijkl}(t) = \Psi^{\pm}_{ijkl}(t) + \Lambda^{\rm pp}_{ijkl}(t) - \left[\Lambda^{\rm pp}_{klij}(t)\right]^*,$$

where the particle-particle ladder term is defined by

$$\Lambda^{\rm pp}_{ijkl}(t) = \sum_{pq}\mathfrak{h}^{\Omega^{\rm pp},\rm corr}_{ijpq}(t)\mathcal{G}_{pqkl}(t)\,. \quad (77)$$

Without the Λ terms we exactly recover the equation of motion for $\mathcal{G}$ in second-order Born approximation. Inclusion of the Λ terms, on the other hand, allows one to take into account multiple scattering and large-angle scattering effects that are important for strongly correlated systems. These terms correspond to the summation of the infinite Born series.

3. $T^{\rm pp}$-G1-G2 equations for the Hubbard model

We now apply this result to the Hubbard Hamiltonian and find,

$$i\hbar\frac{d}{dt}\mathcal{G}^{\uparrow\downarrow\uparrow\downarrow}_{ijkl}(t) - \left[h^{(2),\rm HF}_{\uparrow\downarrow},\mathcal{G}^{\uparrow\downarrow\uparrow\downarrow}\right]_{ijkl}(t) = \Psi^{\uparrow\downarrow\uparrow\downarrow}_{ijkl}(t) + \Lambda^{\rm pp,\uparrow\downarrow\uparrow\downarrow}_{ijkl}(t) - \left[\Lambda^{\rm pp,\uparrow\downarrow\uparrow\downarrow}_{klij}(t)\right]^*,$$

where we introduced the particle-particle ladder term

$$\Lambda^{\rm pp,\uparrow\downarrow\uparrow\downarrow}_{ijkl}(t) = (i\hbar)^2 U(t) \times \sum_{p}\left[G^{>,\uparrow}_{ip}(t)G^{>,\downarrow}_{jp}(t) - G^{<,\uparrow}_{ip}(t)G^{<,\downarrow}_{jp}(t)\right]\mathcal{G}^{\uparrow\downarrow\uparrow\downarrow}_{ppkl}(t)\,. \quad (78)$$

In the present case there exists only one distinct spin combination (two when considering $\uparrow \leftrightarrow \downarrow$) of the particle pair that enters the single-particle EOM [cf. Eqs. (34) and (35)] which simplifies the equations. Numerical results for the T^{pp}-G1-G2 scheme are presented in Sec. VII.

4. T^{pp}-G1-G2 equations for jellium

Turning now to the uniform electron gas, Eq. (39), we again use the interaction matrix of Eq. (40) and define

$$\Lambda^{\mathrm{pp},\alpha\beta}_{\boldsymbol{p},\bar{\boldsymbol{p}},\boldsymbol{q}}(t) := \Lambda^{\mathrm{pp},\alpha\beta\alpha\beta}_{\boldsymbol{p}-\boldsymbol{q},\bar{\boldsymbol{p}}+\boldsymbol{q},\boldsymbol{p},\bar{\boldsymbol{p}}}(t)\,.$$

With that, the equation of motion for the time-diagonal two-particle Green function becomes,

$$\begin{aligned} &i\hbar\frac{d}{dt}\mathcal{G}^{\alpha\beta}_{\boldsymbol{p}\bar{\boldsymbol{p}}\boldsymbol{q}}(t) - \mathcal{G}^{\alpha\beta}_{\boldsymbol{p}\bar{\boldsymbol{p}}\boldsymbol{q}}(t)\big(h^{\mathrm{HF},\alpha}_{\boldsymbol{p}-\boldsymbol{q}} + h^{\mathrm{HF},\beta}_{\bar{\boldsymbol{p}}+\boldsymbol{q}} - h^{\mathrm{HF},\alpha}_{\boldsymbol{p}} - h^{\mathrm{HF},\beta}_{\bar{\boldsymbol{p}}}\big)(t) \\ &\quad = \Psi^{\pm,\alpha\beta}_{\boldsymbol{p}\bar{\boldsymbol{p}}\boldsymbol{q}}(t) + \Lambda^{\mathrm{pp},\alpha\beta}_{\boldsymbol{p},\bar{\boldsymbol{p}},\boldsymbol{q}}(t) - \big[\Lambda^{\mathrm{pp},\alpha\beta}_{\boldsymbol{p}-\boldsymbol{q},\bar{\boldsymbol{p}}+\boldsymbol{q},-\boldsymbol{q}}(t)\big]^*\,, \end{aligned}$$

where the momentum representation of the particle-particle ladder term is given by

$$\begin{aligned} \Lambda^{\mathrm{pp},\alpha\beta}_{\boldsymbol{p},\bar{\boldsymbol{p}},\boldsymbol{q}}(t) &= (i\hbar)^2\big[G^{>,\alpha}_{\boldsymbol{p}-\boldsymbol{q}}(t)G^{>,\beta}_{\bar{\boldsymbol{p}}+\boldsymbol{q}}(t) - G^{<,\alpha}_{\boldsymbol{p}-\boldsymbol{q}}(t)G^{<,\beta}_{\bar{\boldsymbol{p}}+\boldsymbol{q}}(t)\big] \\ &\quad\times\sum_{\boldsymbol{k}} v_{|\boldsymbol{k}-\boldsymbol{q}|}(t)\mathcal{G}^{\alpha\beta}_{\boldsymbol{p}\bar{\boldsymbol{p}}\boldsymbol{k}}(t)\,. \end{aligned} \tag{79}$$

B. Particle-hole T matrix

For the T matrix in the particle-hole channel [28], the derivations of the single-time equations are performed in a similar fashion as for the particle-particle T matrix in Sec. V A. The detailed derivation is given in Appendix C. Here, we summarize the main findings.

1. T^{ph}-G1-G2 equations for a general basis

As for the GW and the TPP approximations, two quasi-Hamiltonians are introduced,

$$\begin{aligned} \mathfrak{h}^{\Omega^{\mathrm{ph}},\mathrm{HF}}_{ijkl}(t) &= \delta_{jl}h^{\mathrm{HF}}_{ik} - \delta_{ik}h^{\mathrm{HF}}_{jl}\,, \\ \mathfrak{h}^{\Omega^{\mathrm{ph}},\mathrm{corr}}_{ijkl}(t) &= (i\hbar)^2\sum_{pq}\big[\mathcal{G}^{\mathrm{F},>}_{iqlp}(t) - \mathcal{G}^{\mathrm{F},<}_{iqlp}(t)\big]w_{pjkq}(t), \end{aligned} \tag{80}$$

and combined into a single quantity,

$$\mathfrak{h}^{\Omega^{\mathrm{ph}}}_{ijkl}(t) = \mathfrak{h}^{\Omega^{\mathrm{ph}},\mathrm{HF}}_{ijkl}(t) + \mathfrak{h}^{\Omega^{\mathrm{ph}},\mathrm{corr}}_{ijkl}(t)\,. \tag{81}$$

The corresponding Møller operator of the particle-hole T matrix again obeys a time-dependent two-particle Schrödinger equation,

$$i\hbar\frac{d}{dt}\Omega^{\mathrm{ph},\gtrless}_{ijkl}(t \gtrless t') = \sum_{pq}\mathfrak{h}^{\Omega^{\mathrm{ph}}}_{ipql}(t)\Omega^{\mathrm{ph},\gtrless}_{qjkp}(t \gtrless t')\,. \tag{82}$$

The time derivative of $\mathcal{G}$ in TPH approximation follows as

$$\begin{aligned} i\hbar\frac{d}{dt}\mathcal{G}_{ijkl}(t) = \Psi^{\pm}_{ijkl}(t) + \sum_{pq}\Big\{&\mathfrak{h}^{\Omega^{\mathrm{ph}}}_{ipql}(t)[\mathcal{G}_{kpqj}(t)]^* \\ &- \mathcal{G}_{ipql}(t)\big[\mathfrak{h}^{\Omega^{\mathrm{ph}}}_{kpqj}(t)\big]^*\Big\}\,. \end{aligned} \tag{83}$$

Again, for practical use, it is convenient to separate the correlation contributions from the mean-field terms via the introduction of an additional quantity:

$$\begin{aligned} &i\hbar\frac{d}{dt}\mathcal{G}_{ijkl}(t) - [h^{(2),\mathrm{HF}},\mathcal{G}]_{ijkl}(t) \\ &\quad = \Psi^{\pm}_{ijkl}(t) + \Lambda^{\mathrm{ph}}_{ijkl}(t) - \big[\Lambda^{\mathrm{ph}}_{klij}(t)\big]^*\,, \end{aligned}$$

where the particle-hole ladder term is defined by

$$\Lambda^{\mathrm{ph}}_{ijkl}(t) = \sum_{pq}\mathfrak{h}^{\Omega^{\mathrm{ph}},\mathrm{corr}}_{ipql}(t)\mathcal{G}_{qjkp}(t)\,. \tag{84}$$

As in the case of the particle-particle T matrix, Sec. V A, neglect of the Λ terms exactly recovers the equation of motion for $\mathcal{G}$ in second-order Born approximation. Inclusion of theses terms, on the other hand, accounts for the entire Born series.

2. T^{ph}-G1-G2 equations for the Hubbard basis

For the Hubbard system (for the definitions, see Sec. III C), we find,

$$\begin{aligned} &i\hbar\frac{d}{dt}\mathcal{G}^{\uparrow\downarrow\uparrow\downarrow}_{ijkl}(t) - \big[h^{(2),\mathrm{HF}}_{\uparrow\downarrow},\mathcal{G}^{\uparrow\downarrow\uparrow\downarrow}\big]_{ijkl}(t) \\ &\quad = \Psi^{\uparrow\downarrow\uparrow\downarrow}_{ijkl}(t) + \Lambda^{\mathrm{ph},\uparrow\downarrow\uparrow\downarrow}_{ijkl}(t) - \big[\Lambda^{\mathrm{ph},\uparrow\downarrow\uparrow\downarrow}_{klij}(t)\big]^*\,, \end{aligned}$$

where we introduced the particle-hole ladder term for the Hubbard system

$$\begin{aligned} \Lambda^{\mathrm{ph},\uparrow\downarrow\uparrow\downarrow}_{ijkl}(t) &= (i\hbar)^2U(t)\sum_{p}\big[G^{>,\uparrow}_{ip}(t)G^{<,\downarrow}_{pl}(t) \\ &\quad - G^{<,\uparrow}_{ip}(t)G^{>,\downarrow}_{pl}(t)\big]\mathcal{G}^{\uparrow\downarrow\uparrow\downarrow}_{pjkp}(t)\,. \end{aligned} \tag{85}$$

Similar to the behavior in the TPP case, only one spin combination (two when considering $\uparrow \leftrightarrow \downarrow$) contributes to the single-particle EOM in Eqs. (34) and (35). The T^{ph}-G1-G2 scheme for the Hubbard model is numerically tested in Sec. VII.

3. T^{ph}-G1-G2 equations for jellium

For the uniform electron gas, Eq. (39), we again use the interaction matrix of Eq. (40), and define

$$\Lambda^{\mathrm{ph},\alpha\beta}_{\boldsymbol{p},\bar{\boldsymbol{p}},\boldsymbol{q}}(t) := \Lambda^{\mathrm{ph},\alpha\beta\alpha\beta}_{\boldsymbol{p}-\boldsymbol{q},\bar{\boldsymbol{p}}+\boldsymbol{q},\boldsymbol{p},\bar{\boldsymbol{p}}}(t)\,.$$

With that, the equation of motion for the time-diagonal two-particle Green function becomes

$$\begin{aligned} &i\hbar\frac{d}{dt}\mathcal{G}^{\alpha\beta}_{\boldsymbol{p}\bar{\boldsymbol{p}}\boldsymbol{q}}(t) - \mathcal{G}^{\alpha\beta}_{\boldsymbol{p}\bar{\boldsymbol{p}}\boldsymbol{q}}(t)\big(h^{\mathrm{HF},\alpha}_{\boldsymbol{p}-\boldsymbol{q}} + h^{\mathrm{HF},\beta}_{\bar{\boldsymbol{p}}+\boldsymbol{q}} - h^{\mathrm{HF},\alpha}_{\boldsymbol{p}} - h^{\mathrm{HF},\beta}_{\bar{\boldsymbol{p}}}\big)(t) \\ &\quad = \Psi^{\pm,\alpha\beta}_{\boldsymbol{p}\bar{\boldsymbol{p}}\boldsymbol{q}}(t) + \Lambda^{\mathrm{ph},\alpha\beta}_{\boldsymbol{p},\bar{\boldsymbol{p}},\boldsymbol{q}}(t) - \big[\Lambda^{\mathrm{ph},\alpha\beta}_{\boldsymbol{p}-\boldsymbol{q},\bar{\boldsymbol{p}}+\boldsymbol{q},-\boldsymbol{q}}(t)\big]^*\,, \end{aligned}$$

with the momentum representation of the particle-hole ladder term, given by

$$\begin{aligned} \Lambda^{\mathrm{ph},\alpha\beta}_{\boldsymbol{p},\bar{\boldsymbol{p}},\boldsymbol{q}}(t) &= (i\hbar)^2\big[G^{>,\alpha}_{\boldsymbol{p}-\boldsymbol{q}}(t)G^{<,\beta}_{\bar{\boldsymbol{p}}}(t) - G^{<,\alpha}_{\boldsymbol{p}-\boldsymbol{q}}(t)G^{>,\beta}_{\bar{\boldsymbol{p}}}(t)\big] \\ &\quad\times\sum_{\boldsymbol{k}} v_{|\boldsymbol{k}|}(t)\mathcal{G}^{\alpha\beta}_{\boldsymbol{p},\bar{\boldsymbol{p}}-\boldsymbol{k},\boldsymbol{q}+\boldsymbol{k}}(t)\,. \end{aligned} \tag{86}$$

VI. DYNAMICALLY-SCREENED-LADDER APPROXIMATION

So far we have considered three important self-energy approximations: the second-Born approximation, GW, and the particle-particle and particle-hole T matrices. While GW

describes dynamical screening, for weakly coupled systems, the T-matrix self energy accounts for strong coupling but neglects dynamical-screening effects. Therefore, the question arises how to combine strong coupling and dynamical screening into a single model in a computationally feasible way. An approximation to realize this, within NEGF theory, is the fluctuating-exchange approximation (FLEX) that combines T matrix and GW contributions according to $\Sigma = \Sigma_{\mathrm{TPP}} + \Sigma_{\mathrm{TPH}} + \Sigma_{GW} - 2\Sigma_{\mathrm{SOA}}$, where the last term is needed to avoid double counting; for more details, see Ref. [28]. A fully self-consistent treatment of dynamical-screening and strong-coupling effects is provided by the dynamically-screened-ladder approximation that has been studied in the context of the bound-state problem in a plasma medium in equilibrium [72]. For more details, see Ref. [73].

The G1-G2 scheme allows for a straightforward way to combine the GW (including exchange) and both T-matrix approximations in a self-consistent way for arbitrary nonequilibrium situations. This is achieved by including in the EOM of the time-diagonal two-particle Green function the terms with all effective Hamiltonians that were derived for GW, the particle-particle and the particle-hole T matrix, respectively, cf. Eqs. (56), (74), and (81). Then, the EOM for $\mathcal{G}$, in a general basis becomes

$$\begin{aligned} i\hbar\frac{d}{dt}\mathcal{G}_{ijkl}(t) &- \left[h^{(2),\mathrm{HF}},\mathcal{G}\right]_{ijkl}(t) \\ &= \Psi^{\pm}_{ijkl}(t) + \sum_{pq}\Big\{\mathfrak{h}^{\varepsilon,\mathrm{corr}}_{qjpl}(t)[\mathcal{G}_{qkpi}(t)]^* \\ &\quad - \mathcal{G}_{qjpl}(t)\left[\mathfrak{h}^{\varepsilon,\mathrm{corr}}_{qkpi}(t)\right]^*\Big\} + \sum_{pq}\Big\{\mathfrak{h}^{\Omega^{\mathrm{pp}},\mathrm{corr}}_{ijpq}(t)[\mathcal{G}_{klpq}(t)]^* \\ &\quad - \mathcal{G}_{ijpq}(t)\left[\mathfrak{h}^{\Omega^{\mathrm{pp}},\mathrm{corr}}_{klpq}(t)\right]^*\Big\} + \sum_{kl}\Big\{\mathfrak{h}^{\Omega^{\mathrm{ph}},\mathrm{corr}}_{ipql}(t)[\mathcal{G}_{kpqj}(t)]^* \\ &\quad - \mathcal{G}_{ipql}(t)\left[\mathfrak{h}^{\Omega^{\mathrm{ph}},\mathrm{corr}}_{kpqj}(t)\right]^*\Big\}. \end{aligned} \tag{87}$$

Alternatively, we can rewrite this equation by using the polarization (Π) and ladder (Λ) terms that were defined by Eqs. (61), (77), and (84),

$$\begin{aligned} i\hbar\frac{d}{dt}\mathcal{G}_{ijkl}(t) - \left[h^{(2),\mathrm{HF}},\mathcal{G}\right]_{ijkl}(t) &= \Psi^{\pm}_{ijkl}(t) \\ + \Pi_{ijkl}(t) - [\Pi_{lkji}(t)]^* + \Lambda_{ijkl}(t) - [\Lambda_{klij}(t)]^*&, \end{aligned} \tag{88}$$

where we combined both ladder terms into

$$\Lambda_{ijkl}(t) = \Lambda^{\mathrm{pp}}_{ijkl}(t) + \Lambda^{\mathrm{ph}}_{ijkl}(t).$$

Obviously, Eq. (88) is a generalization of all previous cases: It additively includes the contributions of the second-order Born self energy (first line), polarization terms that account for dynamical screening and strong-coupling terms. The SOA term that appears in each of the different approximations is included only once, so no double counting occurs. Since all contributions are treated on the same footing, this equation amounts to a simultaneous full account of dynamical screening and strong binary correlations. Alternatively, this approximation can be obtained from reduced-density-operator theory by neglecting three-particle and higher correlations [5]; an early discussion was presented by Wang and Cassing [74].

TABLE I. Scaling of the CPU time with the number of time steps N_t and basis dimension N_b of the traditional non-Markovian HF-GKBA ("standard") and the present time-local scheme (G1-G2), for three relevant basis sets and the self-energy approximations considered in this paper: the second-Born approximation (SOA), GW approximation (GW), the particle-particle (TPP) and particle-hole (TPH) T matrices, and the dynamically-screened-ladder approximation (DSL). Last column: CPU speedup ratio of the G1-G2 scheme compared to standard HF-GKBA. For DSL, currently no standard HF-GKBA version exists. Note that full two-time NEGF simulations always have cubic scaling with N_t.

		HF-GKBA		Speedup
Σ	Basis	Standard	G1-G2	ratio
SOA	general	$\mathcal{O}(N_b^5N_t^2)$	$\mathcal{O}(N_b^5N_t^1)$	$\mathcal{O}(N_t)$
	Hubbard	$\mathcal{O}(N_b^3N_t^2)$	$\mathcal{O}(N_b^4N_t^1)$	$\mathcal{O}(N_t/N_b)$
	jellium	$\mathcal{O}(N_b^3N_t^2)$	$\mathcal{O}(N_b^3N_t^1)$	$\mathcal{O}(N_t)$
GW	general	$\mathcal{O}(N_b^6N_t^3)$	$\mathcal{O}(N_b^6N_t^1)$	$\mathcal{O}(N_t^2)$
	Hubbard	$\mathcal{O}(N_b^3N_t^3)$	$\mathcal{O}(N_b^4N_t^1)$	$\mathcal{O}(N_t^2/N_b)$
	jellium	$\mathcal{O}(N_b^3N_t^3)$	$\mathcal{O}(N_b^3N_t^1)$	$\mathcal{O}(N_t^2)$
TPP	general	$\mathcal{O}(N_b^6N_t^3)$	$\mathcal{O}(N_b^6N_t^1)$	$\mathcal{O}(N_t^2)$
	Hubbard	$\mathcal{O}(N_b^3N_t^3)$	$\mathcal{O}(N_b^4N_t^1)$	$\mathcal{O}(N_t^2/N_b)$
	jellium	$\mathcal{O}(N_b^3N_t^3)$	$\mathcal{O}(N_b^4N_t^1)$	$\mathcal{O}(N_t^2/N_b)$
TPH	general	$\mathcal{O}(N_b^6N_t^3)$	$\mathcal{O}(N_b^6N_t^1)$	$\mathcal{O}(N_t^2)$
	Hubbard	$\mathcal{O}(N_b^3N_t^3)$	$\mathcal{O}(N_b^4N_t^1)$	$\mathcal{O}(N_t^2/N_b)$
	jellium	$\mathcal{O}(N_b^3N_t^3)$	$\mathcal{O}(N_b^4N_t^1)$	$\mathcal{O}(N_t^2/N_b)$
DSL	general	–	$\mathcal{O}(N_b^6N_t^1)$	–
	Hubbard	–	$\mathcal{O}(N_b^4N_t^1)$	–
	jellium	–	$\mathcal{O}(N_b^4N_t^1)$	–

It is easily verified that the entire Eq. (87) requires a CPU time that has the same linear scaling with N_t as all the special cases that were studied before. On the other hand, the polarization and ladder terms determine the scaling with the basis size N_b. This is summarized in Table I and discussed in more detail in Sec. VII.

VII. ANALYSIS OF THE NUMERICAL SCALING

As was shown in the previous sections, the G1-G2 scheme transforms the time-diagonal KBE within the HF-GKBA to a memory-less, time-local form. This means, the theoretical scaling is first order in the propagation duration. This dramatic acceleration is achieved by propagating, in addition to the single-particle Green function, also the time-diagonal two-particle Green function $\mathcal{G}$. This function has, in general, four basis indices and, thus, a dimensionality of N_b^4, where N_b is the single-particle basis dimension. The total scaling of the G1-G2 scheme with N_b depends on the self energy and on the type of basis. In the following, we investigate this scaling more in detail, extending the analysis of Ref. [39].

A. Second-order Born self energy

We start by analyzing the N_b scaling of the SOA-G1-G2 equation for $\mathcal{G}$, Eq. (29), which we rewrite in a different

form

$$
\begin{aligned}
&i\hbar\frac{d}{dt}\mathcal{G}_{ijkl}(t) - \left[h^{(2),\mathrm{HF}},\mathcal{G}\right]_{ijkl}(t)\\
&\quad = (i\hbar)^2\sum_p G^{>}_{ip}(t)\sum_q G^{>}_{jq}(t)\sum_r G^{<}_{rk}(t)\sum_s w^{\pm}_{pqrs}(t)G^{<}_{sl}(t)\\
&\qquad - (i\hbar)^2\sum_p G^{<}_{ip}(t)\sum_q G^{<}_{jq}(t)\sum_r G^{>}_{rk}(t)\sum_s w^{\pm}_{pqrs}(t)G^{>}_{sl}(t)\,.
\end{aligned}
$$

The r.h.s. of this equation contains four sums of dimensionality N_b which are all independent of each other. They are evaluated by successive execution of the occurring tensor contractions. This means the total scaling of the CPU time, in this case, is of order N_b^5.

For the Hubbard basis a first look at Eqs. (36)–(38) suggests an N_b^5-scaling, due to the commutator term in Eq. (36) and the summation in the Φ term of Eq. (38). However, in the Hubbard model the scaling can be further reduced. Note that the Hartree-Fock Hamiltonian, $h^{\mathrm{HF}}(t)$, is a tridiagonal matrix and, thus, the commutator can be computed with N_b^4 effort:

$$
\begin{aligned}
&\left[h^{(2),\mathrm{HF}}_{\uparrow\downarrow},\mathcal{G}^{\uparrow\downarrow\uparrow\downarrow}\right]_{ijkl}(t)\\
&\quad = \sum_p\Big[h^{\mathrm{HF},\uparrow}_{ip}(t)\mathcal{G}^{\uparrow\downarrow\uparrow\downarrow}_{pjkl}(t) + h^{\mathrm{HF},\downarrow}_{jp}(t)\mathcal{G}^{\uparrow\downarrow\uparrow\downarrow}_{ipkl}(t)\\
&\qquad - \mathcal{G}^{\uparrow\downarrow\uparrow\downarrow}_{ijpl}(t)h^{\mathrm{HF},\uparrow}_{pk}(t) - \mathcal{G}^{\uparrow\downarrow\uparrow\downarrow}_{ijkp}(t)h^{\mathrm{HF},\downarrow}_{pl}(t)\Big]\\
&\quad = -i\hbar U(t)\mathcal{G}^{\uparrow\downarrow\uparrow\downarrow}_{ijkl}(t)\big[G^{\downarrow}_{ii}(t) + G^{\uparrow}_{jj}(t) - G^{\downarrow}_{kk}(t) - G^{\uparrow}_{ll}(t)\big]\\
&\qquad - J\sum_p\Big[\delta_{\langle i,p\rangle}\mathcal{G}^{\uparrow\downarrow\uparrow\downarrow}_{pjkl}(t) + \delta_{\langle j,p\rangle}\mathcal{G}^{\uparrow\downarrow\uparrow\downarrow}_{ipkl}(t)\\
&\qquad - \mathcal{G}^{\uparrow\downarrow\uparrow\downarrow}_{ijpl}(t)\delta_{\langle p,k\rangle} - \mathcal{G}^{\uparrow\downarrow\uparrow\downarrow}_{ijkp}(t)\delta_{\langle p,l\rangle}\Big]\,.
\end{aligned}
$$

On the other hand, the Φ term can be simplified by using the identity of Eq. (11):

$$
\begin{aligned}
&\Phi^{\uparrow\downarrow\uparrow\downarrow}_{ijkl}(t)\\
&\quad = (i\hbar)^4\sum_p\left\{\left[G^{<,\uparrow}_{ip}(t) + \frac{1}{i\hbar}\delta_{ip}\right]\left[G^{<,\downarrow}_{jp}(t) + \frac{1}{i\hbar}\delta_{jp}\right]\right.\\
&\qquad \times G^{<,\uparrow}_{pk}(t)G^{<,\downarrow}_{pl}(t) - G^{<,\uparrow}_{ip}(t)G^{<,\downarrow}_{jp}(t)\\
&\qquad \left.\times\left[G^{<,\uparrow}_{pk}(t) + \frac{1}{i\hbar}\delta_{pk}\right]\left[G^{<,\downarrow}_{pl}(t) + \frac{1}{i\hbar}\delta_{pl}\right]\right\}\\
&\quad = (i\hbar)^2(\delta_{ij}-\delta_{kl})G^{<,\uparrow}_{ik}(t)G^{<,\downarrow}_{jl}(t)\\
&\qquad + (i\hbar)^3[G^{<,\uparrow}_{ij}(t)G^{<,\uparrow}_{jk}(t) - G^{<,\uparrow}_{lk}(t)G^{<,\uparrow}_{il}(t)]G^{<,\downarrow}_{jl}(t)\\
&\qquad + (i\hbar)^3[G^{<,\downarrow}_{ji}(t)G^{<,\downarrow}_{il}(t) - G^{<,\downarrow}_{kl}(t)G^{<,\downarrow}_{jk}(t)]G^{<,\uparrow}_{ik}(t)\,.
\end{aligned}
\tag{89}
$$

Here, the leading contribution to the difference, $G^<G^<G^<G^< - G^<G^<G^<G^<$, cancels (contribution with four functions $G^<$) which reduces the complexity. For the Hubbard basis, this reduces the numerical effort of the G1-G2 scheme to a N_b^4 scaling compared to the N_b^5-scaling in the straightforward implementation [39]. In total, an acceleration is achieved for the SOA-G1-G2 scheme, compared to the ordinary HF-GKBA if $N_t \gtrsim N_b$, as summarized in Table I.

The reformulation above that eliminates products of four $G^<$ functions can be made for any basis choice. However, for the general basis this does not result in an improved N_b scaling. For the jellium basis the Eqs. (41)–(43) reveal a particularly favorable scaling with the basis size with N_b^3 for which the above reformulation does not provide further improvement.

B. *GW* self energy

The additional terms of the *GW* approximation can change the N_b scaling compared to the SOA case discussed in the previous section. For the general basis, the leading-order terms for the scaling with the basis size are found in Eqs. (55) and (61) which reveal a N_b^6 scaling. For this case no further reductions are possible, cf. Table I.

For the Hubbard basis the polarization terms [Eqs. (64) and (65)] can be reformulated by again using Eq. (11) to get

$$
\begin{aligned}
\Pi^{\uparrow\downarrow\uparrow\downarrow}_{ijkl}(t) &= -i\hbar U(t)G^{<,\downarrow}_{jl}(t)[\mathcal{G}^{\uparrow\uparrow\uparrow\uparrow}_{ijkj}(t) - \mathcal{G}^{\uparrow\uparrow\uparrow\uparrow}_{ilkl}(t)]\,,\\
\Pi^{\uparrow\uparrow\uparrow\uparrow}_{ijkl}(t) &= -i\hbar U(t)G^{<,\uparrow}_{jl}(t)[\mathcal{G}^{\uparrow\downarrow\uparrow\downarrow}_{ijkj}(t) - \mathcal{G}^{\uparrow\downarrow\uparrow\downarrow}_{ilkl}(t)]\,.
\end{aligned}
$$

From this, it is obvious that, compared to the second-order Born approximation, no further complexity is added for *GW* in the Hubbard case, and the scaling with the basis size remains N_b^4.

To explore the N_b scaling for the jellium basis we recall the polarization term, Eq. (66),

$$
\begin{aligned}
\Pi^{\alpha\beta}_{\boldsymbol{p},\bar{\boldsymbol{p}},\boldsymbol{q}}(t) = \pm(i\hbar)^2\big[&G^{>,\beta}_{\bar{\boldsymbol{p}}+\boldsymbol{q}}(t)G^{<,\beta}_{\bar{\boldsymbol{p}}}(t) - G^{<,\beta}_{\bar{\boldsymbol{p}}+\boldsymbol{q}}(t)G^{>,\beta}_{\bar{\boldsymbol{p}}}(t)\big]\\
&\times v_{|\boldsymbol{q}|}(t)\sum_{\boldsymbol{k},\sigma}\mathcal{G}^{\alpha\sigma}_{\boldsymbol{pkq}}(t)\,.
\end{aligned}
$$

As one can see, the tensor contraction over $\boldsymbol{k}$ can be executed independently of $\bar{\boldsymbol{p}}$. Thus, the full scaling of the *GW*-G1-G2 scheme for a jellium basis remains of order N_b^3, as in the case of the standard HF-GKBA.

C. *T*-matrix self energies

The T-matrix equations [Sec. V] behave very similar to the *GW* equations. For a general basis set with a four-index interaction tensor both, TPP and TPH scale as N_b^6 which can be directly seen from Eqs. (73) and (77), as well as Eqs. (80) and (84).

For the Hubbard basis we can now use Eq. (11) to eliminate contributions that are of second order in $G^<$ from the ladder terms in Eq. (78),

$$
\begin{aligned}
\Lambda^{\mathrm{pp},\uparrow\downarrow\uparrow\downarrow}_{ijkl}(t) = \delta_{ij}U(t)\mathcal{G}^{\uparrow\downarrow\uparrow\downarrow}_{ijkl}(t) + i\hbar U(t)[&G^{<,\downarrow}_{ji}(t)\mathcal{G}^{\uparrow\downarrow\uparrow\downarrow}_{iikl}(t)\\
&+ G^{<,\uparrow}_{ij}(t)\mathcal{G}^{\uparrow\downarrow\uparrow\downarrow}_{jjkl}(t)]\,,
\end{aligned}
$$

as well as in Eq. (85),

$$
\Lambda^{\mathrm{ph},\uparrow\downarrow\uparrow\downarrow}_{ijkl}(t) = i\hbar U(t)[G^{<,\downarrow}_{il}(t)\mathcal{G}^{\uparrow\downarrow\uparrow\downarrow}_{ijki}(t) - G^{<,\uparrow}_{il}(t)\mathcal{G}^{\uparrow\downarrow\uparrow\downarrow}_{ljkl}(t)]\,.
$$

For both cases one can see that the remaining scaling order of the equations is N_b^4 since all internal summations have been eliminated.

In the jellium basis the T matrices show a different scaling behavior compared to *GW*. To see this, we reproduce the two

ladder terms of Eqs. (79) and (86),

$$\Lambda^{\mathrm{pp},\alpha\beta}_{\boldsymbol{p},\bar{\boldsymbol{p}},\boldsymbol{q}}(t) = (i\hbar)^2\big[G^{>,\alpha}_{\boldsymbol{p}-\boldsymbol{q}}(t)G^{>,\beta}_{\bar{\boldsymbol{p}}+\boldsymbol{q}}(t) - G^{<,\alpha}_{\boldsymbol{p}-\boldsymbol{q}}(t)G^{<,\beta}_{\bar{\boldsymbol{p}}+\boldsymbol{q}}(t)\big] \times \sum_{\boldsymbol{k}} v_{|\boldsymbol{k}-\boldsymbol{q}|}(t)\mathcal{G}^{\alpha\beta}_{\boldsymbol{p}\bar{\boldsymbol{p}}\boldsymbol{k}}(t)\,,$$

$$\Lambda^{\mathrm{ph},\alpha\beta}_{\boldsymbol{p},\bar{\boldsymbol{p}},\boldsymbol{q}}(t) = (i\hbar)^2\big[G^{>,\alpha}_{\boldsymbol{p}-\boldsymbol{q}}(t)G^{<,\beta}_{\bar{\boldsymbol{p}}}(t) - G^{<,\alpha}_{\boldsymbol{p}-\boldsymbol{q}}(t)G^{>,\beta}_{\bar{\boldsymbol{p}}}(t)\big] \times \sum_{\boldsymbol{k}} v_{|\boldsymbol{k}|}(t)\mathcal{G}^{\alpha\beta}_{\boldsymbol{p},\bar{\boldsymbol{p}}-\boldsymbol{k},\boldsymbol{q}+\boldsymbol{k}}(t)\,.$$

Evidently, in both cases the tensor contraction of $\boldsymbol{k}$ depends on all other momenta $\boldsymbol{p}$, $\bar{\boldsymbol{p}}$, $\boldsymbol{q}$. Thus, the final scaling with the basis size becomes of order N_b^4. A summary of the numerical scaling with the propagation duration and the basis size is presented in Table. I.

At the same time, any practical implementation of the G1-G2 scheme could, in principle, carry a large overhead that prevents us from achieving the theoretical scaling with the simulation duration and the basis dimension within a relevant parameter range. We, therefore, have implemented the G1-G2 scheme for each of the self energies discussed in this paper and present representative numerical results in Sec. VII D.

D. Numerical results for the Hubbard basis

As we have shown above (cf. Table I), the Hubbard basis is the most unfavorable case for the G1-G2 scheme. Therefore, we choose this case for numerical demonstrations. In Ref. [39] we presented the first numerical tests of this scheme and demonstrated that, for finite Hubbard clusters the predicted linear scaling is indeed achieved for SOA and *GW* self energies, already for rather small values N_t.

Here we extend these simulations to the T-matrix self energies and the DSL approximation. Furthermore, we practically confirm the N_b scaling. As a first test, we verify that the derived formulas of the G1-G2 scheme are equivalent to the original (non-Markovian) HF-GKBA formulation. As a test case we consider, in Fig. 2, the time evolution in a Hubbard dimer for SOA, *GW*, TPP, and TPH self energies. For both considered methods, the original HF-GKBA and the G1-G2 scheme, a fourth-order Runge-Kutta integration scheme with a time step of $\Delta t = 0.02\hbar/J$ is used. The agreement is excellent, and the deviations are mostly due to the original HF-GKBA, as discussed in Ref. [39].

Next, we demonstrate the scaling with the basis dimension N_b for the SOA self energy. In Fig. 3 we show results for a large number of Hubbard chains of varying length, $N_b = 2 \ldots 100$. We clearly confirm the N_b^5 scaling for the standard implementation of the G1-G2 scheme that uses Eq. (38) [39]. This asymptotic behavior is reached already for $N_b \gtrsim 20$. The second curve is for the same setup but uses the optimization, Eq. (89). Again, the predicted improved scaling according to N_b^4 is clearly identified, at least for $N_b \gtrsim 50$. This confirms the expected speedup of the SOA-G1-G2 scheme compared to the standard HF-GKBA, if $N_t \gtrsim N_b$. Thus, even for the most unfavorable case of a Hubbard basis [cf. Table I] the scaling advantage should be reached already for small simulation durations.

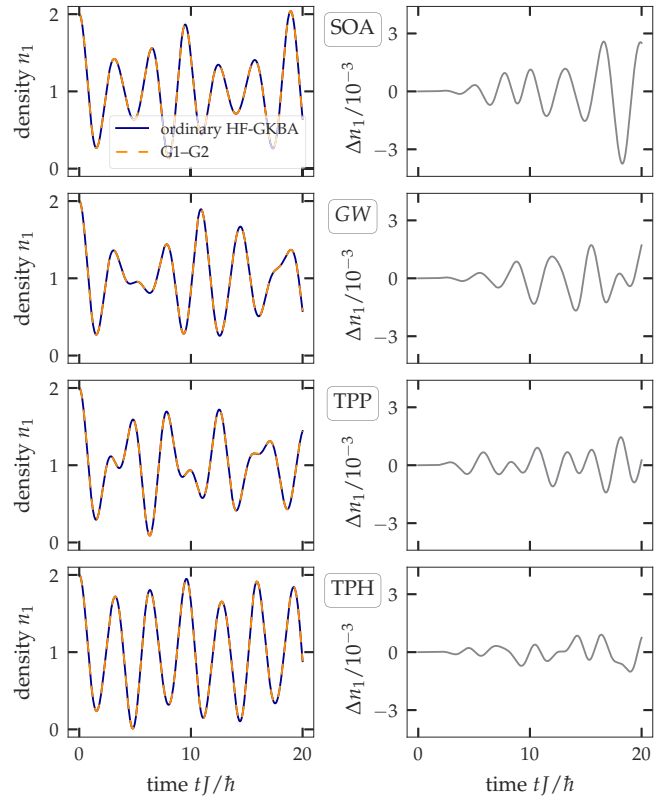

FIG. 2. Comparison of the ordinary HF-GKBA and the G1-G2 scheme for a Hubbard dimer with $U = J$ at half filling. The initial state was uncorrelated with the entire density concentrated at the first lattice site. Rows correspond to SOA, *GW*, TPP, and TPH self energies. Right column shows the deviation $\Delta n_1(t) = n_1^{\mathrm{G1-G2}}(t) - n_1^{\mathrm{ordinary}}(t)$ of the densities of both schemes on site 1.

To explore the scaling with N_t in more detail we have performed a series of simulations for all self-energy approximations, comparing the standard HF-GKBA to the G1-G2 scheme. The results are shown in Fig. 4 and confirm the quadratic (cubic) scaling of the CPU time with N_t, for the standard HF-GKBA with SOA (*GW*) self energy. Similar cubic scaling is observed for the two T-matrix approximations

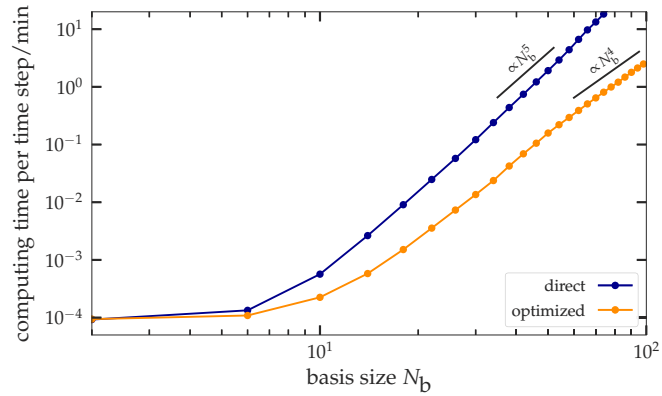

FIG. 3. CPU-time scaling of the SOA-G1-G2 scheme with the basis size N_b comparing the direct, Eq. (39) [39], and the optimized implementation, Eq. (89). Results are for a 1D Hubbard chain.

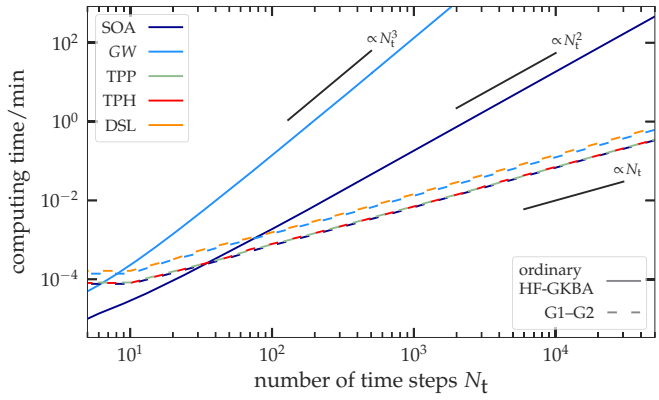

FIG. 4. CPU-time scaling with the simulation duration N_t, comparing the standard HF-GKBA to the G1-G2 scheme. G1-G2 data are shown for five self-energy approximations (indicated in the legend) all of which clearly exhibit linear scaling. In contrast, the standard HF-GKBA scales as N_t^2, for SOA, and N_t^3, for *GW*. Results are for a 10-site Hubbard chain.

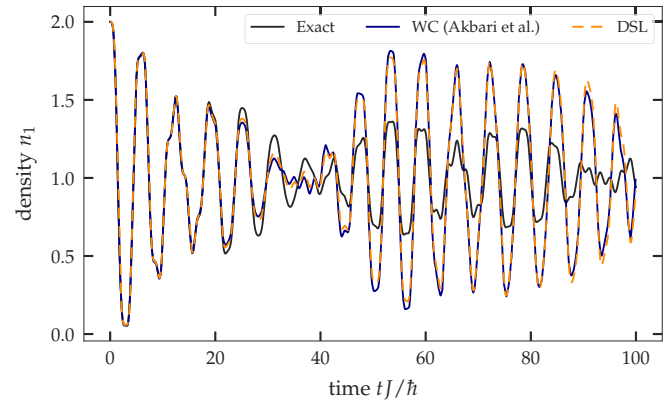

FIG. 5. Density evolution comparing the DSL-G1-G2 scheme to the results of Ref. [75] (WC) and exact-diagonalization simulations. The system is a four-site Hubbard chain at $U = 0.1J$ and half filling; the simulations started from a noninteracting (uncorrelated) initial state, where the first two sites are doubly occupied.

(not shown) whereas simulations with DSL approximation are not possible, at the moment. Let us now turn to the G1-G2 results (dashed lines). Each of the curves exhibits the predicted linear scaling, already for $N_t \gtrsim 20$. Interestingly, in the G1-G2 scheme, the CPU time required for the rather involved T-matrix approximations is only slightly above the time required for the comparatively simple SOA case. Equally remarkable is the observation that the *GW* and DSL approximations, which, in Hubbard, rely on cross-coupling spin components, are rather close to the former self energies.

Note that, for the present small system (10-site Hubbard chain) "break even" of the G1-G2 scheme is reached for all self energies compared to the ordinary SOA-HF-GKBA (dark blue curve) well below $N_t = 100$ whereas the original *GW*-HF-GKBA (light blue) is unfavorable, practically from the start. For larger times, the ordinary *GW*-HF-GKBA quickly turns out unfeasible (e.g., for $N_t \sim 10^3$ it requires 10^4 times longer simulations than *GW*-G1-G2), and the same applies to the T-matrix self energies. Thus, we conclude that, it is not just a quantitative gain in CPU time that the G1-G2 scheme delivers but, in many cases, highly accurate simulations (beyond the simple SOA self energy) become possible at all that are (currently) impossible otherwise.

In particular, at increased coupling, $U/J \gtrsim 2$, the SOA self energy is known to be inaccurate (for an analysis see Ref. [28]), and for reliable simulations, more advanced approximations are crucial. In that context the DSL approximation is particularly attractive because it contains the dominant correlation effects self consistently. Until now such simulations have only occasionally been reported, for very small systems and short propagation times. An example of a four-site Hubbard chain is shown in Fig. 5. We observe excellent agreement of our DSL-G1-G2 scheme to the Wang-Cassing (WC) approximation simulations of Akbari *et al.* [75] confirming the equivalence of the two approximations. The results show excellent quantitative agreement with exact-diagonalization data (black curve), however, for times $tJ/\hbar \gtrsim 30$ deviations are growing.

VIII. DISCUSSION AND OUTLOOK

In this paper we analyzed the properties of nonequilibrium Green functions in the frame of the generalized Kadanoff-Baym ansatz with Hartree-Fock propagators (HF-GKBA). Due to the non-Markovian structure of the collision integral, HF-GKBA simulations have an unfavorable quadratic (cubic) scaling with the number of time steps, for second-order Born (more complicated) self energies. At the same time, it has been reported earlier that this memory integral can be formally eliminated in favor of coupled time-local differential equations for the single-particle and two-particle density matrix [5,40]. An equivalent formulation in the framework of nonequilibrium Green functions has been established in Ref. [39]—the G1-G2 scheme. The formal equivalence between both approaches is important because it means that the G1-G2 scheme retains all attractive properties of the HF-GKBA: It is total-energy conserving and time reversible [56]. Furthermore, the most prominent self-energy approximations from NEGF theory that have been derived, e.g., using diagrammatic techniques, can be transformed into a time-local form, by applying the HF-GKBA.

The earlier analyses of the time-linear equations [5,40] concentrated mainly on spatially homogeneous systems (jellium) and did not include computational aspects such as the CPU-time requirement. The scaling with the propagation time and basis size have only recently been analyzed in detail in conjunction with the G1-G2 scheme [39], and it was confirmed that the N_t^1 scaling can be achieved in practice. Here, we substantially extended these results, including additional high-level self energies such as the particle-particle and particle-hole T-matrix self energies and the screened-ladder approximation. In each case N_t^1 scaling of the CPU time could be confirmed giving rise to a remarkable N_t^2-scaling advantage compared to the standard HF-GKBA scheme (Fig. 4) which was found to be independent of the single-particle basis used for the simulations. Furthermore, we re-analyzed the CPU-time scaling with the basis dimension N_b and observed that the G1-G2 scheme has an overhead, compared to standard HF-GKBA, that is, *at most*, first order in N_b, cf. Table I.

Even for the most unfavorable basis—the Hubbard basis—the G1-G2 scheme has only a N_b^1 overhead (down from a N_b^2 overhead reported in Ref. [39]) which could be achieved by a reformulation of the scattering term in the G2 equation, cf. Sec. VII A. Thus, we expect that the G1-G2 scheme outperforms the standard HF-GKBA approach, in all cases of practical relevance, which can be seen from the CPU-time scaling ratio summarized in the right column of Table I.

With the G1-G2 scheme NEGF simulations (within the HF-GKBA) have been brought to the same CPU-time scaling as many other time-dependent approaches, including semiclassical molecular dynamics, hydrodynamics, Boltzmann-type kinetic equations, TDDFT (adiabatic approximation), and the time-dependent Schrödinger equation. Most importantly, now long simulations are feasible that were previously prohibited by the memory structure (resulting in the N_t^2 or N_t^3 scaling discussed above) without compromising the quality of the treatment of electronic correlations. We also showed that the inclusion of initial correlations in the G1-G2 scheme is trivial, and their propagation again requires a CPU-time effort that is of order N_t. Also the precomputation of the correlated initial state, e.g., via imaginary-time stepping or adiabatic switching, see, e.g., Ref. [21], can be carried out separately and does not affect the propagation scaling.

While we presented numerical results only for the Hubbard model, even larger gains, compared to the standard HF-GKBA, are predicted for jellium (e.g., electron gas, dense quantum plasmas, electron-hole plasmas etc.) and for more general basis sets where the interaction tensor has four indices (e.g., electron dynamics in atoms and molecules). At the same time, the removal of the memory integral as the main CPU-time bottleneck was achieved by computing the dynamics of an additional quantity—the time-diagonal two-particle Green function $\mathcal{G}_{ijkl}$. Thus, the new bottleneck in the G1-G2 scheme is the memory cost to store this four-dimensional tensor (only the current values are required), but this can be mitigated by suitable parallelization concepts.

By mapping NEGF simulations to a time-local scheme for single-time quantities, it should be expected that close connections exist with reduced-density-operator theory (RDO) [5,39,40]. The latter has been an independent many-body approach that has been successfully applied in many areas, including semiconductor optics, see, e.g., Refs. [76,77], dense plasmas [32], correlated electrons [64,75,78], nuclear matter [79], and cold atoms [80]. Our results indicate the correspondence between important self-energy approximations of NEGF theory to closure relations of RDO and confirm and extend earlier results on the particle-particle T matrix [71] and the GW approximation [64]. We also investigated the simultaneous treatment of strong coupling and dynamical-screening effects by combining ladder and polarization terms in the equation for $\mathcal{G}$. This led us to the dynamically-screened-ladder approximation (DSL) in Sec. VI. This approximation includes all two-particle interaction contributions and is, thus, equivalent to an approximation considered by Wang and Cassing before [74]. The equivalence of the two approximations was confirmed by the excellent agreement with the numerical results of Akbari *et al.* [75] for a small Hubbard cluster, cf. Fig. 5. Consequently, all self-energy contributions that go beyond the DSL correspond to the (partial) account of three-particle correlations and, thus, additionally require (at least) the propagation of the time-diagonal three-particle Green function, when mapped to a time-linear scheme.

Despite the high quality of the DSL, we also observed that it is in quantitative agreement with exact diagonalization (CI) data (black curve in Fig. 5) only during the initial relaxation phase (for times $tJ/\hbar \lesssim 30$) [75]. So, clearly, more systematic comparisons to CI results, for a broader range of coupling strengths and filling fractions, are desirable to understand the applicability limits of the DSL. While CI simulations are limited to very small particle numbers (basis size N_b) the G1-G2 scheme in DSL and simpler approximations can treat much larger systems. To go beyond those parameters where the DSL approximation is valid, further improved approximations are in high demand. This will require one to partially include three-particle correlations. Examples are the Kirkwood superposition approximation of classical statistical physics [81] (for recent applications see Refs. [82,83]), the approximation by Nakatsuji and Yasuda [84,85], and self-energy corrections to the BBGKY hierarchy [5]. Another route to improvements starts from nonequilibrium Green functions theory where one approach is to apply the GKBA but replace the Hartree-Fock propagators by correlated propagators [21]. Another concept is to replace the GKBA entirely by an improved reconstruction ansatz. In both cases, the procedure outlined in the present paper will allow one to derive the corresponding improved G1-G2 scheme. Since the applicability limits of the GKBA are still not fully explored, full two-time NEGF simulations will remain indispensable for tests and benchmarks, see, e.g., Ref. [86].

In conclusion, let us come back to the remarkable capability of the G1-G2 scheme to efficiently perform long-time simulations of correlated-electron dynamics. With this it should be feasible to reach thermodynamic equilibrium (or a quasistationary or prethermalized state) of the electrons. At the same time, slower processes, such as the equilibration with heavier particles (e.g., with the lattice in solids or with ions in dense plasmas) will make it desirable to develop a multiscale approach. This can be based on approximate solutions of the G1-G2 equations, e.g., by using retardation expansions [5] or the correlation-time approximation [87], eventually approaching the Markovian Boltzmann equation or local thermodynamic equilibrium. In that case a connection of the kinetic simulations to quantum hydrodynamic models, see, e.g., Refs. [88,89], could be a promising approach.

ACKNOWLEDGMENTS

We thank K. Balzer and C. Makait for valuable comments. We acknowledge computing time at the North German Supercomputing Alliance (HLRN) via Grant SHP00015.

J.-P.J. and N.S. contributed equally to this work.

APPENDIX A: PROPERTIES OF THE TIME-EVOLUTION OPERATOR

In the following, we derive important properties of the one- and two-particle propagators.

1. Symmetry relations

The single-particle time-evolution operator $\mathcal{U}$ fulfills the symmetry

$$[\mathcal{U}_{ji}(t',t)]^* = \left[G^{\mathrm{R}}_{ji}(t',t) - G^{\mathrm{A}}_{ji}(t',t)\right]^* = -\mathcal{U}_{ij}(t,t')\,, \quad \text{(A1)}$$

where $[G^{\mathrm{A/R}}_{ji}(t,t')]^* = G^{\mathrm{R/A}}_{ij}(t',t)$ has been used. Likewise, the two-particle propagator obeys,

$$\left[\mathcal{U}^{(2)}_{klij}(t,t')\right]^* = [\mathcal{U}_{ki}(t,t')]^*[\mathcal{U}_{lj}(t,t')]^* = \mathcal{U}^{(2)}_{ijkl}(t',t)\,,$$

where Eq. (A1) has been used.

2. Group property

When applying the HF-GKBA the retarded and advanced propagators, $G^{\mathrm{R}}(t,t')$ and $G^{\mathrm{A}}(t,t')$, are used in HF approximation and, thus, obey the group property [36] for $t > \bar{t} > t'$:

$$G^{\mathrm{A}}_{ij}(t',t) = -i\hbar \sum_k G^{\mathrm{A}}_{ik}(t',\bar{t})G^{\mathrm{A}}_{kj}(\bar{t},t)\,, \quad \text{(A2)}$$

$$G^{\mathrm{R}}_{ij}(t,t') = i\hbar \sum_k G^{\mathrm{R}}_{ik}(t,\bar{t})G^{\mathrm{R}}_{kj}(\bar{t},t')\,. \quad \text{(A3)}$$

In the following, the group property for the propagator $\mathcal{U}$ is derived for all relevant time orderings. Starting with

$$i\hbar \sum_k \mathcal{U}_{ik}(t,\bar{t})\mathcal{U}_{kj}(\bar{t},t') = i\hbar \sum_k \left[G^{\mathrm{R}}_{ik}(t,\bar{t}) - G^{\mathrm{A}}_{ik}(t,\bar{t})\right]\left[G^{\mathrm{R}}_{kj}(\bar{t},t') - G^{\mathrm{A}}_{kj}(\bar{t},t')\right],$$

five different cases have to be considered. For $t = \bar{t} = t'$ one gets

$$\sum_k \mathcal{U}_{ik}(t,t)\mathcal{U}_{kj}(t,t) = \sum_k \frac{\delta_{ik}\delta_{kj}}{(i\hbar)^2} = \frac{\delta_{ij}}{(i\hbar)^2} = \frac{1}{i\hbar}\mathcal{U}_{ij}(t,t)\,.$$

For $t = \bar{t}$ one gets

$$\sum_k \mathcal{U}_{ik}(t,t)\mathcal{U}_{kj}(t,t') = \sum_k \frac{1}{i\hbar}\delta_{ik}\mathcal{U}_{kj}(t,t') = \frac{1}{i\hbar}\mathcal{U}_{ij}(t,t')\,,$$

as well as for $\bar{t} = t'$,

$$\sum_k \mathcal{U}_{ik}(t,t')\mathcal{U}_{kj}(t',t') = \sum_k \mathcal{U}_{ik}(t,t')\frac{1}{i\hbar}\delta_{kj} = \frac{1}{i\hbar}\mathcal{U}_{ij}(t,t')\,.$$

For $t > \bar{t} > t'$, the propagators reduce to $\mathcal{U}_{ij}(t,t') = G^{\mathrm{R}}_{ij}(t,t')$, for which Eq. (A3) is directly applicable. For the analogous case, $t < \bar{t} < t'$, one obtains $\mathcal{U}_{ij}(t,t') = -G^{\mathrm{A}}_{ij}(t,t')$ which, together with Eq. (A2), leads to

$$i\hbar \sum_k \mathcal{U}_{ik}(t,\bar{t})\mathcal{U}_{kj}(\bar{t},t') = \mathcal{U}_{ij}(t,t')\,, \quad \text{(A4)}$$

for all t, t'. A direct consequence of this group property is [cf. Eq. (21)],

$$\mathcal{U}^{(2)}_{ijkl}(t,t') = (i\hbar)^2 \sum_{pq} \mathcal{U}^{(2)}_{ijpq}(t,\bar{t})\mathcal{U}^{(2)}_{pqkl}(\bar{t},t')\,, \quad \text{(A5)}$$

for the two-particle propagator.

3. Equations of motion

Using the EOM for the retarded/advanced Green functions, Eq. (23), the EOMs for the modified propagator immediately follows, where we separately consider the time evolution along the first and second time arguments:

$$\begin{aligned} i\hbar\frac{d}{dt}\mathcal{U}_{ij}(t,t') &= \sum_k h^{\mathrm{HF}}_{ik}(t)G^{\mathrm{R}}_{kj}(t,t') + \delta_{ij}\delta(t,t') \\ &\quad - \sum_k h^{\mathrm{HF}}_{ik}(t)G^{\mathrm{A}}_{kj}(t,t') - \delta_{ij}\delta(t,t') \\ &= \sum_k h^{\mathrm{HF}}_{ik}(t)\mathcal{U}_{kj}(t,t')\,, \quad \text{(A6)} \\ i\hbar\frac{d}{dt}\mathcal{U}_{ij}(t',t) &= -\sum_k G^{\mathrm{R}}_{ik}(t',t)h^{\mathrm{HF}}_{kj}(t) - \delta_{ij}\delta(t,t') \\ &\quad + \sum_k G^{\mathrm{A}}_{ik}(t',t)h^{\mathrm{HF}}_{kj}(t) + \delta_{ij}\delta(t,t') \\ &= -\sum_k \mathcal{U}_{ik}(t',t)h^{\mathrm{HF}}_{kj}(t)\,. \quad \text{(A7)} \end{aligned}$$

Obviously, $\mathcal{U}$ has no time-singular term but obeys a Schrödinger-type equation of motion. For the two-particle propagator follows

$$\begin{aligned} \frac{d}{dt}\left[\mathcal{U}^{(2)}_{ijkl}(t,\bar{t})\right] &= \frac{d}{dt}[\mathcal{U}_{ik}(t,\bar{t})]\mathcal{U}_{jl}(t,\bar{t}) \\ &\quad + \mathcal{U}_{ik}(t,\bar{t})\frac{d}{dt}[\mathcal{U}_{jl}(t,\bar{t})] \\ &= \left[\frac{1}{i\hbar}\sum_p h^{\mathrm{HF}}_{ip}(t)\mathcal{U}_{pk}(t,\bar{t})\right]\mathcal{U}_{jl}(t,\bar{t}) \\ &\quad + \mathcal{U}_{ik}(t,\bar{t})\left[\frac{1}{i\hbar}\sum_p h^{\mathrm{HF}}_{jp}(t)\mathcal{U}_{pl}(t,\bar{t})\right] \\ &= \frac{1}{i\hbar}\sum_p h^{\mathrm{HF}}_{ip}(t)\mathcal{U}^{(2)}_{pjkl}(t,\bar{t}) \\ &\quad + \frac{1}{i\hbar}\sum_p h^{\mathrm{HF}}_{jp}(t)\mathcal{U}^{(2)}_{ipkl}(t,\bar{t})\,. \quad \text{(A8)} \end{aligned}$$

To simplify the notation, we use the two-particle Hartree-Fock Hamiltonian [cf. Eq. (26)] so that

$$\sum_{pq} h^{(2),\mathrm{HF}}_{ijpq}(t)\mathcal{U}^{(2)}_{pqkl} = \sum_p h^{\mathrm{HF}}_{ip}(t)\mathcal{U}^{(2)}_{pjkl}(t,\bar{t}) + \sum_p h^{\mathrm{HF}}_{jp}(t)\mathcal{U}^{(2)}_{ipkl}(t,\bar{t})\,,$$

and Eq. (A8) can be rewritten as

$$\frac{d}{dt}\left[\mathcal{U}^{(2)}_{ijkl}(t,\bar{t})\right] = \frac{1}{i\hbar}\sum_{pq} h^{(2),\mathrm{HF}}_{ijpq}(t)\mathcal{U}^{(2)}_{pqkl}(t,\bar{t})\,.$$

In the same way the derivative with respect to the second time argument is found,

$$\begin{aligned}\frac{d}{dt}\big[\mathcal{U}^{(2)}_{ijkl}(\bar{t},t)\big] &= \frac{d}{dt}[\mathcal{U}_{ik}(\bar{t},t)]\mathcal{U}_{jl}(\bar{t},t)\\ &\quad+\mathcal{U}_{ik}(\bar{t},t)\frac{d}{dt}[\mathcal{U}_{jl}(\bar{t},t)]\\ &= \left[-\frac{1}{i\hbar}\sum_p \mathcal{U}_{ip}(\bar{t},t)h^{\mathrm{HF}}_{pk}(t)\right]\mathcal{U}_{jl}(\bar{t},t)\\ &\quad+\mathcal{U}_{ik}(\bar{t},t)\left[-\frac{1}{i\hbar}\sum_p \mathcal{U}_{jp}(\bar{t},t)h^{\mathrm{HF}}_{pl}(t)\right]\\ &= -\frac{1}{i\hbar}\sum_{pq}\mathcal{U}^{(2)}_{ijpq}(\bar{t},t)h^{(2),\mathrm{HF}}_{pqkl}(t).\end{aligned}$$

APPENDIX B: TIME-LINEAR INTEGRAL SOLUTION FOR $\mathcal{G}$

As we show in Sec. III B, the non-Markovian structure of the time-diagonal two-particle Green function, Eq. (22), can be eliminated by converting the problem into two coupled differential equations for $G^<(t)$ and $\mathcal{G}(t)$. Here we show for completeness that, alternatively, time-linear scaling can also be achieved within an integral representation of $\mathcal{G}$. To reveal the time-linear core of Eq. (22) for Hartree-Fock propagators, we consider a time $T+\Delta$ for which the time integral can be split into two intervals $[t_0, T]$ and $[T, T+\Delta]$, resulting in

$$\begin{aligned}\mathcal{G}_{ijkl}(T+\Delta) &= \mathcal{G}^{\Delta}_{ijkl}(T) + (i\hbar)^3\sum_{pqrs}\int_{t_0}^{T} d\bar{t}\\ &\quad\times\mathcal{U}^{(2)}_{ijpq}(T+\Delta,\bar{t})\Psi^{\pm}_{pqrs}(\bar{t})\mathcal{U}^{(2)}_{rskl}(\bar{t},T+\Delta),\end{aligned}$$

with

$$\begin{aligned}\mathcal{G}^{\Delta}_{ijkl}(T) &:= (i\hbar)^3\sum_{pqrs}\int_{T}^{T+\Delta} d\bar{t}\\ &\quad\times\mathcal{U}^{(2)}_{ijpq}(T+\Delta,\bar{t})\Psi^{\pm}_{pqrs}(\bar{t})\mathcal{U}^{(2)}_{rskl}(\bar{t},T+\Delta).\end{aligned}$$

Applying the group property of the two-particle propagator, Eq. (A5), leads to

$$\begin{aligned}\mathcal{G}_{ijkl}(T+\Delta) &= \mathcal{G}^{\Delta}_{ijkl}(T) + (i\hbar)^7\sum_{pqrsuvxy}\int_{t_0}^{T} d\bar{t}\\ &\quad\times\mathcal{U}^{(2)}_{ijpq}(T+\Delta,T)\mathcal{U}^{(2)}_{pqrs}(T,\bar{t})\\ &\quad\times\Psi^{\pm}_{rsuv}(\bar{t})\mathcal{U}^{(2)}_{uvxy}(\bar{t},T)\mathcal{U}^{(2)}_{xyjm}(T,T+\Delta),\end{aligned}$$

where we identify the two-particle Green function at time T,

$$\begin{aligned}\mathcal{G}_{ijkl}(T+\Delta) &= \mathcal{G}^{\Delta}_{ijkl}(T) + (i\hbar)^4\sum_{pqrs}\mathcal{U}^{(2)}_{ijpq}(T+\Delta,T)\\ &\quad\times\mathcal{G}_{pqrs}(T)\mathcal{U}^{(2)}_{rskl}(T,T+\Delta).\end{aligned}\tag{B1}$$

The above expression only contains a time integral of fixed length Δ. Thus, provided that the solution $\mathcal{G}(T)$ is known, the propagation to $T+\Delta$ can be done in a constant amount of time, independent of T. This way Eq. (B1) provides the basis for a time-linear propagation scheme. At the same time, we found that, for current applications, the integral form is less favorable for numerical implementation, compared to the independent approach that uses coupled time-local differential equations (G1-G2 scheme [39]) that is derived in Sec. III B and, therefore, forms the basis of the present paper.

APPENDIX C: PARTICLE-HOLE T MATRIX

For the T matrix in the particle-hole channel [28], the derivation of the G1-G2 scheme is performed in similar fashion as for the particle-particle T matrix in Sec. V A. The self energy has the form,

$$\Sigma^{\gtrless}_{ij}(t,t') = i\hbar\sum_{kl}T^{\mathrm{ph},\gtrless}_{ikjl}(t,t')G^{\gtrless}_{lk}(t,t'),\tag{C1}$$

where now the particle-hole T matrix is expressed as

$$T^{\mathrm{ph},\gtrless}_{ijkl}(t,t') = \sum_{pq}w_{ipql}(t)\Omega^{\mathrm{ph},\gtrless}_{qjkp}(t,t'),\tag{C2}$$

which allows us to rewrite the self energy (C1):

$$\Sigma^{\gtrless}_{ij}(t,t') = i\hbar\sum_{klpq}w_{ipql}(t)\Omega^{\mathrm{ph},\gtrless}_{qkjp}(t,t')G^{\gtrless}_{lk}(t,t').\tag{C3}$$

In Eqs. (C2) and (C3), Ω^{ph} denotes the nonequilibrium generalization of the Møller operator in the particle-hole channel. The collision integral (10) of the time-diagonal equation then becomes

$$\begin{aligned}I_{ij}(t) &= i\hbar\sum_{klpqr}w_{ipqr}(t)\int_{t_0}^{t}d\bar{t}\left[\Omega^{\mathrm{ph},>}_{qlkp}(t,\bar{t})\mathcal{G}^{\mathrm{F},<}_{krlj}(\bar{t},t)\right.\\ &\quad\left.-\Omega^{\mathrm{ph},<}_{qlkp}(t,\bar{t})\mathcal{G}^{\mathrm{F},>}_{krlj}(\bar{t},t)\right]\\ &= \pm i\hbar\sum_{klp}w_{iklp}(t)\mathcal{G}_{lpjk}(t),\end{aligned}$$

which results in the following expression for the time-diagonal element of the two-particle Green function,

$$\begin{aligned}\mathcal{G}_{ijkl}(t) &= \pm\sum_{pq}\int_{t_0}^{t}d\bar{t}\left[\Omega^{\mathrm{ph},>}_{iqpl}(t,\bar{t})\mathcal{G}^{\mathrm{F},<}_{pjqk}(\bar{t},t)\right.\\ &\quad\left.-\Omega^{\mathrm{ph},<}_{iqpl}(t,\bar{t})\mathcal{G}^{\mathrm{F},>}_{pjqk}(\bar{t},t)\right].\end{aligned}\tag{C4}$$

By construction, the particle-hole T matrix obeys the following symmetry [cf. Eq. (13)],

$$T^{\mathrm{ph},\gtrless}_{ijkl}(t,t') = T^{\mathrm{ph},\lessgtr}_{jilk}(t',t).$$

The particle-hole T matrix sums up the particle-hole collisions via the recursive equation (again the singular part has

been subtracted compared to its standard definition [28])

$$T^{\mathrm{ph},\gtrless}_{ijkl}(t,t') = \pm i\hbar \sum_{pqrs} w_{iqpl}(t) G^{\mathrm{F},\gtrless}_{psqr}(t,t') w^{\pm}_{rjks}(t') + i\hbar \sum_{pqrs} w_{iqpl}(t) \Bigg[\int_{t_0}^{t} d\bar{t}\, \big(G^{\mathrm{F},>}_{psqr}(t,\bar{t}) - G^{\mathrm{F},<}_{psqr}(t,\bar{t}) \big) T^{\mathrm{ph},\gtrless}_{rjks}(\bar{t},t') + \int_{t_0}^{t'} d\bar{t}\, G^{\mathrm{F},\gtrless}_{psqr}(t,\bar{t}) \big(T^{\mathrm{ph},<}_{rjks}(\bar{t},t') - T^{\mathrm{ph},>}_{rjks}(\bar{t},t') \big) \Bigg],$$

whereas the Møller operator obeys

$$\begin{aligned}
\Omega^{\mathrm{ph},\gtrless}_{ijkl}(t,t') &= \pm i\hbar \sum_{pq} G^{\mathrm{F},\gtrless}_{iplq}(t,t') w^{\pm}_{qjkp}(t') + i\hbar \sum_{pqrs} \Bigg[\int_{t_0}^{t} d\bar{t}\, \big(G^{\mathrm{F},>}_{iplq}(t,\bar{t}) - G^{\mathrm{F},<}_{iplq}(t,\bar{t}) \big) w_{qrsp}(\bar{t}) \Omega^{\mathrm{ph},\gtrless}_{sjkr}(\bar{t},t') \\
&\quad + \int_{t_0}^{t'} d\bar{t}\, G^{\mathrm{F},\gtrless}_{iplq}(t,\bar{t}) w_{qrsp}(\bar{t}) \big(\Omega^{\mathrm{ph},<}_{sjkr}(\bar{t},t') - \Omega^{\mathrm{ph},>}_{sjkr}(\bar{t},t') \big) \Bigg] \\
&= \pm i\hbar \sum_{pq} G^{\mathrm{F},\gtrless}_{iplq}(t,t') w^{\pm}_{qjkp}(t') + i\hbar \sum_{pqrs} \Bigg[\int_{t_0}^{t} d\bar{t}\, \big(G^{\mathrm{F},<}_{piql}(\bar{t},t) - G^{\mathrm{F},>}_{piql}(\bar{t},t) \big) \Omega^{\mathrm{ph},\lessgtr}_{rqps}(t',\bar{t}) \\
&\quad + \int_{t_0}^{t'} d\bar{t}\, G^{\mathrm{F},\lessgtr}_{piql}(\bar{t},t) \big(\Omega^{\mathrm{ph},>}_{rqps}(t',\bar{t}) - \Omega^{\mathrm{ph},<}_{rqps}(t',\bar{t}) \big) \Bigg] w_{sjkr}(t').
\end{aligned}$$

The time-diagonal equation for Ω^{ph} can be further simplified,

$$\begin{aligned}
\Omega^{\mathrm{ph},\gtrless}_{ijkl}(t,t) &= \pm i\hbar \sum_{pq} G^{\mathrm{F},\gtrless}_{iplq}(t) w^{\pm}_{qjkp}(t) + i\hbar \sum_{pqrs} \int_{t_0}^{t} d\bar{t}\, \big(\mathcal{G}^{\mathrm{F},<}_{piql}(\bar{t},t) \Omega^{\mathrm{ph},>}_{rqps}(t,\bar{t}) - \mathcal{G}^{\mathrm{F},>}_{piql}(\bar{t},t) \Omega^{\mathrm{ph},<}_{rqps}(t,\bar{t}) \big) w_{sjkr}(t) \\
&= \pm i\hbar \sum_{pq} G^{\mathrm{F},\gtrless}_{iplq}(t) w^{\pm}_{qjkp}(t) \pm i\hbar \sum_{pq} \mathcal{G}_{ipql}(t) w_{qjkp}(t).
\end{aligned}$$

1. T^{ph} approximation within the HF-GKBA

Applying the HF-GKBA to Eq. (C4) yields

$$\mathcal{G}_{ijkl}(t) = \pm (i\hbar)^2 \sum_{pqrs} \int_{t_0}^{t} d\bar{t}\, \mathcal{U}_{jr}(t,\bar{t}) \mathcal{U}_{sk}(\bar{t},t) \big[\Omega^{\mathrm{ph},>}_{iqpl}(t,\bar{t}) \mathcal{G}^{\mathrm{F},<}_{prqs}(\bar{t}) - \Omega^{\mathrm{ph},<}_{iqpl}(t,\bar{t}) \mathcal{G}^{\mathrm{F},>}_{prqs}(\bar{t}) \big],$$

and, for the Møller operator,

$$\begin{aligned}
\Omega^{\mathrm{ph},\gtrless}_{ijkl}(t \geqslant t') &= \pm (i\hbar)^3 \sum_{pqrs} \mathcal{U}_{ir}(t,t') G^{\mathrm{F},\gtrless}_{rpsq}(t') \mathcal{U}_{sl}(t',t) w^{\pm}_{qjkp}(t') \\
&\quad + (i\hbar)^3 \sum_{pqrsuv} \Bigg[\int_{t_0}^{t} d\bar{t}\, w_{qrsp}(\bar{t}) \mathcal{U}_{iu}(t,\bar{t}) \big(G^{\mathrm{F},>}_{upvq}(t,\bar{t}) - G^{\mathrm{F},<}_{upvq}(t,\bar{t}) \big) \mathcal{U}_{vl}(\bar{t},t) \Omega^{\mathrm{ph},\gtrless}_{sjkr}(\bar{t},t') \\
&\quad + \int_{t_0}^{t'} d\bar{t}\, \mathcal{U}_{iu}(t,\bar{t}) G^{\mathrm{F},\gtrless}_{upvq}(t,\bar{t}) \mathcal{U}_{vl}(\bar{t},t) w_{qrsp}(\bar{t}) \big(\Omega^{\mathrm{ph},<}_{sjkr}(\bar{t},t') - \Omega^{\mathrm{ph},>}_{sjkr}(\bar{t},t') \big) \Bigg],
\end{aligned} \tag{C5}$$

where $\mathcal{U}$ obeys Eqs. (A6) and (A7). With Eq. (C5) we obtain the time derivative,

$$\begin{aligned}
\frac{d}{dt} \Omega^{\mathrm{ph},\gtrless}_{ijkl}(t \geqslant t') &= \frac{1}{i\hbar} \sum_{p} \big\{ h^{\mathrm{HF}}_{ip}(t) \Omega^{\mathrm{ph},\gtrless}_{pjkl}(t \geqslant t') - \Omega^{\mathrm{ph},\gtrless}_{ijkp}(t \geqslant t') h^{\mathrm{HF}}_{pl}(t) \big\} \\
&\quad \pm i\hbar \sum_{pqrs} \big[\mathcal{G}^{\mathrm{F},>}_{iplq}(t) - \mathcal{G}^{\mathrm{F},<}_{iplq}(t) \big] w_{qrsp}(t) \Omega^{\mathrm{ph},\gtrless}_{sjkr}(t \geqslant t') \\
&= \frac{1}{i\hbar} \sum_{pq} \big[\mathfrak{h}^{\Omega^{\mathrm{ph}},\mathrm{HF}}_{ipql}(t) + \mathfrak{h}^{\Omega^{\mathrm{ph}},\mathrm{corr}}_{ipql}(t) \big] \Omega^{\mathrm{ph},\gtrless}_{qjkp}(t \geqslant t'),
\end{aligned}$$

where we introduced the Hamiltonians

$$\mathfrak{h}^{\Omega^{\rm ph},\rm HF}_{ijkl}(t) = \delta_{jl} h^{\rm HF}_{ik} - \delta_{ik} h^{\rm HF}_{jl}\,,$$
$$\mathfrak{h}^{\Omega^{\rm ph},\rm corr}_{ijkl}(t) = (i\hbar)^2 \sum_{pq} \left[\mathcal{G}^{\rm F,>}_{iplq}(t) - \mathcal{G}^{\rm F,<}_{iplq}(t)\right] w_{qjkp}(t)$$

that can be combined to

$$\mathfrak{h}^{\Omega^{\rm ph}}_{ijkl}(t) = \mathfrak{h}^{\Omega^{\rm ph},\rm HF}_{ijkl}(t) + \mathfrak{h}^{\Omega^{\rm ph},\rm corr}_{ijkl}(t)\,,$$

and the Møller operator obeys a Schrödinger equation,

$$i\hbar \frac{d}{dt} \Omega^{\rm ph,\gtrless}_{ijkl}(t \gtrless t') = \sum_{pq} \mathfrak{h}^{\Omega^{\rm ph}}_{ipql}(t) \Omega^{\rm ph,\gtrless}_{qjkp}(t \gtrless t')\,.$$

2. $T^{\rm ph}$-G1-G2 equations for a general basis

Next, we compute the time derivative of $\mathcal{G}$,

$$\frac{d}{dt}\mathcal{G}_{ijkl}(t) = \left[\frac{d}{dt}\mathcal{G}_{ijkl}(t)\right]_{\int} + \left[\frac{d}{dt}\mathcal{G}_{ijkl}(t)\right]_{\Omega^{\rm ph}} + \left[\frac{d}{dt}\mathcal{G}_{ijkl}(t)\right]_{\mathcal{U}},$$

and obtain for the first part,

$$\begin{aligned}
\left[\frac{d}{dt}\mathcal{G}_{ijkl}(t)\right]_{\int} &= \pm \sum_{pq} \left[\Omega^{\rm ph,>}_{iqpl}(t,t)\mathcal{G}^{\rm F,<}_{pjqk}(t,t) - \Omega^{\rm ph,<}_{iqpl}(t,t)\mathcal{G}^{\rm F,>}_{pjqk}(t,t)\right] \\
&= i\hbar \sum_{pqrs} w^{\pm}_{rqps}(t)\left[\mathcal{G}^{\rm F,>}_{islr}(t)\mathcal{G}^{\rm F,<}_{pjqk}(t) - \mathcal{G}^{\rm F,<}_{islr}(t)\mathcal{G}^{\rm F,>}_{pjqk}(t)\right] + i\hbar \sum_{pqrs} \mathcal{G}_{isrl}(t) w_{rqps}(t)\left[\mathcal{G}^{\rm F,<}_{pjqk}(t) - \mathcal{G}^{\rm F,>}_{pjqk}(t)\right] \\
&= \frac{1}{i\hbar}\Psi^{\pm}_{ijkl}(t) - \frac{1}{i\hbar}\sum_{pq}\left[\mathfrak{h}^{\Omega^{\rm ph},\rm corr}_{kqpj}(t)\right]^* \mathcal{G}_{iqpl}(t)\,,
\end{aligned}$$

and, for the second part,

$$\begin{aligned}
\left[\frac{d}{dt}\mathcal{G}_{ijkl}(t)\right]_{\Omega^{\rm ph}} &= \pm (i\hbar)^2 \sum_{pqrs}\int_{t_0}^{t} d\bar{t}\, \mathcal{U}_{jr}(t,\bar{t})\left[\left(\frac{d}{dt}\Omega^{\rm ph,>}_{iqpl}(t,\bar{t})\right)\mathcal{G}^{\rm F,<}_{prqs}(\bar{t}) - \left(\frac{d}{dt}\Omega^{\rm ph,<}_{iqpl}(t,\bar{t})\right)\mathcal{G}^{\rm F,>}_{prqs}(\bar{t})\right]\mathcal{U}_{sk}(\bar{t},t) \\
&= \frac{1}{i\hbar}\sum_{pq}\left[\mathfrak{h}^{\Omega^{\rm ph},\rm HF}_{ipql}(t) + \mathfrak{h}^{\Omega^{\rm ph},\rm corr}_{ipql}(t)\right]\mathcal{G}_{qjkp}(t),
\end{aligned}$$

and, for the third part,

$$\begin{aligned}
\left[\frac{d}{dt}\mathcal{G}_{ijkl}(t)\right]_{\mathcal{U}} &= \pm (i\hbar)^2 \sum_{pqrs}\int_{t_0}^{t} d\bar{t}\left(\frac{d}{dt}\mathcal{U}_{jr}(t,\bar{t})\right)\left[\Omega^{\rm ph,>}_{iqpl}(t,\bar{t})\mathcal{G}^{\rm F,<}_{prqs}(\bar{t}) - \Omega^{\rm ph,<}_{iqpl}(t,\bar{t})\mathcal{G}^{\rm F,>}_{prqs}(\bar{t})\right]\mathcal{U}_{sk}(\bar{t},t) \\
&\quad \pm (i\hbar)^2 \sum_{pqrs}\int_{t_0}^{t} d\bar{t}\,\mathcal{U}_{jr}(t,\bar{t})\left[\Omega^{\rm ph,>}_{iqpl}(t,\bar{t})\mathcal{G}^{\rm F,<}_{prqs}(\bar{t}) - \Omega^{\rm ph,<}_{iqpl}(t,\bar{t})\mathcal{G}^{\rm F,>}_{prqs}(\bar{t})\right]\left(\frac{d}{dt}\mathcal{U}_{sk}(\bar{t},t)\right) \\
&= \frac{1}{i\hbar}\sum_{pq}\mathcal{G}_{ipql}(t)\mathfrak{h}^{\Omega^{\rm ph},\rm HF}_{jqpk}(t).
\end{aligned}$$

Combining the three contributions yields the derivative,

$$i\hbar\frac{d}{dt}\mathcal{G}_{ijkl}(t) = \Psi^{\pm}_{ijkl}(t) + \sum_{kl}\left\{\mathfrak{h}^{\Omega^{\rm ph}}_{ipql}(t)[\mathcal{G}_{kpqj}(t)]^* - \mathcal{G}_{ipql}(t)\left[\mathfrak{h}^{\Omega^{\rm ph}}_{kpqj}(t)\right]^*\right\},$$

which is the result presented in the main part of the paper.

APPENDIX D: INTEGRAL SOLUTION $\mathcal{G}(t)$ AND INITIAL CORRELATIONS FOR HIGHER-ORDER SELF ENERGIES

While initial correlations are trivially added to the differential G1-G2 scheme as an initial condition, as we demonstrated in Sec. III E, for the integral representation of $\mathcal{G}$, this problem is more involved. We, therefore, outline, in this Appendix, the

solution for higher-order self energies by extending our SOA result, Eq. (46). Since the derivations are carried out analogously to Sec. III E and Appendix B, respectively, we only give the resulting equations. Performing the time derivative of the integral expressions recovers the differential equations for the respective self energy, cf. Eqs. (59), (76), and (83).

1. *GW* self energy

In the case of the *GW* self energy Eq. (46) becomes

$$\mathcal{G}_{ijkl}(t) = (i\hbar)^4 \sum_{pqrs} \int_{t_0}^{t} d\bar{t}\, \mathcal{U}^{(2),\varepsilon}_{lqjs}(t,\bar{t}) \left[\delta(t_0,\bar{t}) \mathcal{G}^0_{pqrs} + \frac{1}{i\hbar} \Psi_{pqrs}(\bar{t}) \right] \left[\mathcal{U}^{(2),\varepsilon}_{irkp}(t,\bar{t}) \right]^* ,$$

where

$$\mathcal{U}^{(2),\varepsilon}_{ijkl}(t,t') = \mathcal{U}_{kj}(t,t')\mathcal{U}_{li}(t',t) + i\hbar \sum_{pqrs} \int_{t'}^{t} d\bar{t}\, \mathcal{U}_{kp}(t,\bar{t}) \mathcal{U}_{qi}(\bar{t},t) \mathfrak{h}^{\varepsilon,\mathrm{corr}}_{rpsq}(\bar{t}) \mathcal{U}^{(2),\varepsilon}_{rjsl}(\bar{t},t') .$$

The equation of motion for these modified propagators can also be brought to a differential form:

$$i\hbar \frac{d}{dt} \mathcal{U}^{(2),\varepsilon}_{ijkl}(t \geqslant t') = \sum_{pq} \mathfrak{h}^{\varepsilon}_{pkqi}(t) \mathcal{U}^{(2),\varepsilon}_{pjql}(t \geqslant t') . \tag{D1}$$

As one observes, $\mathcal{U}^{(2),\varepsilon}$ obeys the same equation as $\varepsilon^{-1,\gtrless}$ itself [cf. Eq. (57)]. They are, however, not identical, since the time-diagonal values differ [cf. Eqs. (18) and (53)].

2. *T* matrix in the particle-particle channel

For the particle-particle T-matrix approximation similar equations can be derived. The equivalent of Eq. (46) takes the form,

$$\mathcal{G}_{ijkl}(t) = (i\hbar)^4 \sum_{pqrs} \int_{t_0}^{t} d\bar{t}\, \mathcal{U}^{(2),\Omega^{\mathrm{pp}}}_{ijpq}(t,\bar{t}) \left[\delta(t_0,\bar{t}) \mathcal{G}^0_{pqrs} + \frac{1}{i\hbar} \Psi^{\pm}_{pqrs}(\bar{t}) \right] \left[\mathcal{U}^{(2),\Omega^{\mathrm{pp}}}_{klrs}(t,\bar{t}) \right]^* ,$$

where

$$\mathcal{U}^{(2),\Omega^{\mathrm{pp}}}_{ijkl}(t,t') = \mathcal{U}^{(2)}_{ijkl}(t,t') + i\hbar \sum_{pqrs} \int_{t'}^{t} d\bar{t}\, \mathcal{U}^{(2)}_{ijpq}(t,\bar{t}) \mathfrak{h}^{\Omega^{\mathrm{pp}},\mathrm{corr}}_{pqrs}(\bar{t}) \mathcal{U}^{(2),\Omega^{\mathrm{pp}}}_{rskl}(\bar{t},t') .$$

The corresponding differential equation for the two-particle propagator mirrors the respective equation for Ω^{pp} [cf. Eq. (75)],

$$i\hbar \frac{d}{dt} \mathcal{U}^{(2),\Omega^{\mathrm{pp}}}_{ijkl}(t \geqslant t') = \sum_{pq} \mathfrak{h}^{\Omega^{\mathrm{pp}}}_{ijpq}(t) \mathcal{U}^{(2),\Omega^{\mathrm{pp}}}_{pqkl}(t \geqslant t') . \tag{D2}$$

As for *GW*, the time-diagonal values of both quantities do, however, not coincide.

3. *T* matrix in the particle-hole channel

Finally, in the particle-hole T-matrix approximation Eq. (46) is replaced by

$$\mathcal{G}_{ijkl}(t) = i\hbar \sum_{pqrs} \int_{t_0}^{t} d\bar{t}\, \mathcal{U}^{(2),\Omega^{\mathrm{ph}}}_{ispl}(t,\bar{t}) \left[\delta(t_0,\bar{t}) \mathcal{G}^0_{pqrs} + \frac{1}{i\hbar} \Psi^{\pm}_{pqrs}(\bar{t}) \right] \left[\mathcal{U}^{(2),\Omega^{\mathrm{ph}}}_{kqrj}(t,\bar{t}) \right]^* ,$$

with

$$\mathcal{U}^{(2),\Omega^{\mathrm{ph}}}_{ijkl}(t,t') = \mathcal{U}_{ik}(t,t')\mathcal{U}_{jl}(t',t) + i\hbar \sum_{pqrs} \int_{t'}^{t} d\bar{t}\, \mathcal{U}_{iq}(t,\bar{t}) \mathcal{U}_{pl}(\bar{t},t) \mathfrak{h}^{\Omega^{\mathrm{ph}},\mathrm{corr}}_{qrsp}(\bar{t}) \mathcal{U}^{(2),\Omega^{\mathrm{ph}}}_{sjkr}(\bar{t},t') .$$

The last equation can again be transformed into its differential form,

$$i\hbar \frac{d}{dt} \mathcal{U}^{(2),\Omega^{\mathrm{ph}}}_{ijkl}(t \geqslant t') = \sum_{pq} \mathfrak{h}^{\Omega^{\mathrm{ph}}}_{ipql}(t) \mathcal{U}^{(2),\Omega^{\mathrm{ph}}}_{qjkp}(t \geqslant t') ,$$

which matches Eq. (82) for Ω^{ph} in analogy to Eqs. (D1) and (D2).

[1] L. Keldysh, Diagram technique for nonequilibrium processes, Sov. Phys. JETP **20**, 1018 (1965) [Zh. Eksp. Teor. Fiz. **47**, 1515 (1964)].

[2] M. Bonitz, A.-P. Jauho, M. Sadovskii, and S. Tikhodeev, In memoriam Leonid V. Keldysh, Phys. Status Solidi B **256**, 1800600 (2019).

[3] L. Kadanoff and G. Baym, *Quantum Statistical Mechanics* (Benjamin, New York, 1962).

[4] H. Haug and A.-P. Jauho, *Quantum Kinetics in Transport and Optics of Semiconductors* (Springer, Berlin, Heidelberg, 2008).

[5] M. Bonitz, *Quantum Kinetic Theory*, 2nd ed., Teubner-Texte zur Physik (Springer, Cham, 2016).

[6] G. Stefanucci and R. van Leeuwen, *Nonequilibrium Many-Body Theory of Quantum Systems: A Modern Introduction* (Cambridge University Press, Cambridge, 2013).

[7] P. Danielewicz, Quantum theory of nonequilibrium processes II. Application to nuclear collisions, Ann. Phys. **152**, 305 (1984).

[8] H. S. Köhler, Memory and correlation effects in nuclear collisions, Phys. Rev. C **51**, 3232 (1995).

[9] W. Schäfer and M. Wegener, *Semiconductor Optics and Transport Phenomena* (Springer, Berlin, Heidelberg, 2002).

[10] D. Semkat, D. Kremp, and M. Bonitz, Kadanoff-Baym equations with initial correlations, Phys. Rev. E **59**, 1557 (1999).

[11] D. Kremp, T. Bornath, M. Bonitz, and M. Schlanges, Quantum kinetic theory of plasmas in strong laser fields, Phys. Rev. E **60**, 4725 (1999).

[12] N. E. Dahlen and R. van Leeuwen, Solving the Kadanoff-Baym Equations for Inhomogeneous Systems: Application to Atoms and Molecules, Phys. Rev. Lett. **98**, 153004 (2007).

[13] K. Balzer, S. Bauch, and M. Bonitz, Efficient grid-based method in nonequilibrium Green's function calculations: Application to model atoms and molecules, Phys. Rev. A **81**, 022510 (2010).

[14] K. Balzer, S. Bauch, and M. Bonitz, Time-dependent second-order Born calculations for model atoms and molecules in strong laser fields, Phys. Rev. A **82**, 033427 (2010).

[15] M. P. von Friesen, C. Verdozzi, and C.-O. Almbladh, Successes and Failures of Kadanoff-Baym Dynamics in Hubbard Nanoclusters, Phys. Rev. Lett. **103**, 176404 (2009).

[16] M. Puig von Friesen, C. Verdozzi, and C.-O. Almbladh, Kadanoff-Baym dynamics of Hubbard clusters: Performance of many-body schemes, correlation-induced damping and multiple steady and quasi-steady states, Phys. Rev. B **82**, 155108 (2010).

[17] S. Hermanns, N. Schlünzen, and M. Bonitz, Hubbard nanoclusters far from equilibrium, Phys. Rev. B **90**, 125111 (2014).

[18] N. Schlünzen, S. Hermanns, M. Bonitz, and C. Verdozzi, Dynamics of strongly correlated fermions: *Ab initio* results for two and three dimensions, Phys. Rev. B **93**, 035107 (2016).

[19] N. Schlünzen and M. Bonitz, Nonequilibrium green functions approach to strongly correlated fermions in lattice systems, Contrib. Plasma Phys. **56**, 5 (2016).

[20] K. Balzer, M. R. Rasmussen, N. Schlünzen, J.-P. Joost, and M. Bonitz, Doublon Formation by Ions Impacting a Strongly Correlated Finite Lattice System, Phys. Rev. Lett. **121**, 267602 (2018).

[21] M. Bonitz, K. Balzer, N. Schlünzen, M. Rasmussen, and J.-P. Joost, Ion impact induced ultrafast electron dynamics in correlated materials and finite graphene clusters, Phys. Status Solidi B **257**, 1800490 (2019).

[22] N. Schlünzen, K. Balzer, M. Bonitz, L. Deuchler, and E. Pehlke, Time-dependent simulation of ion stopping: Charge transfer and electronic excitations, Contrib. Plasma Phys. **59**, e201800184 (2019).

[23] H. S. Köhler, N.-H. Kwong, and H. A. Yousif, A Fortran code for solving the Kadanoff-Baym equations for a homogeneous fermion system, Comput. Phys. Commun. **123**, 123 (1999).

[24] M. Bonitz and D. Semkat, Generalized quantum kinetic equations, in *Introduction to Computational Methods in Many Body Physics*, edited by M. Bonitz and D. Semkat (Rinton Press, Princeton, 2006), pp. 94–102.

[25] A. Marini, C. Hogan, M. Grüning, and D. Varsano, yambo: An ab initio tool for excited state calculations, Comput. Phys. Commun. **180**, 1392 (2009).

[26] N. Schlünzen, J.-P. Joost, and M. Bonitz, Comment on "On the unphysical solutions of the Kadanoff-Baym equations in linear response: Correlation-induced homogeneous density-distribution and attractors," Phys. Rev. B **96**, 117101 (2017).

[27] N. Schlünzen, J.-P. Joost, F. Heidrich-Meisner, and M. Bonitz, Nonequilibrium dynamics in the one-dimensional Fermi-Hubbard model: Comparison of the nonequilibrium Green-functions approach and the density matrix renormalization group method, Phys. Rev. B **95**, 165139 (2017).

[28] N. Schlünzen, S. Hermanns, M. Scharnke, and M. Bonitz, Ultrafast dynamics of strongly correlated fermions – Nonequilibrium Green functions and selfenergy approximations, J. Phys.: Condens. Matter **32**, 103001 (2020).

[29] E. Gull, A. J. Millis, A. I. Lichtenstein, A. N. Rubtsov, M. Troyer, and P. Werner, Continuous-time Monte Carlo methods for quantum impurity models, Rev. Mod. Phys. **83**, 349 (2011).

[30] P. Lipavský, V. Špička, and B. Velický, Generalized Kadanoff-Baym ansatz for deriving quantum transport equations, Phys. Rev. B **34**, 6933 (1986).

[31] M. Bonitz, D. Kremp, D. C. Scott, R. Binder, W. D. Kraeft, and H. S. Köhler, Numerical analysis of non-Markovian effects in charge-carrier scattering: One-time versus two-time kinetic equations, J. Phys.: Condens. Matter **8**, 6057 (1996).

[32] M. Bonitz and D. Kremp, Kinetic energy relaxation and correlation time of nonequilibrium many-particle systems, Phys. Lett. A **212**, 83 (1996).

[33] K. Balzer and M. Bonitz, *Nonequilibrium Green's Functions Approach to Inhomogeneous Systems* (Springer, Berlin, Heidelberg, 2013).

[34] S. Latini, E. Perfetto, A.-M. Uimonen, R. van Leeuwen, and G. Stefanucci, Charge dynamics in molecular junctions: Nonequilibrium Green's function approach made fast, Phys. Rev. B **89**, 075306 (2014).

[35] A. Marini, Competition between the electronic and phonon–mediated scattering channels in the out–of–equilibrium carrier dynamics of semiconductors: An ab-initio approach, J. Phys.: Conf. Ser. **427**, 012003 (2013).

[36] D. Karlsson, R. van Leeuwen, E. Perfetto, and G. Stefanucci, The generalized Kadanoff-Baym ansatz with initial correlations, Phys. Rev. B **98**, 115148 (2018).

[37] E. Perfetto, A.-M. Uimonen, R. van Leeuwen, and G. Stefanucci, First-principles nonequilibrium Green's-function approach to transient photoabsorption: Application to atoms, Phys. Rev. A **92**, 033419 (2015).

[38] E. V. Boström, A. Mikkelsen, C. Verdozzi, E. Perfetto, and G. Stefanucci, Charge separation in donor-C60 complexes with real-time green functions: The importance of nonlocal correlations, Nano Lett. **18**, 785 (2018).

[39] N. Schlünzen, J.-P. Joost, and M. Bonitz, Achieving the Scaling Limit for Nonequilibrium Green Functions Simulations, Phys. Rev. Lett. **124**, 076601 (2020).

[40] S. Hermanns, K. Balzer, and M. Bonitz, Few-particle quantum dynamics–comparing nonequilibrium Green functions with the generalized Kadanoff–Baym ansatz to density operator theory, J. Phys.: Conf. Ser. **427**, 012008 (2013).

[41] U. Schneider, L. Hackermüller, J. P. Ronzheimer, S. Will, S. Braun, T. Best, I. Bloch, E. Demler, S. Mandt, D. Rasch, and A. Rosch, Fermionic transport and out-of-equilibrium dynamics in a homogeneous Hubbard model with ultracold atoms, Nat. Phys. **8**, 213 (2012).

[42] K. Balzer, M. Bonitz, R. van Leeuwen, A. Stan, and N. E. Dahlen, Nonequilibrium Green's function approach to strongly correlated few-electron quantum dots, Phys. Rev. B **79**, 245306 (2009).

[43] Throughout this work, "±" refers to bosons/fermions.

[44] The commutator of two single-particle quantities $A(t)$ and $B(t)$ is defined as $[A,B]_{ij}(t) = \sum_k [A_{ik}(t)B_{kj}(t) - B_{ik}(t)A_{kj}(t)]$.

[45] The commutator of two two-particle quantities $A(t)$ and $B(t)$ is defined as $[A,B]_{ijkl}(t) = \sum_{pq}[A_{ijpq}(t)B_{pqkl}(t) - B_{ijpq}(t)A_{pqkl}(t)]$.

[46] J. Hubbard and B. H. Flowers, Electron correlations in narrow energy bands, Proc. R. Soc. London A **276**, 238 (1963).

[47] I. Bloch, Probing and controlling quantum matter using ultracold quantum gases in optical lattices, in *Quantum Information and Coherence*, edited by E. Andersson and P. Öhberg, Scottish Graduate Series (Springer International Publishing, Cham, 2014), pp. 31–63.

[48] J. Kajala, F. Massel, and P. Törmä, Expansion Dynamics in the One-Dimensional Fermi-Hubbard Model, Phys. Rev. Lett. **106**, 206401 (2011).

[49] T. Dornheim, S. Groth, and M. Bonitz, The uniform electron gas at warm dense matter conditions, Phys. Rep. **744**, 1 (2018).

[50] J. M. Ziman, *Electrons and Phonons: The Theory of Transport Phenomena in Solids* (Oxford University Press, Oxford, 1960).

[51] G. D. Mahan, *Many-Particle Physics* (Springer, Boston, MA, 1990).

[52] D. Semkat, D. Kremp, and M. Bonitz, Kadanoff–Baym equations and non-Markovian Boltzmann equation in generalized T-matrix approximation, J. Math. Phys. **41**, 7458 (2000).

[53] M. Hopjan and C. Verdozzi, Initial correlated states for the generalized Kadanoff-Baym Ansatz without adiabatic switching-on of interactions in closed systems, Eur. Phys. J.: Spec. Top. **227**, 1939 (2019).

[54] D. Semkat, D. Kremp, and M. Bonitz, Generalized T-matrix approximation in quantum kinetic equations, Contrib. Plasma Phys. **42**, 31 (2002).

[55] A. Rios, B. Barker, M. Buchler, and P. Danielewicz, Towards a nonequilibrium Green's function description of nuclear reactions: One-dimensional mean-field dynamics, Ann. Phys. **326**, 1274 (2011).

[56] M. Bonitz, M. Scharnke, and N. Schlünzen, Timereversal invariance of quantum kinetic equations II: Density operator formalism, Contrib. Plasma Phys. **58**, 1036 (2018).

[57] D. Semkat, M. Bonitz, and D. Kremp, Relaxation of a quantum many-body system from a correlated initial state. A general and consistent approach, Contrib. Plasma Phys. **43**, 321 (2003).

[58] D. Gericke, M. Murillo, D. Semkat, M. Bonitz, and D. Kremp, Relaxation of strongly coupled Coulomb systems after rapid changes of the interaction potential, J. Phys. A: Math. Gen. **36**, 6087 (2003).

[59] M. Moeckel and S. Kehrein, Interaction Quench in the Hubbard Model, Phys. Rev. Lett. **100**, 175702 (2008).

[60] M. Eckstein, M. Kollar, and P. Werner, Interaction quench in the hubbard model: Relaxation of the spectral function and the optical conductivity, Phys. Rev. B **81**, 115131 (2010).

[61] M. Bonitz, D. Semkat, D. Gericke, and M. Murillo, Short-time dynamics of quantum many-body systems following a spin statistics switch, in *Progress in Nonequilibrium Green's functions II*, edited by M. Bonitz and D. Semkat (World Scientific Publ., Singapore, 2003), pp. 94–102.

[62] D. Gericke, M. Murillo, M. Bonitz, and D. Semkat, Temperature estimates for quantum systems after an ionization iduced rapid switch of the spin statistics, J. Phys. A: Math. Gen. **36**, 6095 (2003).

[63] L. Hedin, New method for calculating the one-particle Green's function with application to the electron-gas problem, Phys. Rev. **139**, A796 (1965).

[64] U. Hohenester and W. Pötz, Density-matrix approach to nonequilibrium free-carrier screening in semiconductors, Phys. Rev. B **56**, 13177 (1997).

[65] R. Balescu, Irreversible processes in ionized gases, Phys. Fluids **3**, 52 (1960).

[66] A. Lenard, On Bogoliubov's kinetic equation for a spatially homogeneous plasma, Ann. Phys. **10**, 390 (1960).

[67] Y. Klimontovich, *Kinetic Theory of Nonideal Gases and Nonideal Plasmas* (Pergamon, Oxford, 1982).

[68] G. Stefanucci, Y. Pavlyukh, A.-M. Uimonen, and R. van Leeuwen, Diagrammatic expansion for positive spectral functions beyond GW: Application to vertex corrections in the electron gas, Phys. Rev. B **90**, 115134 (2014).

[69] J.-P. Joost, N. Schlünzen, and M. Bonitz, Femtosecond electron dynamics in graphene nanoribbons – a nonequilibrium Green functions approach within an extended Hubbard model, Phys. Status Solidi B **257**, 1800498 (2019).

[70] J. R. Taylor (ed.), *Scattering Theory: The Quantum Theory of Nonrelativistic Collisions* (Dover, Mineola, NY, 1983).

[71] D. Kremp, M. Bonitz, W. Kraeft, and M. Schlanges, Non-Markovian Boltzmann equation, Ann. Phys. **258**, 320 (1997).

[72] R. Zimmermann, K. Kilimann, W. D. Kraeft, D. Kremp, and G. Röpke, Dynamical screening and self-energy of excitons in the electron–hole plasma, Phys. Status Solidi B **90**, 175 (1978).

[73] W. Kraeft, D. Kremp, W. Ebeling, and G. Röpke, *Quantum Statistics of Charged Particle Systems* (Akademieverlag, Berlin, 1986).

[74] W. Shun-jin and W. Cassing, Explicit treatment of n-body correlations within a density-matrix formalism, Ann. Phys. **159**, 328 (1985).

[75] A. Akbari, M. J. Hashemi, A. Rubio, R. M. Nieminen, and R. van Leeuwen, Challenges in truncating the hierarchy of time-dependent reduced density matrices equations, Phys. Rev. B **85**, 235121 (2012).

[76] M. Lindberg and S. W. Koch, Effective Bloch equations for semiconductors, Phys. Rev. B **38**, 3342 (1988).

[77] V. M. Axt and A. Stahl, A dynamics-controlled truncation scheme for the hierarchy of density matrices in semiconductor optics, Z. Phys. B: Condens. Matter **93**, 195 (1994).

[78] D. Lacroix, S. Hermanns, C. M. Hinz, and M. Bonitz, Ultrafast dynamics of finite Hubbard clusters: A stochastic mean-field approach, Phys. Rev. B **90**, 125112 (2014).

[79] P. Schuck and M. Tohyama, Self-consistent RPA and the time-dependent density matrix approach, Eur. Phys. J. A **52**, 307 (2016).

[80] S. Krönke and P. Schmelcher, Born-Bogoliubov-Green-Kirkwood-Yvon hierarchy for ultracold bosonic systems, Phys. Rev. A **98**, 013629 (2018).

[81] J. G. Kirkwood, Statistical mechanics of fluid mixtures, J. Chem. Phys. **3**, 300 (1935).

[82] A. Singer, Maximum entropy formulation of the Kirkwood superposition approximation, J. Chem. Phys. **121**, 3657 (2004).

[83] V. E. Fortov, O. F. Petrov, and O. S. Vaulina, Dusty-Plasma Liquid in the Statistical Theory of the Liquid State, Phys. Rev. Lett. **101**, 195003 (2008).

[84] H. Nakatsuji and K. Yasuda, Direct Determination of the Quantum-Mechanical Density Matrix Using the Density Equation, Phys. Rev. Lett. **76**, 1039 (1996).

[85] F. Lackner, I. Březinová, T. Sato, K. L. Ishikawa, and J. Burgdörfer, High-harmonic spectra from time-dependent two-particle reduced-density-matrix theory, Phys. Rev. A **95**, 033414 (2017).

[86] N. H. Kwong, M. Bonitz, R. Binder, and H. S. Köhler, Semiconductor Kadanoff-Baym equation results for optically excited electron-hole plasmas in quantum wells, Phys. Status Solidi B **206**, 197 (1998).

[87] M. Bonitz, Correlation time approximation in non-Markovian kinetics, Phys. Lett. A **221**, 85 (1996).

[88] Z. A. Moldabekov, M. Bonitz, and T. S. Ramazanov, Theoretical foundations of quantum hydrodynamics for plasmas, Phys. Plasmas **25**, 031903 (2018).

[89] M. Bonitz, Z. A. Moldabekov, and T. S. Ramazanov, Quantum hydrodynamics for plasmas–quo vadis? Phys. Plasmas **26**, 090601 (2019).